COMPUTATIONAL MODELING OF WIND FLOW AND WIND-INDUCED LOADS ON LOW BUILDINGS

Theodore Potsis

A Thesis

In the Department of

Building, Civil and Environmental Engineering

Presented in Partial Fulfillment of the Requirements

For the Degree of

Doctor of Philosophy (Building Engineering) at

Concordia University

Montreal, Quebec, Canada

October, 2024

CONCORDIA UNIVERSITY

SCHOOL OF GRADUATESTUDIES

This is to certify that the thesis prepared

By: Theodore Potsis

Entitled: Computational Modeling of Wind Flow and Wind-Induced Loads on Low Buildings

and submitted in partial fulfillment of the requirements for the degree of

Doctor of Philosophy (Building Engineering)

complies with the regulations of the University and meets the accepted standards with respect to originality and quality.

Signed by the final examining committee:

______________________________ Chair
Dr. Carol Fung

______________________________ External Examiner
Dr. Ashraf A. El Damatty

______________________________ Arms-Length Examiner
Dr. Hoi Dick Ng

______________________________ Examiner
Dr. Samuel Li

______________________________ Examiner
Dr. Anjan Bhowmick

______________________________ Thesis Supervisor
Dr. Theodore Stathopoulos

Approved by ______________________________
Dr. Mohamed Ouf, Graduate Program Director

1/13/2025

____
Dr. Mourad Debbabi, Dean, Gina Cody School of Engineering and Computer Science

ABSTRACT

COMPUTATIONAL MODELING OF WIND FLOW AND WIND-INDUCED LOADS ON LOW BUILDINGS

Theodore Potsis, Ph.D.

Concordia University, 2024

Moving towards a new era where structural engineering applications will rely more on Computational Fluid Dynamics as means to evaluate wind related characteristics, this thesis demonstrates a novel computational technique to model wind flow and wind-induced structural loads. During the last decades there have been continuous efforts in modelling efficiently turbulent flows by the practice and scientific community. Various methodologies have been discussed in the literature, but their applicability for structural design remains problematic, thus wind design standards and codes of practice hesitate to adopt computational procedures for structural loads. Therefore, a new tool that serves the engineering needs while respecting the scientific requirements has been developed.

The so-called Dynamic Terrain method utilizes velocity time series extracted from the Concordia Wind Tunnel as inlet conditions. A first target achieved was to model accurately the energy of the fluctuations of turbulence scales that are smaller than the building characteristic dimensions. This accomplishment covers a research gap in the state-of-the-art identified during a comprehensive review study. Another achievement is the ability of the method to model various exposure conditions, in addition to the characteristic standard open, suburban and urban exposures. Quasi-

steady conditions are assumed for the inlet time series as to respect physical aspects such as the divergence-free criteria and numerical stability. The final pressure time series are extracted by filtering the numerical data to account for the inherent discontinuity of the inlet conditions and their propagation in the computational domain.

With this engineering tool, modeling of wind flow and peak pressures on building envelopes become possible via simple procedures and advantageous techniques, compared with similar approaches currently available. Validation of wind flow and pressure characteristics are presented for various structural applications. Mean, std and peak pressures have been validated for loads on low-rise buildings based on experiments from TPU, NIST and the Concordia Wind Tunnel. The accuracy is within acceptable margins established by comparisons among the experimental results from respective wind tunnel facilities. The tool is incorporated in an open database, where experimental data from the Concordia Wind Tunnel and OpenFOAM libraries are included for free usage by practitioners and scientific groups.

Acknowledgments

First, I want to thank myself for enduring the pain and discomfort of not knowing the answers to the questions that kept me sleepless at night for the last 5 years. Second, I want to thank my family who has been the driving force to conclude this thesis. My mother, who has been worrying about the many hours of work and the quality of food I put in my stomach. Mom, I can finally admit that I did not have the courage to tell you half of it, not to worry you more. My sister, for inspiring and pushing me to achieve my dreams. My father, who is the reason why I am passionate with nature and its physical and mathematical interpretation. Father, I am so proud of you and so thankful. This thesis, every paper, every presentation, and every dream I have ever achieved (and hopefully will do in the future), is devoted to them.

There is one more person that I want to thank from the bottom of my heart - Prof. Ted Stathopoulos, my mentor, supervisor, and scientific father. We met in a crowded place in Athens for an interview in July 2019 and from that moment on he has supported me like family. He is most of all an amazing human and then an amazing and passionate mentor and researcher. He has always been there to help me and take my mind of things when research was too much to handle. Mr. Stathopoulos, thank you for giving the opportunity and tools to answer the questions I have had since I first encountered Wind Engineering.

I would also like to acknowledge the support from colleagues. Dear Murad, thank you for the endless talks. Dear Hatem and Natasha, thank you for the guidance and coffee breaks. Dear Jianhan, you are my first memory in the lab and our talks will always have a special place in my heart. Prof. Bert Blocken thank you for the constructive conversations that gave me new perspectives in my research. Prof. Alessio Ricci, thank you for the inspiring words and the trust in my work. Prof. Tominaga, thank you for your contribution as a co-author in our paper – it is a tremendous honor to collaborate with you and share thoughts and ideas. I have been so blessed to meet and discuss with all these amazing and passionate scientists.

During my stay in Montreal for the last 5 years I have encountered many people that I would like to thank for not only enduring but caring about me. Adamantia, Marco, Niz, Kris, Ale, Fede, Matteo, Claudio, Nathan, Gabri, Claudine, Kristina, Seb. You have all played a role in this achievement and I thank you individually for supporting me. Sarah, thank you for being the most beautiful human being I have encountered. I would also like to thank my second family that has always been there to listen and understand me, even from 7596 km far. Lou, Yianni, George, Marko, Yanno, Brouma thank you for reminding me who I am.

Contribution of Authors

This thesis includes material from two published peer review journal papers included in Chapters 2, and 4. The papers were co-authored with my supervisor Prof. Ted Stathopoulos, whose contribution was vital in terms of conceptualization, reviewing and editing. The paper in Chapter 2 was co-authored also with Prof. Yoshihide Tominaga, who contributed in great extent to the conceptualization, reviewing and editing. I am really grateful for their contributions.

There are a few things in a human's life that create inspiration and inspire creation due to lack of understanding.

For me all of those things revolve around piano and wind so I eagerly devote my freedom to them.

Here is the result.

TABLE OF CONTENTS

LIST OF FIGURES

LIST OF TABLES

NOMENCLATURE

Acronyms

ABL	Atmospheric Boundary Layer
AIJ	Architectural Institute of Japan
ASCE	American Society of Civil Engineers
CAD	Computer Aided Design
CFD	Computational Fluid Dynamics
CWE	Computational Wind Engineering
CWT	Concordia Wind Tunnel
DT	Dynamic Terrain
DNS	Direct Numerical Simulations
EVA	Extreme Value Analysis
GIS	Geographic Information Systems
HPC	High Performance Computing
LES	Large Eddy Simulation
LES-DT	Large Eddy Simulation – Dynamic Terrain
NBCC	National Building Code of Canada
NIST	National Institute of Standards and Technologies
NS	Navier-Stokes
MDSRFG	Modified Discretizing Synthetic Random Flow Generator

PDF	Probability Density Function
PoA	Percentage of Accuracy
PRMSE	Percentage of Root Mean Square Error
RANS	Reynolds Averaged Navier Stokes
RMS	Root Mean Square
SEI	Structural Engineering Institute
TPU	Tokyo Polytechnique University
UBL	Urban Boundary Layer
UCL	Urban Canopy Layer
URANS	Unsteady Reynolds Averaged Navier Stokes
V&V	Validation and Verification
WALE	Wall Adaptive Local Eddy viscosity

Latin letters

Cp	Pressure coefficient
f	Frequency (Hz)
f_c	Cut-off frequency of LES filter (Hz)
n_c	Normalised cut-off frequency of LES filter
H	Building height (m)
Iu	Turbulence intensity in the streamwise direction
t*	Normalised time

p	Pressure (Pa)
Re	Reynolds Number
S	Strain rate tensor (s^{-1})
u	Instantaneous wind velocity (m/s)
U	Mean wind velocity (m/s)
U_{ref}	Mean wind velocity at reference height (m/s)
v	Kinematic viscosity (m^2/s)
v_t	Turbulent kinematic viscosity (m^2/s)
Q	Q-criterion (s^{-2})

Greek letters

δ	Kronecker delta
Δ	Filter of LES
μ	Viscosity (kg/m·s)
ρ	Density (kg/m^3)
τ	Reynolds stress tensor
Φ	Convergence parameter

Subscripts

i	Streamwise direction (x-axis)

j	Lateral direction (y-axis)
k	Vertical direction (z-axis)
mean	Mean value
peak	Peak value
std	Standard deviation

CHAPTER 1: INTRODUCTION

1.1 Wind in the atmosphere of the globe

Wind is a natural expression of the physical existence of our globe. The atmosphere generates vast air masses at large heights with the purpose of keeping the temperature in an equilibrium state. As seen in Figure 1.1, three main regions of wind exchange areas are formed, from the equator until the north pole. As the air descends it interacts with the solid surface of the earth and macro and meso scales of the atmosphere are formed. The atmospheric boundary layer (ABL) that is created from this interaction and is found in the first 400 m ~ 800 m from the ground surface, is the scale of interest for the purposes of this thesis. In the present work, wind engineering is discussed and computational techniques that have been researched will be thoroughly explained and presented. For the sake of completeness, this chapter introduces the reader to the field of wind engineering and computational wind engineering in chronological order.

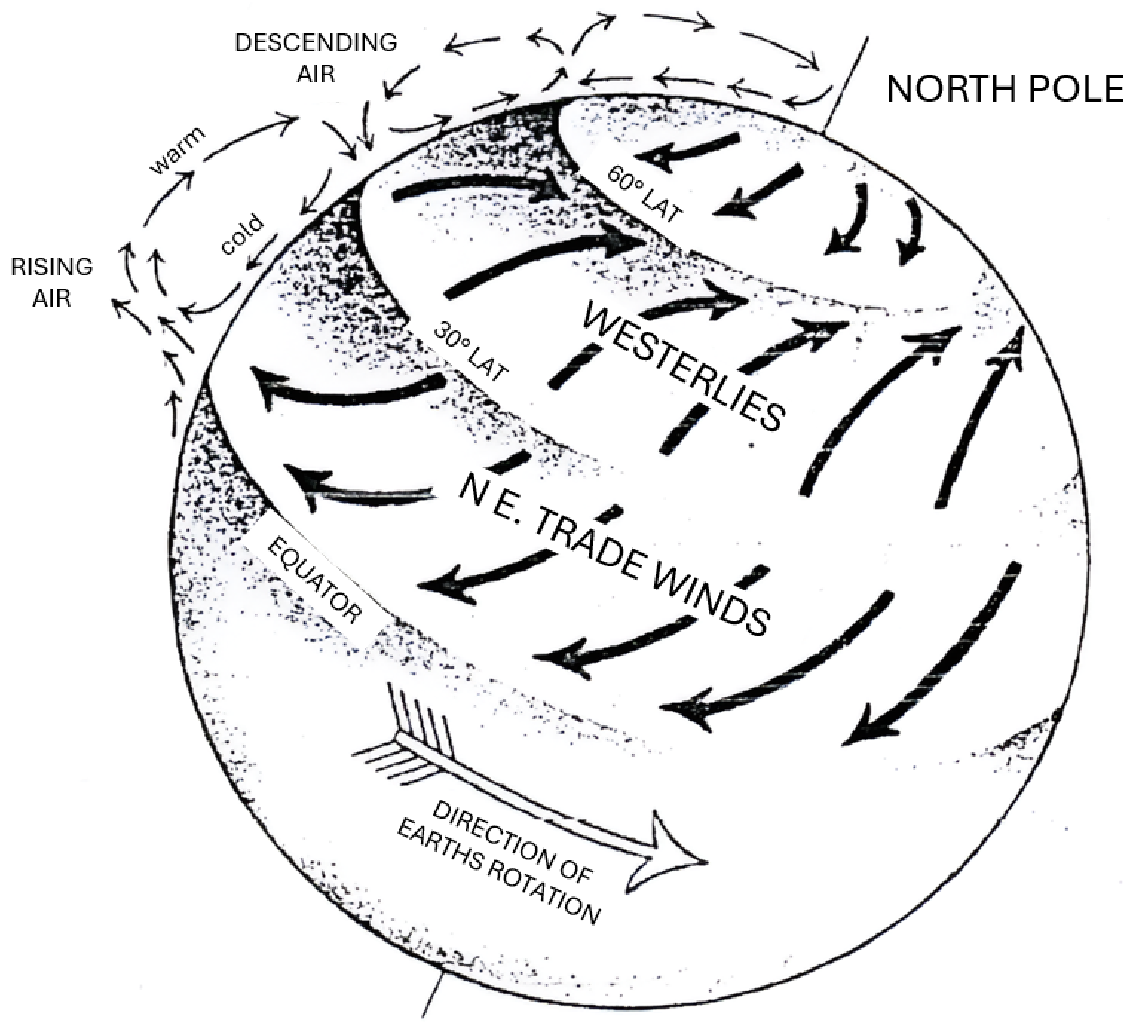

Figure 1.1: Air exchanges in the atmosphere of the globe (Stathopoulos T., 2020)

Throughout the years of economic prosperity and technological advancements of humanity, scientists have focused on a variety of subjects that target to expand the understanding of natural phenomena and their mathematical interpretations. The engineering realm exists between the boundaries of science and the applicability of theoretical and mathematical ideas. Observing the consequences of wind in the ABL early in the 19th century created the idea that wind should be understood in more detail, both for scientific and engineering reasons. For example, one of the first documented wind-induced disasters was reported in 1836 in Brighton Chain Pier, England. The engineer that created the sketches in Figure 1.2, tried to report the way that the bridge eventually "gave away" during a storm on 20 of November of that year.

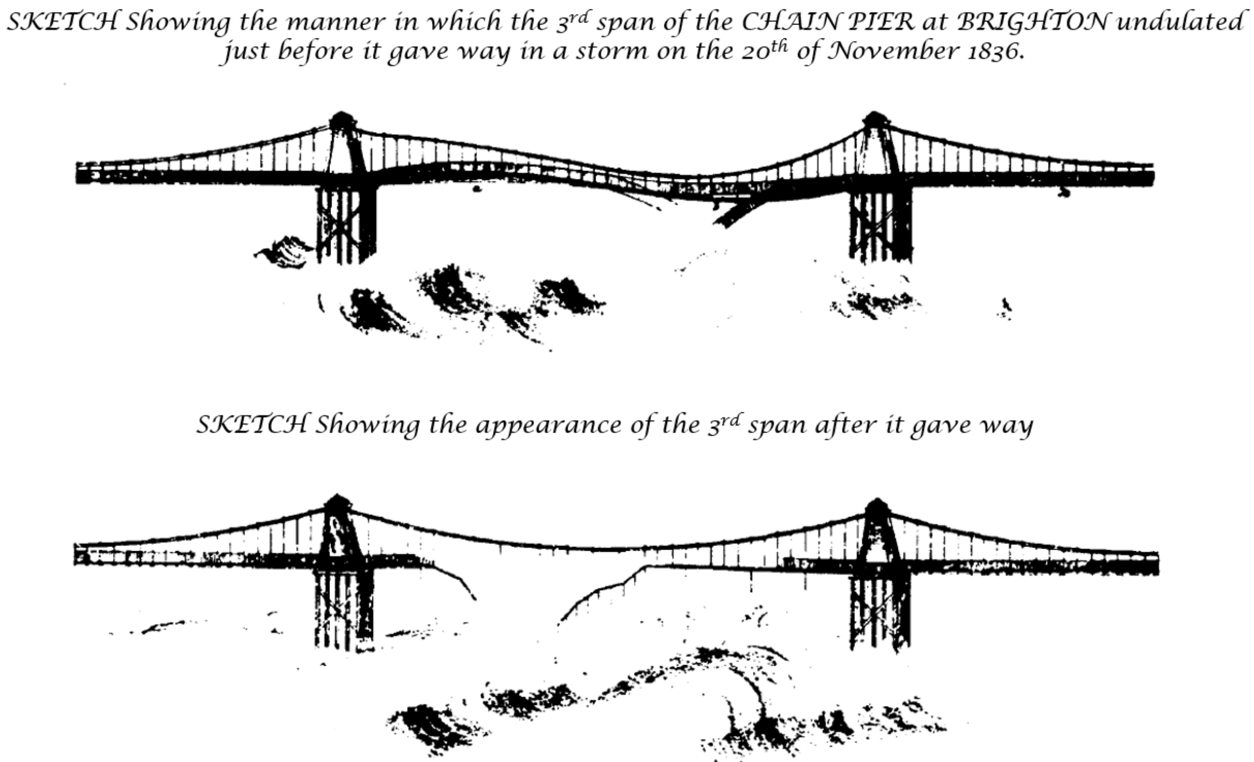

Figure 1.2: Sketch of the conditions under which the Brighton Chain Pier "gave way" (modified after Holmes J.D., 2003)

Similar events have been reported through the decades, but the formal definition of wind engineering was introduced by Cermak, 1975: "The rational treatment of the interaction between wind in the atmospheric boundary layer and humans and their works on the surface of Earth". The definition presented is a slight modification to the original one, in which the word "man" is found instead of a human, as to remove any gender-related bias. The main aspect that makes wind engineering a complicated field for research and applications is its multi-disciplinary nature. The fields that are combined refer to meteorological sciences, structural dynamics, statistics, probability theories, and fluid mechanics among others.

Meteorological sciences usually have the role of defining the wind regime in regions of the globe and providing important information regarding the velocities that are expected as close to the ABL as possible. Structural dynamics are another aspect of wind engineering, to understand the consequences of wind on structural systems and conclude a safe and economical design. Air is a fluid; thus, fluid mechanics also consists of an important field in wind engineering. Wind flow in the ABL can be categorized as incompressible turbulent flow and it should obey to the principal laws of fluid motion. The chaotic nature of high turbulence creates the need for statistical interpretation of results and many assumptions concerning probability theory.

It is interesting to see how wind engineering has combined these fields during the last decades to form an entirely new scientific and engineering path. Professor Alan G Davenport is considered the father of wind engineering since he was the first to document properly the interaction of wind and structures. One of the most signification contributions he made in wind engineering regards the wind loading chain that is presented in Figure 1.3. The theoretical concept of the wind loading chain is found - in one way or another – in all similar efforts by scientists that worked on wind engineering ever since. That is simply because it rationalizes the important parameters. The chain starts from the wind velocity time series in the natural wind that results in a force on the surface of a (structural) element, which creates a dynamic excitation/response. According to Davenport, the spectrum is the basis of formatting a correct representation of these quantities, as usually used in structural dynamics applications. For this reason, the aerodynamic admittance is the link between the velocity and the force spectrums, while the mechanical admittance is the link between the force and the response spectrum. Probability density functions are also of great importance for all three components, to ensure the level of confidence in each aspect and assumption.

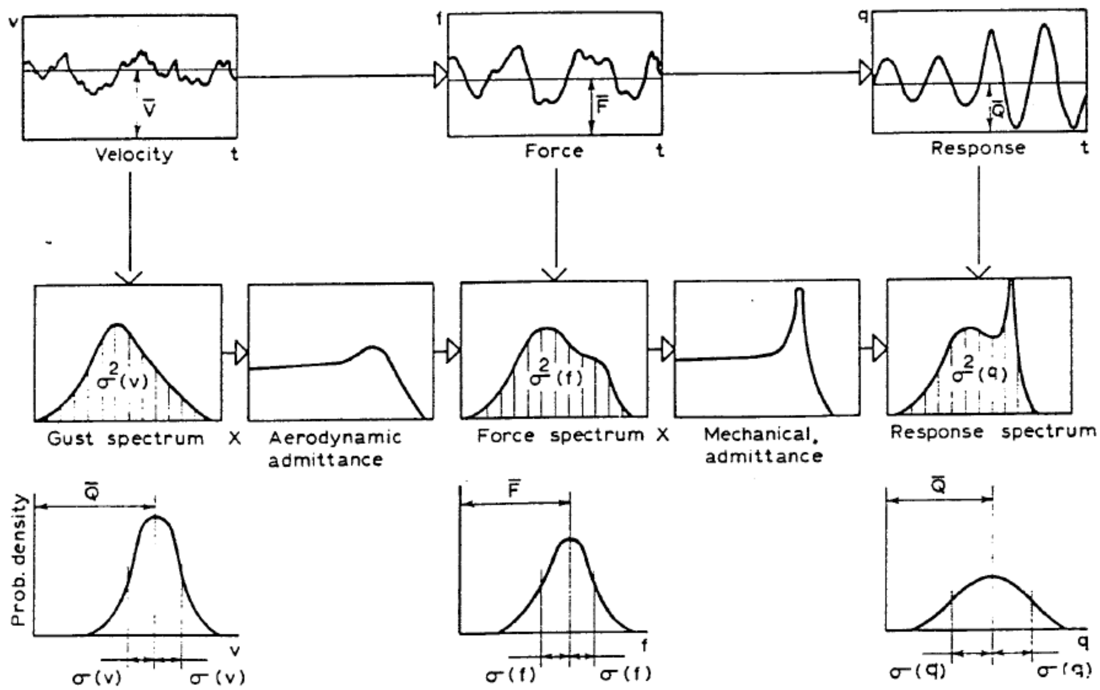

Figure 1.3: Wind loading chain (after Davenport. 1969)

This thesis focuses more on the first two parts of the Davenport chain. The scope is to be able to estimate wind velocities and their forces on solid obstacles, that refers to buildings, and not focus to their response. For this reason, the theoretical and mathematical tools that have been utilized focus more of fluid motion laws for incompressible turbulent flows. The physical values of interest refer to velocity and pressure.

1.2 Turbulent incompressible flow: theoretical and mathematical interpretation

Fluid mechanics theory has been developing since the 19th century, by some of the most competent scholars that science has ever known. The narrative of fluid mechanics from the authors' point of view, starts with Bernoulli's equation. It was the first conception of the physical correlation between the velocity of a fluid and the pressure generated in a free stream, laminar, and irrotational flow. The equation is presented in Equation 1.1. After that, the next step was understanding flows around bluff bodies, and the pressures created on solid surfaces. In turbulent (non-idealistic) conditions the pressure is expressed in Equation 1.2, where Cp is the pressure coefficient that depends on the characteristics of the bluff body and flow quantities.

$$P + 0.5 \cdot \rho \cdot U^2 = constant \qquad \textit{Equation 1.1}$$

$$C_p = \frac{p - p_{ref}}{0.5 \cdot \rho \cdot U^2} \qquad \textit{Equation 1.2}$$

To understand the outcome of the wind on a solid surface, first, a deeper understanding of the flow field is necessary. The first universal law that is assumed in fluid mechanics refers to the conservation of mass. Let us consider a control volume (c.v) of a fluid in a cartesian system with velocities u, v, and w at the direction x, y, and z, as displayed in Figure 1.4. For the mass to be conserved, Equation 1.3 can be derived. Adopting a Newtonian system means that not only mass is conserved but also momentum. This creates the momentum equations in Equation 1.4 for a three-dimensional flow. Accelerations out of the system (denoted as $\vec{a}$ in Figure 1.4) are assumed to be zero.

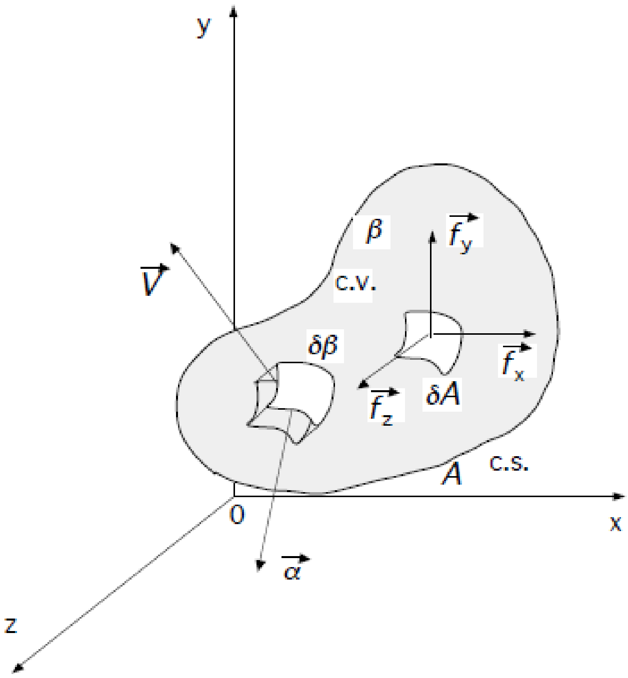

Figure 1.4: Control volume (c.v) of a fluid in incompressible flow conditions (Vatistas G.., 2020)

Conservation of mass *Equation 1.3*

$$\frac{\partial u}{\partial x}+\frac{\partial v}{\partial y}+\frac{\partial w}{\partial z}=\vec{\nabla}\cdot\vec{V}=0$$

x − momentum

$$\rho\left\{\frac{\partial u}{\partial t}+u\frac{\partial u}{\partial x}+v\frac{\partial u}{\partial y}+w\frac{\partial u}{\partial z}\right\}=-\frac{\partial p}{\partial x}+\mu\nabla^2 u$$

y − momentum

Equation 1.4

$$\rho\left\{\frac{\partial v}{\partial t}+u\frac{\partial v}{\partial x}+v\frac{\partial v}{\partial y}+w\frac{\partial v}{\partial z}\right\}=-\frac{\partial p}{\partial y}+\mu\nabla^2 v$$

z − momentum

$$\rho\left\{\frac{\partial w}{\partial t}+u\frac{\partial w}{\partial x}+v\frac{\partial w}{\partial y}+w\frac{\partial w}{\partial z}\right\}=-\frac{\partial p}{\partial z}+\mu\nabla^2 w$$

This set of equations are known as the Navier-Stokes (NS hereafter) equations and as can be seen they are second order non-linear partial differential equations. Immediately after generating this system of equations, it was understood that an analytical solution is not viable, thus numerical techniques were searched. It took about one century until computational resources became available, so the solution of this system of equations could be approximated.

1.3 Turbulent incompressible flow: numerical interpretation

There are two main approaches on how to numerically solve the NS equations. First, by assuming time averaging techniques such as, Reynolds Averaged Navier Stokes (RANS) and Unsteady Reynolds Averaged Navier Stokes (URANS) and second via spatial averaging such as Direct Numerical Simulation (DNS) and Large Eddy Simulation (LES). The first category is primarily used in environmental wind engineering applications, as further discussed in Section 2.2.1. This is due to the fact that time averaging techniques are unable to provide reliable information regarding instantaneous or peak velocity or pressure values in the NS system of equations.

Large-Eddy Simulation modeling process is complex since it depends explicitly on the exact solution, the computational grid and the numerical method, making each problem appear unique. Therefore, it is necessary to find some mathematical models for the Large-Eddy Simulation problem which will mimic its main features, the most important one being the removal of the small scales of the exact solution. A simplified heuristic view of this problem is illustrated in Figure 1.5 (Sagaut, 2006). As seen, the size of the mesh divides the resolved and the modelled eddies in physical (Δ) and Fourier space (k_c).

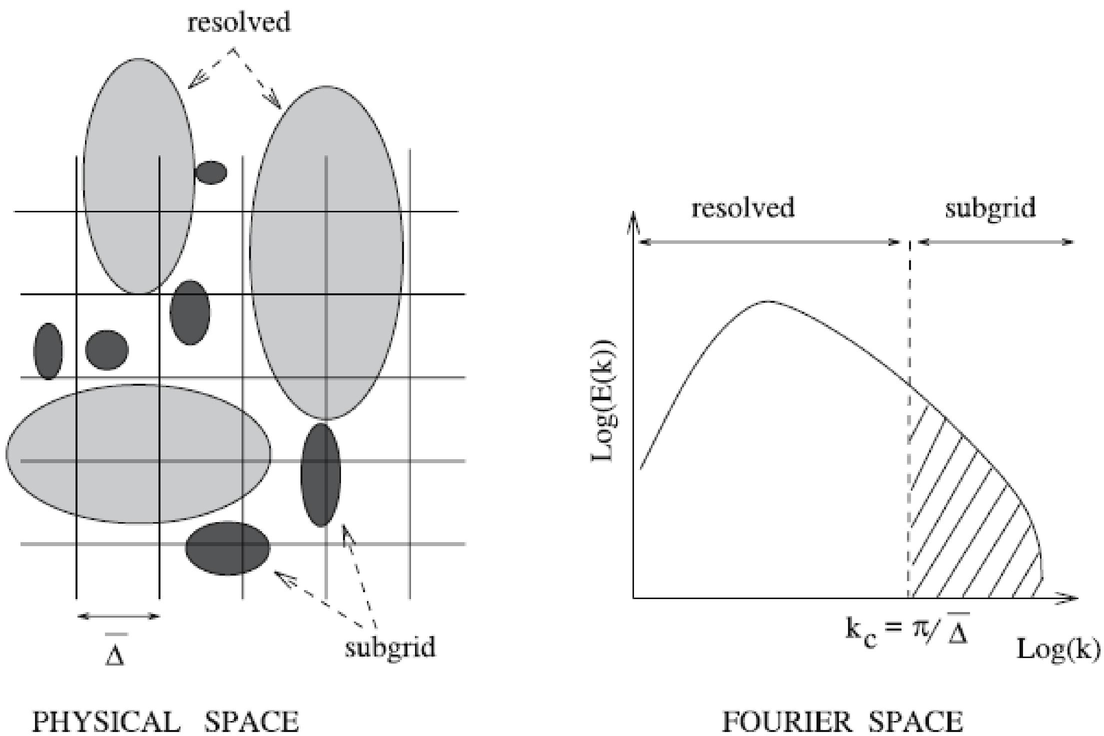

Figure 1.5: Schematic view of the simplest scale separation operator (Segaut, 2006)

Depending on the value of Δ and corresponding kc, a range of scales will be directly resolved, and the rest will be calculated by the subgrid model. If the cut-off limit is so small that it includes even the smallest scales of turbulence then the analysis is equivalent to a DNS, meaning that the kinematic viscosity will dissipate the energy entirely. If this is not possible, the unfiltered NS equations take the form presented in Equation 1.5 and Equation 1.6 using the Einstein notation. Using the filtered decomposition where its instantaneous value is equal to the summation of the filtered ($\overline{u_i} or \overline{p}$) and the subgrid ($\acute{u_i}$ or $\acute{p}$) contributions, the filtered NS can be extracted in Equation 1.7. On the left-hand side, first, there is the time dependent term, then the non-linear convected term, while on the right-hand side the pressure term, the molecular diffusion term and finally the Reynolds stress term. By virtue of Leonard's decomposition (Sagaut, 2006), this term can be modelled only based on the filtered values (Equation 1.8), thus there is no explicit need to calculate the subgrid contribution a priori during the computation. According to the Boussinesq approximation, similar to the molecular diffusion term, the Reynolds stresses (τij) in Equation 1.8, are equal to a viscosity constant multiplied by the shear strain rate Sij, as seen in Equation 1.9 and Equation 1.10. This constant is not the kinematic viscosity v, but the so-called eddy viscosity v_t. The term v_t is a numerical parameter to compensate for the fact that the dissipation of the energy can not be entirely due to the kinematic viscosity v, since the mesh is not as small as the smallest possible (Kolmogorov) scale. There are various ways to model this parameter, but the one selected as more efficient for this thesis is based on the Wall-Adaptive Local Eddy viscosity. The set of Equations that correspond to that are found in Equation 1.11, Equation 1.12 and Equation 1.13. The WALE model was selected since it behaves more efficiently than other models for boundary layer flows (Potsis and Stathopoulos, 2022).

Conservation of mass

$$\frac{\partial u_i}{\partial x_i} = 0 \qquad \textit{Equation 1.5}$$

Conservation of momentum

$$\frac{\partial u_i}{\partial t} + \frac{\partial}{\partial x_j}(u_i u_j) = -\frac{1}{\rho}\frac{\partial p}{\partial x_i} + v\frac{\partial}{\partial x_j}\left(\frac{\partial u_i}{\partial x_j} + \frac{\partial u_j}{\partial x_i}\right), i = 1,2,3 \qquad \textit{Equation 1.6}$$

Conservation of momentum - filtered

$$\frac{\partial \overline{u_i}}{\partial t} + \frac{\partial}{\partial x_j}(\overline{u_i}\,\overline{u_j}) = -\frac{1}{\rho}\frac{\partial \bar{p}}{\partial x_i} + v\frac{\partial}{\partial x_j}\left(\frac{\partial \overline{u_i}}{\partial x_j} + \frac{\partial \overline{u_j}}{\partial x_i}\right) - \frac{\partial \tau_{ij}}{\partial x_j} \qquad \textit{Equation 1.7}$$

$$\tau_{ij} = \overline{u_i u_j} - \overline{u_i}\,\overline{u_j} \qquad \textit{Equation 1.8}$$

$$\tau_{ij} - \frac{1}{3}\tau_{kk}\delta_{ij} = -2v_t\bar{S}_{ij}$$ *Equation 1.9*

$$\bar{S}_{ij} = \frac{1}{2}\left(\frac{\partial \bar{u}_i}{\partial x_j} + \frac{\partial \bar{u}_j}{\partial x_i}\right)$$ *Equation 1.10*

$$v_t = \left(C_W V^{1/3}\right)^2 \frac{\left(\mathcal{S}_{ij}^d \mathcal{S}_{ij}^d\right)^{3/2}}{\left(\bar{S}_{ij}\bar{S}_{ij}\right)^{5/2} + \left(\mathcal{S}_{ij}^d \mathcal{S}_{ij}^d\right)^{5/4}}$$ *Equation 1.11*

$$\mathcal{S}_{ij}^d = \frac{1}{2}\left(\bar{g}_{ij}^2 + \bar{g}_{ij}^2\right) - \frac{1}{2}\delta_{ij}\bar{g}_{kk}^2$$ *Equation 1.12*

$$\bar{g}_{ij} = \frac{\partial \bar{u}_i}{\partial x_j}, \bar{g}_{ij}^2 = \bar{g}_{ik}\bar{g}_{kj}$$ *Equation 1.13*

1.4 Motivation of thesis

From the above numerical interpretation of the NS system of equations, it becomes evident that the mesh size will dictate the accuracy of LES. Based on Choin and Moin, (1976) the mesh size should follow specific guidelines to conduct accurate LES and depend on the Reynolds number. Given that the wind flows in the ABL are accompanied by large Reynolds numbers, the mesh needed to conduct traditional LES is very small, which leads to a huge computational burden. Besides that, the mesh for DNS is even smaller and it would be impossible to solve even with the most advanced High-Performance Computers available. This forced the field of computational wind engineering to search for different modeling techniques and ways to reduce the computational necessities.

This is the main issue that the thesis is addressing – numerical means to optimize the balance between computational efficiency, complexity, and accuracy in LES. All this from the scope of engineering applications that target to model wind flow in the ABL, and wind induced structural loads. Low buildings have been selected as the ideal structures for the case studies in the thesis, due to the fact that they interact with higher turbulence near the ground. Because of that, the flow field has a strong three-dimensional character in contrast to high-rise buildings, where the flow field tends to be more two-dimensional. This makes the flow field and wind induced pressures more random and complicated to model computationally, creating a research gap in the current state-of-the-art. To close this research gap and address the issue at hand a novel inflow generation methodology has been researched and developed for this thesis – the so-called Dynamic Terrain method.

1.5 Structure of thesis

The thesis presented hereafter includes material from published papers and traditional chapters that link the trajectory of research to make it more concise.

In **Chapter 2** the findings in Potsis et al.., (2023) are partially presented which refer to the advancements of computational wind engineering for structural applications since its formal birth in 1992. This Chapter acts as the basis of the literature review and defines the state-of-the-art and research gaps that the thesis is based on.

In **Chapter 3** focus is given to engineering needs and the computational targets of computational wind engineering for structural applications. It is a traditional thesis chapter and acts as a connecting link.

In **Chapter 4**, is based on the published paper Potsis and Stathopoulos, (2024). The so-called Dynamic Terrain method via LES (LES-DT) is presented. Two validation studies are found in this chapter and comparisons with other state-of-the-art tools.

In **Chapter 5** the open database that relates to Chapter 4 is discussed with guidelines and further applications on its validation. It consists of two more validation studies, and it is a traditional thesis chapter. Further documentation of the open database is found in **Appendix A**.

Finally, in **Chapter 6** the main findings and conclusions of the thesis are presented and in **Chapter 7** some future perspectives are discussed.

CHAPTER 2: STATE-OF-THE-ART: CWE FOR WIND INDUCED LOADS

This chapter summarises the progress of the CWE field since its formal birth in 1992. It is based on material from Potsis et al.., (2023). Some modifications of the published paper were made for uniformity reasons.

2.1. Introduction

Following the pioneering Computational Wind Engineering conference in Tokyo in 1992 (CWE92) organized by Prof. Shuzo Murakami, the so-called father of Computational Wind Engineering (CWE), the use of Computational Fluid Dynamics (CFD) has rapidly expanded in both scientific research and practical applications. This is due, first, to the improvement of computational power, which has made it possible to perform large-demand calculations in less time. Second, the spread of commercial and open-source CFD codes has lowered the barriers to entry into these topics for the users and made it easier to cooperate with other software such as computer aided design (CAD) and geographic information systems (GIS).

As stated in the definition of wind engineering (Cermak, 1975), the chaotic nature of the wind flow can be translated in physical terms by the large range of length and time scales, in which the various vortexes fluctuate and interact with each other and solid surfaces. The computational and analytical understanding of this interaction with humans and their works in the atmospheric boundary layer

(ABL) has been the subject of research of CWE since 1992, for environmental and structural applications in building engineering. Depicting the interaction of this wide range of scales in the CFD environment has proven challenging, although important milestones have already been reached.

There have been many excellent review papers on CWE so far (Murakami, 1990; Murakami, 1993; Murakami, 1997; Stathopoulos, 1997; 2002; Tamura 1999; Mochida et al., 2008; Tamura, 2008; Mochida et al., 2011; Fernando et al., 2010; Fernando, 2010; Barlow, 2013; 2014; Blocken, 2014; Blocken 2015; Daniels and Xie, 2022). Murakami (1990) first presented the concept of CWE and reviewed its state of the art. Murakami (1997) outlined the difficulties in modeling wind flows in the atmosphere with CFD, compared various turbulence models and concluded that Large Eddy Simulation (LES) will focus the attention of researchers in the future of CWE. Stathopoulos (1997) compared various computational assumptions and corresponding results regarding structural loads on building envelopes and concluded that the imminent future target should be to express correct the turbulent features and that CFD and experiments should be run in parallel, but the final decision of design must be based on the latter. Tamura (1999) discussed various CFD techniques for the aeroelastic behavior of cylinder type-structures and concluded that their reliability is sufficient. Tamura (2008) revised the status of the field in terms of wind effects on buildings, velocities affected by a 3D hill, wind configuration in cities, environmental applications, and combined methods with meso-scale meteorological models. As conclusions, the study mentioned the problems in estimating peak forces on building envelopes, gust velocities in various terrains and concentration fluctuation in the dispersion of hazardous gases. Also, the study concluded that LES is expected to be free from the wind tunnel techniques and be introduced as an independent and powerful tool. Fernando (2010) reviewed the dynamics of airflows intrinsic to urban areas in complex terrain by employing idealized flow configurations to illustrate fundamental processes. Barlow (2014) reviewed the progress made in studies of the urban boundary layer (UBL) in terms of a conceptual framework spanning microscale to mesoscale determinations of UBL structure and evolution. Blocken (2014) extensively reviewed the CWE development from the perspective of a 50-year anniversary. Daniels and Xie (2022) conducted an overview of LES applications on slender structures with focus on inflow generation methods for isolated high-rise buildings and bridge decks. The improvement of the numerical methods in the last decade for these applications is clear, although the authors mention the increasing need for best practice guidelines with LES and the necessity of experiments to validate/complement numerical results.

In most of these review papers, it is not explicitly distinguished whether CFD was applied to structural or environmental problems, or only one aspect was addressed. However, the requirements of practical use of CFD in the environmental field and those in the structural field are very different. In the case of environmental problems, most of the required information about the wind flow can be obtained from the time-averaged quantities, whereas in the case of structural problems, time-averaged values alone are not sufficient, and information on instantaneous (peak) values is often indispensable. This directly leads to the choice of turbulence modelling approach as discussed later.

On the other hand, recent advances in computing power are removing the barriers between the environmental and structural methodologies. Therefore, the authors believe that discussing structural and environmental issues separately is not beneficial for the further development of

CWE; rather, the time has come to integrate the findings of both. Although this integration is important, this Chapter reviews in more detail the progress of CWE from the perspective of structural problems and attempts to discuss the direction of future development. Interested readers for environmental applications of CWE are referred to Potsis et al.., (2023).

The following subsection summarizes the overview of progress depending on the turbulence model, ABL modeling and inflow generation techniques and verification, validation and best practice guidelines. Next, in Section 2.3, some of the key research efforts on structural computational wind engineering applications are discussed. In Section 2.4, some future perspectives are discussed, and on 2.5 the Chapter is summarized and some conclusions are drawn.

2.2 Overview of Progress in Computational Approaches and Methodologies

2.2.1 Choice of turbulence models

Since the beginning of CWE, one of the main concerns for researchers has been the appropriate choice of turbulence models. It is necessary to understand the characteristics and limitations of each turbulence model before selecting an appropriate one. Direct Numerical Simulation (DNS) that solves Navier-Stokes (N-S) equations (Equation 1.3 and Equation 1.4) directly, is the most accurate approach; however, its computational burden is unreachable, even from the most modern High-Performance Computing clusters. Therefore, two paths can be chosen based on the averaging technique that is implemented into the system: Reynolds (Ensemble)-averaging and spatial-averaging. A modeling approach that solves Reynolds-averaged N-S equations is called RANS (Reynolds-Averaged N-S equations) model. The term of time in the equations is switched off, leading to a steady-state analysis (steady RANS), but when the term is switched on, unsteady analyses (unsteady RANS) are carried out. Since the Reynolds' stresses appear as new unknowns when applying Reynolds-averaging to the N-S equations, various models have been proposed to close the system of equations as the so-called 'turbulence closure' (Ferziger and Peric, 2002; Versteeg and Malalasekera, 2007). Although the two-equation models such as k-ε and k-ω are well-known for this modeling approach, many variations exist in a hierarchical manner.

One modeling approach that solves grid size-averaged N-S equations by filtering techniques is called LES. The mesh size is used as a filter to distinguish large and sub-grid scale (SGS) eddies: the latter are modeled, whereas the former is directly solved. SGS models are divided into eddy viscosity models and velocity gradient models. Amongst the eddy viscosity the most used ones are the constant-coefficient Smagorinsky model (Smagorinsky, 1963) and the dynamic Smagorinsky (Germano et al., 1991). In the velocity gradient models, the Wall Adaptive Local Eddy-viscosity (WALE) model (Nicoud and Ducros, 1999) has been implemented in many works referenced in this Chapter and its numerical interpretation can be found in Chapter 1 of the thesis.

Starting with the work of Murakami et al. (1990), comparisons between LES and RANS have been made on various subjects (e.g. Murakami et al., 1992; Murakami, 1993; Murakami et al., 1996; Rodi, 1997; Cheng et al., 2003; Tominaga et al., 2008a; Blocken et al., 2011; Caciolo et al., 2012; Chew et al., 2018; Blocken, 2018; Zhang et al., 2020; Vita et al., 2020). RANS equations model all turbulent fluctuations; therefore, it provides only ensemble-averaged values, which are usually time-averaged, but it is simple to use, computationally affordable, and economical (Hanjalic, 2005). On the other hand, LES models only the fluctuations smaller than the grid scale, thus the spatial and temporal resolutions must be very fine, resulting in high computational cost (e.g. Blocken, 2015). Of course, LES has the advantage of obtaining instantaneous values of pressure and velocity because it directly calculates wind velocity fluctuations. This is essential with respect to its application to structural problems. It should be noted, however, that even in predicting the mean flow field, RANS, especially steady-RANS, have some shortcomings: the RANS tends to predict a wider and stronger recirculation flow in the wake region behind the building, although it gives relatively good predictions for the strong velocity region. This is because the steady-RANS cannot predict large-scale unsteady fluctuations such as the Karman vortex, therefore underestimates the momentum mixing behind buildings (Tominaga et al., 2008a). This shortcoming in the mean flow prediction by steady-RANS for the weak velocity region has been recognized. Numerous examples of investigating the impacts of turbulence models in RANS simulations have been reported for a variety of flow fields (e.g. Mochida et al., 2002; Tominaga and Stathopoulos, 2009; Elkhoury, 2016; Moen et al., 2019). Calibration of the coefficients in the RANS turbulence models has also been proposed (e.g. Guillas et al., 2014; Gimenez and Bre, 2019; Shirzadi et al., 2020c). However, the current consensus is that individual sensitivity studies are necessary because it is difficult to generalize these results to various types of flow fields.

2.2.2 Modeling of atmospheric boundary layers (ABL) - Turbulence inflow conditions

In the lower atmosphere abutting Earth's surface, heat, momentum, and mass fluxes are controlled by the ground, i.e., by the ABL. Factitious elements and anthropogenic forcing cause the ABL over urban areas, called the UBL (Fernando, 2010). Buildings and other components within urban areas form an urban canopy layer (UCL). Figure 2.1 illustrates these names and relationships. The modeling and parameterization over these boundary layers have been comprehensively reviewed in Fernando et al. (2010), Fernando (2010), and Barlow (2013; 2014). In many CWE applications, the UCL is resolved and simulated directly, while the properties of ABL and UBL are set as boundary conditions. Needless to say, when reproducing various environmental and structural phenomena occurring at the building scale, it is important to accurately predict the ABL and UBL at larger scales. In addition, the UCLs of areas outside of the analyzed area must be properly modeled. Barlow (2014) suggested the structure is determined not only by urban surface characteristics but also by mesoscale thermal circulations, referring to a scale of 10–100 km, and by day with weak synoptic forcing (i.e., low wind, sunny conditions) buoyant up-draughts over the hotter urban surface can induce an urban thermal circulation. That is to say, the appropriate modeling of ABL/UBL/UCL can be the groundwork to accurately model winds on flat terrains as well as on complex areas for a large spectrum of topics in CWE. Meteorological research dealing with ABL/UBL/UCL and engineering research dealing directly with the building scales have developed separately, but the barriers between the two research fields have become smaller. Some studies of coupling micro-scale CFD with mesoscale analysis using regional scale models have been reported. It is expected that research results from different research fields will be cross-referenced and revitalized in the future.

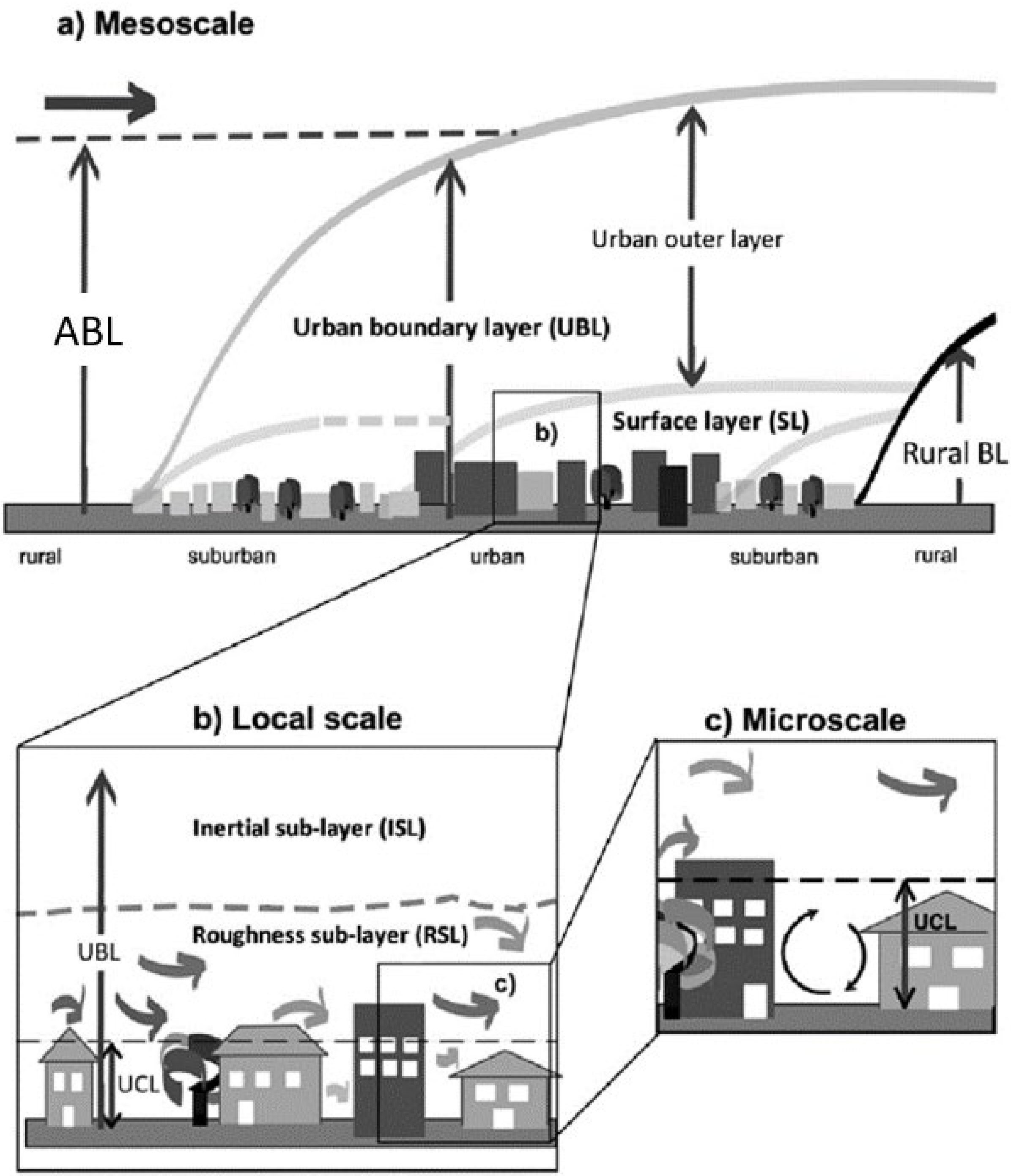

Figure 2.1. Sketch of the urban boundary-layer structure indicating the various sub-layers and their names (from Rotach et al. 2005; modified after Oke 1987, Piringer et al., 2007).

The traditional modeling of ABL or UBL in wind engineering has been based on the power or logarithmic laws of the mean wind speed profiles both experimentally and numerically (Davenport, 1960). One of the major changes since 1992 is the gained attention to the horizontal homogeneity of the ABL over the computational domain in CWE simulations. Richards and Hoxey (1993) first pointed out that the inflow boundary condition and the turbulence model should be consistent for homogeneous boundary layer flow. Later, Blocken et al. (2007) clarified the relationship between the sand-grain roughness wall functions and the horizontal homogeneity, and these findings has been extended and sophisticated by the several follow-up studies (Yang et al., 2009; Gorlé et al., 2009; Richards and Norris, 2011; Parente et al., 2011).

Although the above investigations were considered for RANS, the setting of inflow boundary conditions for LES are even more challenging because of the need to provide fluctuating velocity field varying in time and space. These difficulties turned the attention of the community to the inlet conditions in the last decades since they are directly related to reducing computational effort while achieving accurate results for the velocity and pressure distributions. In the paper of Lund (1998) the recycling techniques were first introduced, based on a precursor analysis in an empty computational domain, where the flow recirculates from inlet to outlet, until the target statistics are achieved. The time series of the velocity field are extracted from a plane and re-introduced as inlet conditions in the main analysis, where the building resides. This technique provided essential information to the field regarding the difficulties in capturing the appropriate fluctuating field by recirculating the flow. These findings defined dramatically the trajectory of the subsequent research since many works have attempted to solve these issues and used recycling methods as a benchmark. At the same time, attention was turned into synthetic methods to define the inlet boundary and the necessary velocity fluctuations, as to overcome the problems of generalizing the recycling approach. The Random Flow Generator (RFG) technique was the first introducing the concept of synthetic turbulence generation (Kondo et al., 1997). In this case a summation of sinusoidal waves with a range of amplitudes, frequencies and phase shifts is used to generate the velocity time series. Great improvements of this method were achieved afterwards by introducing the correct spectral representation at the inlet plane, making it appropriate for ABL flows (Smirnov et al., 2001, Castro and Paz, 2013, Aboshosha et al., 2015b, Yu et al., 2018, Patruno and Ricci, 2018, Bervida et al., 2020 and Melaku and Bitsuamlak, 2021). Another technique was proposed by super-positioning natural vortices into the mean velocity (Jarrin et al., 2006). Results of the method indicated that although the velocity statistics are achieved, the pressure fluctuations on the building envelope were unphysical until a divergent-free criterion was included (Poletto et al., 2013, Yan and Li, 2015). The method was further improved by introducing the multi-scale eddy approach (Luo et al., 2017). Also, Digital Filtering methods were investigated in order to synthetically generate turbulence (Klein et al. 2003). The principal work is to filter random data and superimpose them on the mean values of the flow field. The methodology was later improved by introducing mass flow correction and divergent free condition (Kim et al., 2013); assumptions that were further investigated later by Patruno and de Miranda (2020). Further discussion regarding inflow turbulence generation methods can be found in Dhamankar et al.., (2018) and Potsis and Stathopoulos, (2022).

2.2.3 Verification, validation, and best practice guidelines

Since 1992, the recognition that the verification and validation processes are prerequisites for CFD simulations has propagated. The fundamental strategy of verification relies on the identification and quantification of the error in the computational model and its solutions. On the other hand, the fundamental strategy of validation is to assess how accurately the computational results compare with the experimental data, with quantified error and uncertainty estimates for both (Oberkampf and Trucano, 2002; Oberkampf et al., 2004). In other words, validation is the process of determining the degree to which a model accurately represents the real world regarding the intended uses of the model (AIAA, 1998). In order to perform high-quality validations and uncertainty evaluations of CFD simulations, reliable experimental data are indispensable. Moreover, it should be noted that the validation of LES results is not as straightforward as that for models based on RANS, as addressed by Harms et al. (2011). For LES, validation procedures are complicated because comparisons must be based not only on mean quantities but also on the frequency distributions of statistically representative ensembles of results. Hertwig et al. (2011) proposed and applied a novel validation strategy for LES, consisting of a multilevel hierarchy of comparative analysis methods, in which not only low-order statistical moments but also higher-order eddy statistics and structural turbulence information are compared.

Since 1992, quantitative evaluation of CFD performance using validation metrics has become established (Robins et al., 2000; Schatzmann et al., 2010; Di Sabatino et al., 2011). In order to perform such quantitative evaluations, reliable and high-resolution measurement results are required. In that sense, an advance is the availability of open database of experimental results for benchmark cases for CFD validation. In the environmental field, there are database by AIJ (Yoshie et al., 2007; Architectural Institute of Japan, 2016) and the university of Hamburg (CEDVAL, 2006). In the structural field, databases generated by the University of Western Ontario (NIST, 2003) and Tokyo Polytechnic University (TPU, 2013) are available. For more general industrial applications, QNET-CFD, which was developed under the European Union R&D program, is available (Hirsch, 2006). It would be important to disclose the measurement database, by including details such as experimental conditions and measurement uncertainty.

Regarding structural applications, standardized procedures via LES have been proposed in terms of benchmarking pressures on building envelopes of low- and high-rise structures. The first endeavor (Tamura et al., 2008) is based on the procedures and findings of Nozawa et al. (2002) and Nozawa (2003). Lately, a standard CFD procedure was proposed (Thordal et al., 2020 a, b) for the CAARC high-rise building, based on the digital wind tunnel approach. Results regarding the peak structural response were improved when compared with previous practical proposals by Elshaer et al. (2016) and Ricci et al. (2018). It is worth noting that the state-of-the-art lacks a generalized procedure for peak load estimation in computational domains that respects the limits of computational resources and complexity for practical use. Therefore, design for wind loads via CFD is not permitted in most code provisions worldwide. On the other hand, results from applications of practical guidelines of CFD can be included in the final design decisions for environmental problems. The topic of validation and verification for structural applications in CWE is further explored in Section 3.3.

2.3. Structural Wind Engineering

Structural wind Engineering from a computational perspective regards the use of CFD to calculate the mean and fluctuating pressures on envelopes in order to carry out the final design. The lateral force-resisting system should be checked by means of dynamic or static procedures and the limit states of design should be acceptable according to each case. Since 1992, the field has reached some very important milestones that are worth referring to. The most seminal works introduced new features in the procedure to calculate the mean and statistical moments for the fluctuating pressures. Step by step after each of these works various benchmarks were established that were used for the evolution of the state-of-the-art. Although the main topic of this thesis is low buildings it is very important to discuss the applications in high buildings as well in the state-of-the-art, thus in this subsection focus is placed both on low and high buildings and wind directionality.

2.3.1 Low rise buildings

Initially, focus was given to capturing the essential characteristics of the flow and the consequence pressures in terms of the mean values, mainly using low-rise structures as benchmarks. Few works mention fluctuating values of the pressure regime. A computational study was concluded at the beginning of the first decade, to calculate the pressures on an L-shaped building, with the k-ε model by using steady-RANS (Stathopoulos and Zhou, 1993). When comparing mean pressures on the symmetry line of the roof for an oblique wind direction of 30°, the results were considered representative, in the same way as the previous studies. But, when comparing pressures at the edge of the roof, the results were unacceptable, as can be seen in Figure 2.2. This observation proves that near the points of separation, the mean flow character needs special treatment, especially on the roof of low-rise structures and that the comparisons should regard corner zones and oblique wind directions. This study can be considered as a starting point to demonstrate how the field has progressed since 1992. Two years later, roof pressures were evaluated by using the steady-RANS, with a comprehensive grid size parametric study (Stathopoulos and Zhou, 1995). Results indicate the sensitivity of the grid size to capture the essential flow features and the limited ability of steady-

RANS to capture the main pressure regime on the roof, as the height of the building increases and the wind direction becomes oblique.

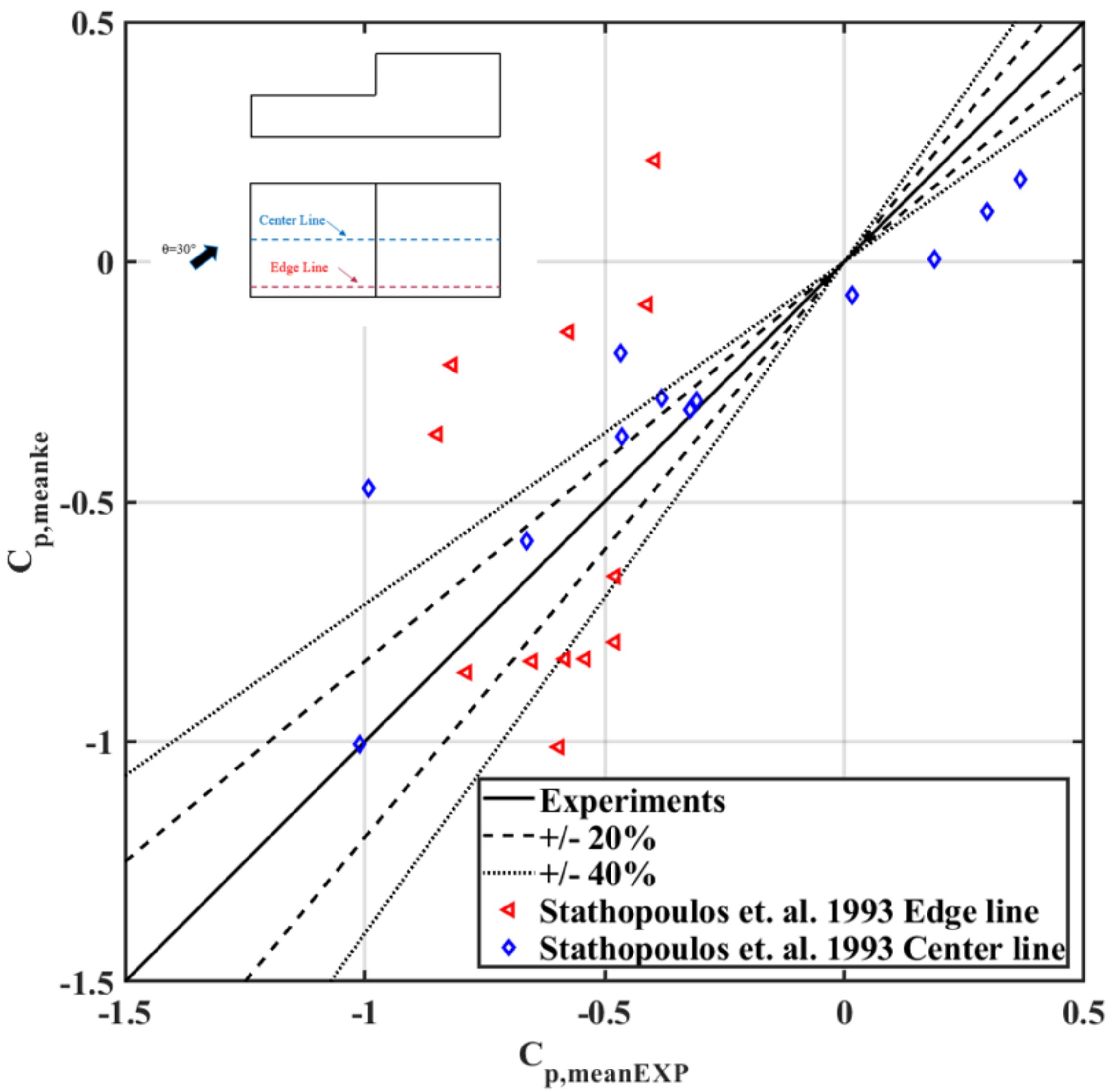

Figure 2.2: Correlation of mean pressure coefficient between experiments and k-ε model results, along the center and edge line of a stepped roof building for wind direction of 30 degrees (Stathopoulos and Zhou, 1993)

The Texas Tech University (TTU) model has been thoroughly represented in computational domains during all three decades, with great accuracy for the mean values from early on (Mochida et al., 1993, Selvam, 1997). Richards and Hoxey (1992) noticed that the errors between full-scale and experimental results have the same range as the ones between full-scale and CFD techniques for the mean pressure coefficients when the k-ε model is used. Similar accuracy was accomplished by studies of that decade (Delaunay et al., 1995, Murakami et al., 1992) for a cube structure. After these works, a very valuable conclusion was reached; by using the minimized computational effort of the steady-RANS approach with the k-ε models, the mean values of the pressures were evaluated accurately. The mean conditions of the pressure field were captured in all the works presented for the center line, except maybe some points on the roof where the separation occurs (Murakami, 1993; Tsuchiya et al., 1997). Although, this achievement is of relatively small importance when design conditions are sought.

The final target of structural computational wind engineering is to calculate the fluctuating nature of the pressure regime to evaluate the peak (design) values. In order to achieve that, the statistical moments of these pressure coefficients started to be investigated, with more gravity given to the second-order statistics, the root mean square (rms). Very quickly the community realized that this is impossible to be achieved by modeling the turbulence features using the averaging techniques of steady or unsteady RANS with the k-ε models. Particularly since the results are extremely sensitive to the averaging times selected and can be manipulated according to each case. The research trajectory focused on LES and the imminent target became improving the mean values and capturing the fluctuating features of the pressure regime.

One more benchmark was reached in the first decade, which was of great importance and defined to a great extent the trajectory of the coming research. This refers to the incoming turbulent statistics of the flow field and the inlet conditions that are applied in the computational domain where the structure resides. In the latest review of the field (Stathopoulos, 1997), this concluding remark is presented. The target is to express as accurately as possible the vertical distribution of the velocity statistics at the location of interest, to enhance the pressure fluctuations in the building envelope, and match the physical conditions measured in wind tunnels. With the work of Lund (1998), the recycling techniques were established and used for the prediction of the fluctuating pressures for a low-rise building with aspect ratios of 1:1:0.5 (Nozawa and Tamura, 2002). Results regarding the mean pressure coefficient do not provide any strong variation when compared with similar work where smooth steady flow inlet conditions were assumed (Tamura, 1997), but the rms distribution was finally introduced accurately.

Although there are certain advantages in recycling methods for the inlet conditions, attention was turned to synthetic methods for the generation of the velocity time series, since they provide better control regarding the turbulence length and time scales, and their corresponding spatial evolution in the domain. In 1997 it was the first endeavor in this respect (Kondo et al., 1997) and quickly more focus was given to improving the existing methods and creating new ones. As synthetic techniques developed rapidly through the years, studies dealt with fluctuating pressure values in cubes (Irtaza et al., 2013, Richards and Norris, 2015, Ong et al., 2020, and Papp et al., 2021). For the mean values of the pressure coefficient, the symmetry line was used, and the results are presented in Figure 2.3. The grey area represents the range of values as extracted from experiments and full-scale data found. Improvements were found when comparing k-ε with LES, especially near the corner region of the roof and the windward side. The various assumptions of each study that uses LES seem to play a negligible role in the mean pressure coefficient on the leeward side.

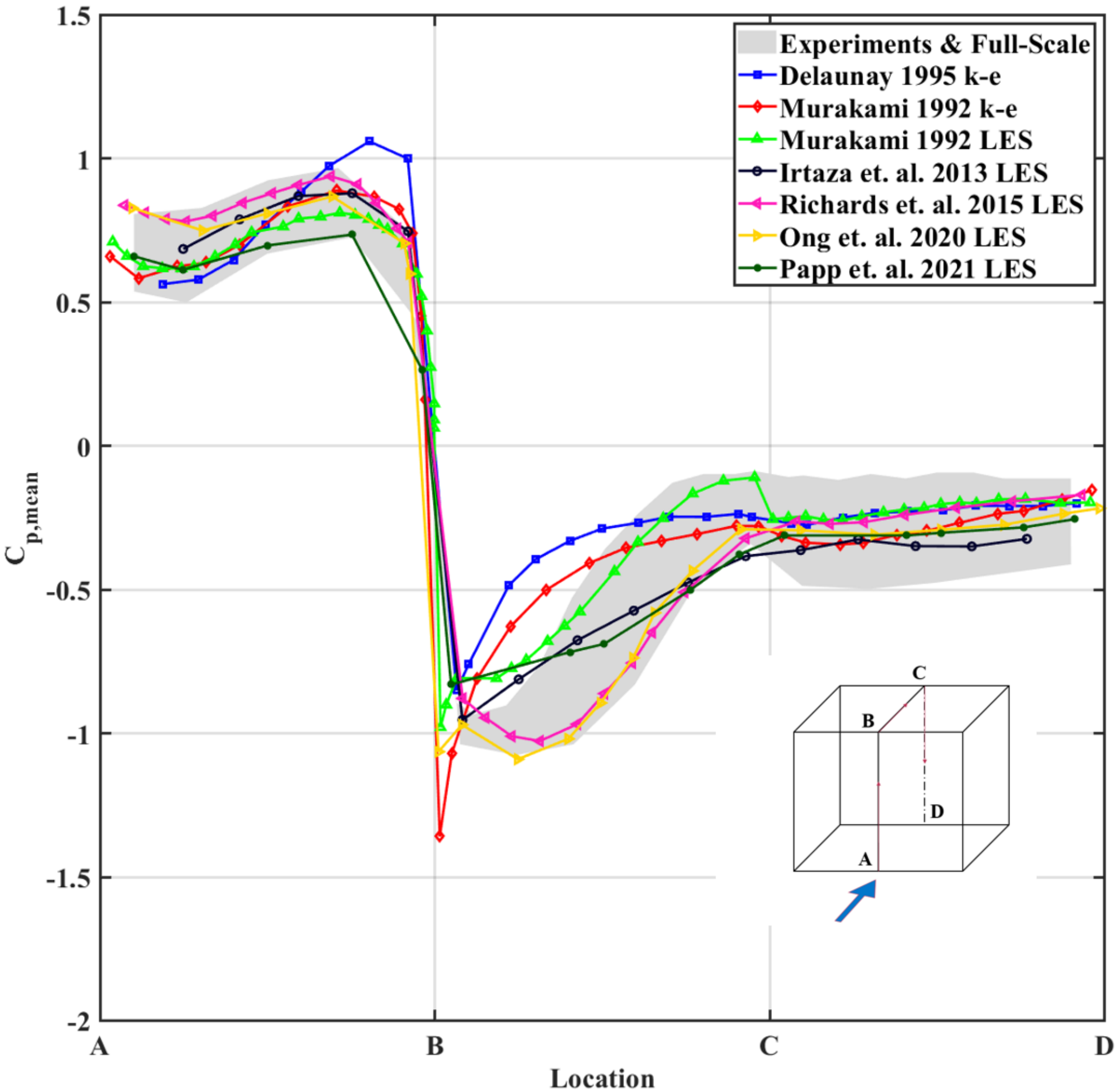

Figure 2.3: Mean pressure coefficient for wind perpendicular to AB for a cube (Delaunay, 1995, Murakami, 1992, Irtaza et al., 2013, Richards et al., 2015, Ong et al., 2020, Papp et al., 2021).

Regarding the distribution of rms, Figure 2.4 displays the correlation between the LES results and the experimental and full-scale values. Each result was correlated with the target experiments on which the study was based. Comparisons with full-scale data proved to be at the same level of accuracy (Richards and Norris, 2015 and Guichard, 2019). Despite the various inlet conditions used by these studies, most of their results have less than 20% error. Focusing on low-rise structures with different aspect ratios, valuable data are found in Nozawa and Tamura (2002) and the work of Ricci et al. (2017) which are also presented in Figure 2.4. It is important to notice that the low-rise structure with aspect ratios 1:1:0.5 was proposed as a benchmark for the establishment of AIJ CFD provisions (Tamura et al., 2008). The evolution of the accuracy is evident, although, in a small percentage, vis-à-vis the rms prediction of LES has not seen significant improvements in the last two decades for low-rise building design. Similar comparisons in non-symmetry lines are limited and more focus should be given in the future on this field, to assess whether these methods can capture the pressure regime in the entire building envelope.

High length scales of turbulence interact with low-rise buildings; these scales might be further augmented when the actual surroundings are also modelled. For example, the influence of neighboring structures in the pressure regime has been investigated for a low-rise cube with a hybrid RANS-LES approach (Gough et al., 2019). Comparisons were conducted with full-scale and wind tunnel data. The difficulty in capturing the mean pressures with the inclusion of the neighboring structures is evident in the results.

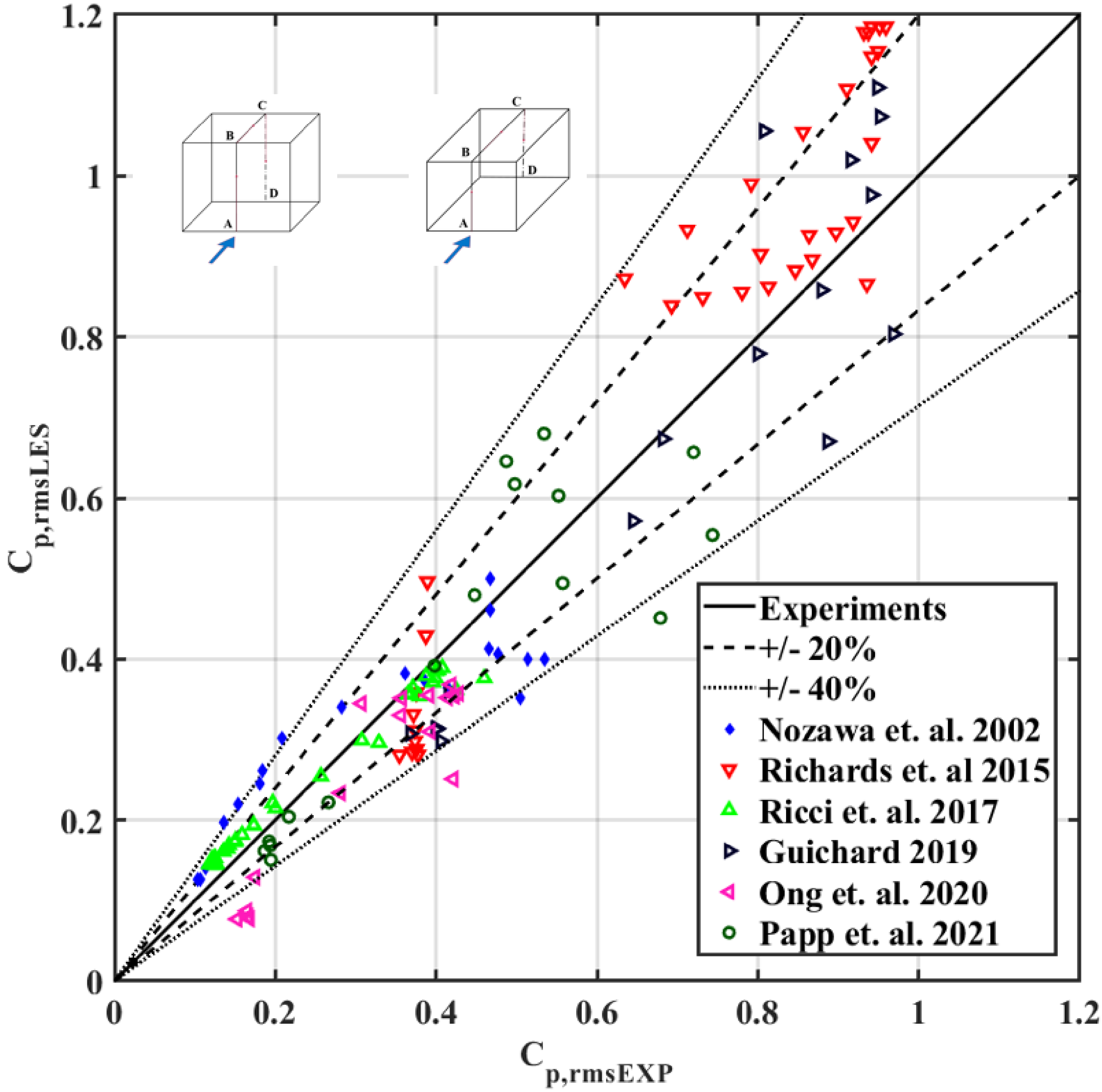

Figure 2.4: Correlation between LES and experiments for the rms pressure coefficient in the center line of the building envelope for cubes (Richards and Norris, 2015, Guichard, 2019, Ong et al., 2020 and Papp et al., 2021) and low rise building with aspect ratios 1:1:0.5(Nozawa et al., 2002) and 1:1.5:0.5 (Ricci et al., 2017).

2.3.2 High rise buildings

Structural wind engineering applications with CFD for high rise structures started appearing at the beginning of 2010s. The CAARC standard building has been the main point of focus, with many computational works comparing experimental results from National Aeronautic Establishment (NAE), National Physical Laboratory (PHL), University of Bristol, City University, Monash University and Tong Ji (TJ) University. In this period inlet conditions were also examined by various works that can be considered seminal (Daniels et al., 2013, Yan and Li, 2015 and Elshaer et al., 2016). The mean values of the pressure coefficient can be captured accurately despite the inlet assumptions, although this is not the case for the rms values. According to Figure 2.5 the rms distribution in the building envelope ranges based on each case. The vortex method seems to be overestimating the fluctuations. The improved version of the discretizing and synthesizing RFG (DSRFG) method (Elshaer et al., 2016), seems to provide more valid results than the previous one (Huang et al., 2010). Each inflow generation method uses a different approach to model the turbulence statistics and the spectral content in the location where the CAARC building interacts with the flow field in the computational domain. Since the energy of the velocity fluctuations is not the same from each approach, differences in the rms distribution are expected. This makes further elaboration of the results a more difficult task. Pressure distribution in geometrical modification of the CAARC building were also investigated by using the RFG method with the scope to establish the level of improvement in the aeroelastic response (Alminhana et al., 2018).

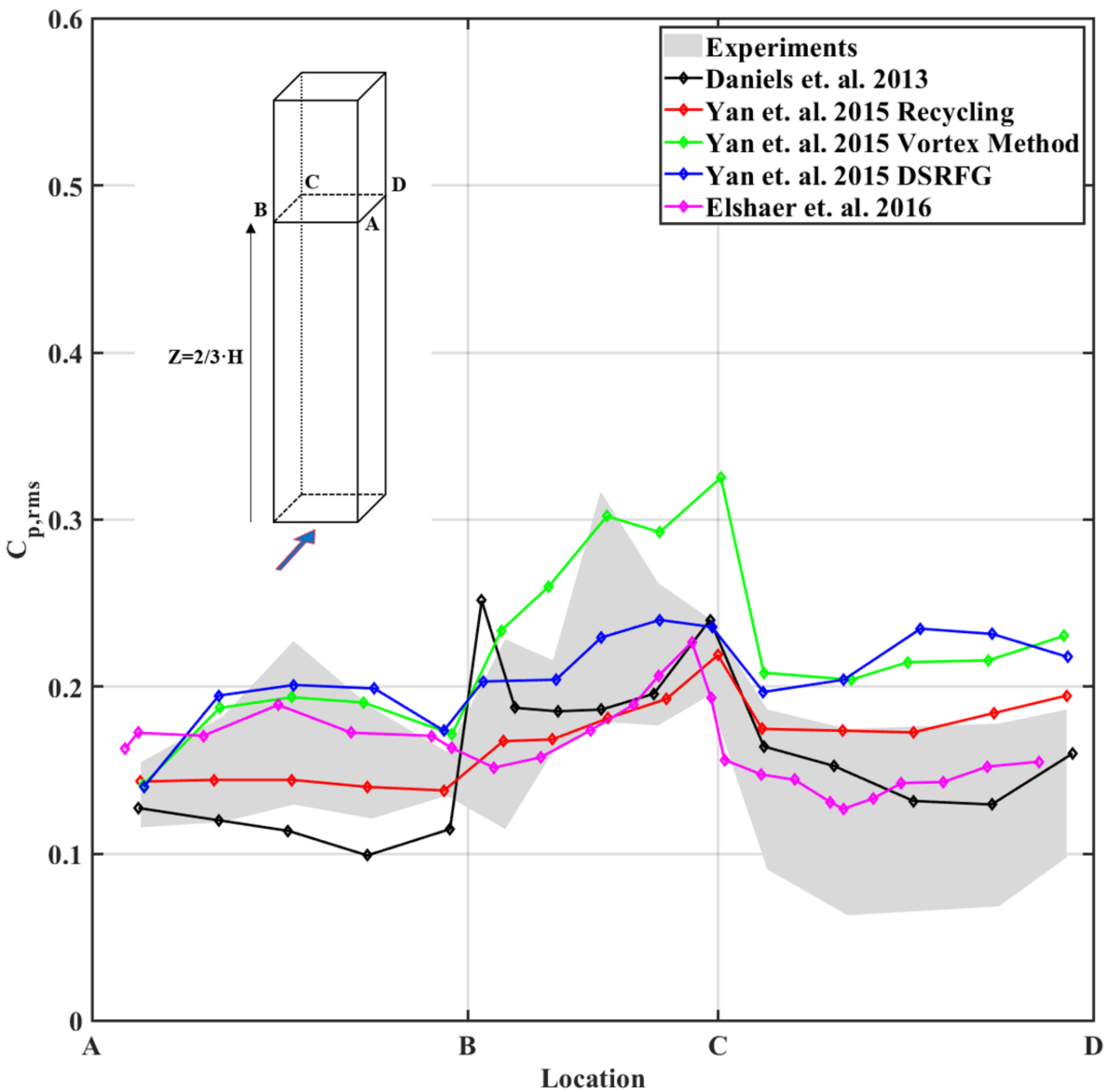

Figure 2.5: LES and experiments for rms pressure coefficient at 2/3H of the CAARC building

Pressure coefficients in urban areas with dense building configurations have also been examined. Recycling techniques were used for a complex urban domain with the target of extracting pressure values of a non-orthogonal high-rise building. Results correlated well with experiments for mean pressure statistics and total force distribution, but the rms, and maximum values were not reproduced that accurately (Nozu et al., 2015). In a similarly dense environment, the CAARC building was investigated, where results of the DSRFG method proved adequate regarding the total force distribution with height on the building, by comparing the displacements and accelerations with experiments (Elshaer et al., 2016).

Besides the CAARC benchmark other studies focused on square sections of high-rise buildings. For example, the flow around a 1:1:8.3 building was investigated based on an improvement of the RFG method (Huang et al., 2010). The DSRFG improves the spectral content of the streamwise velocity and results regarding the along and across-wind forces and base moment were in good comparison with experiments. Later, the DSRFG method was improved to better capture the spectral content of the velocity fluctuations. The consistent discrete RFG (CDRFG) method was applied in a similar building, where the results of the total force distributions were more accurate (Aboshosha et al., 2015b). In the aforementioned study, a code is public for reconstructing the inlet turbulent field. The abilities of the method were extended by modifying the spatial distribution of the turbulent field and introducing a narrowband synthetic procedure (NSRFG), which provided better accuracy for the rms values (Yu et al., 2018). Based on the NSRFG method, a high-rise building with an aspect ratio of 1:1:9 was later investigated (Feng et al., 2019). The following year one more study was published that used a synthetic RFG method and wall-modeled LES to capture the pressures in a high-rise building with an aspect ratio of 1:1:5 (Wang et al.., 2020). The novel approach correlated very well with the target experiments. The same building configuration was selected in a comprehensive study that applied Lattice-Boltzmann method (fluid particles collision) (Buffa et al., 2021). The rms results for the aforementioned papers are presented in Figure 2.6. It is obvious that by increasing the height of the structure the results become less accurate, with errors close to 40%, although, no general conclusion regarding the improved accuracy of one of the approaches can be made. More work is needed in that area to understand the advantages and disadvantages of these methods.

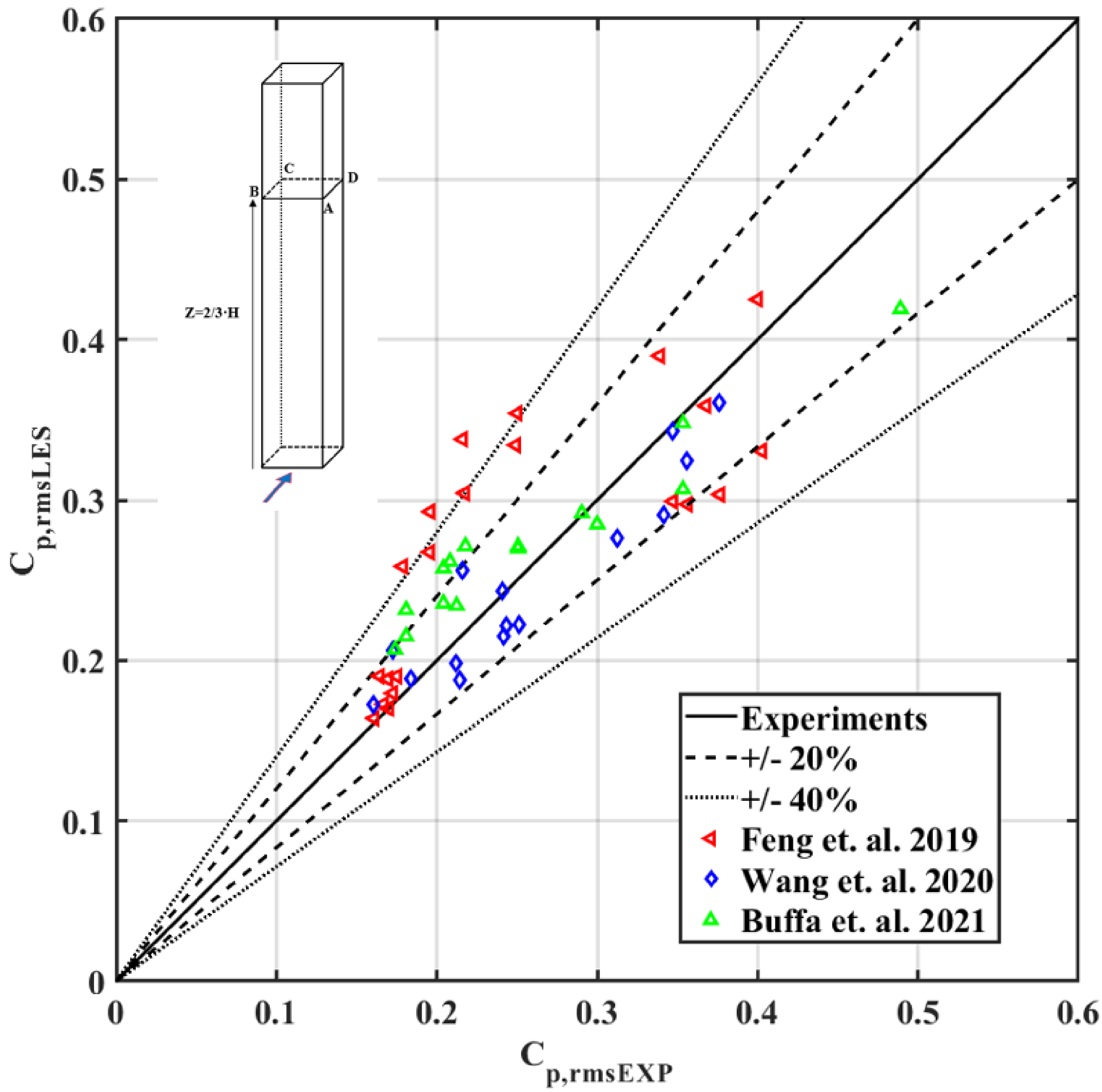

Figure 2.6: Correlation between LES and experiments for rms pressure coefficient at 2/3H of the 1:1:5 building (Wang et al.., 2020 and Buffa et al., 2021) and 1:1:9 (Feng et al., 2019)

Local loads in high rise structures were also examined in Lamberti et al., (2020). The high-rise structure of aspect ratio 1:3.3:6.6 was imposed in a synthetic inlet that was previously optimized by the authors (Lamberti et al., 2018). The sensitive analysis included the roughness length, turbulence kinetic energy and streamwise integral time-scale, as defined in the synthetic approach. The "sensitivity bounds" agree with great accuracy with the experimental results regarding local values of mean, rms and peak pressure coefficients.

2.3.3 Wind directionality

Wind direction is another fundamental parameter in wind engineering and computational procedures. Wind flows perpendicular to the building facades might be considered the most critical for calculating the total structural response (area loads), although that might not be the case for the design of cladding elements (local loads). Especially when considering roof loads, the conical vortices, and the various zones in which the peak values are distributed are of crucial essence for an accurate design. The LES study by Ono et al. (2008) included oblique direction of 45° for a low-rise building with an aspect ratio of 1:1:0.5, by following the already established technique of the benchmark by Nozawa and Tamura (2002). Results seem to capture the main features of the flow field in the contours presented. Later, in the works of Ricci et al. (2017) and Ricci et al. (2018) one oblique wind direction of 45° was included for the estimation of the pressures on a corresponding low- and high-rise structure by using a modified version of the RFG technique of Castro et al. (2013).The mean and rms values were predicted in the same manner for all wind directions of the low-rise, but more difficulties were noticed in the high-rise building, especially near the corner zone.

After that, a comparison of mean and rms pressures was conducted for a square section of a high-rise structure with aspect ratios 1:1:3 and 1:1:4 for 0° and 15° angles of attack, by using the recycling technique (Cao et al., 2019). The mean and rms values were underestimated when compared with the experimental results for the windward and the side faces. Papp et al. (2021) included the oblique 45° of wind direction in the study, where a similar conclusion can be drawn as in Ricci et al. (2017). Figure 2.7 presents results from the aforementioned works in terms of their correlation with the target experiments of each study for the mean values, and Figure 2.8 the corresponding rms values. As before, it is difficult to generalize the relative accuracy of each method and the assumptions under which the results were extracted, although it is obvious that small steps of improvement can be noticed.

The inherent difficulty in modelling non-perpendicular wind directions can be described by the more interactive turbulent structures in the wake region. This has a dramatic impact on the mesh size, as to choose the correct y^+ values and filter size for LES. In all the above works, finer mesh was needed to model oblique wind attacks. More research is needed in this area, in order to quantify these needs in more applications both for low- and high-rise structures.

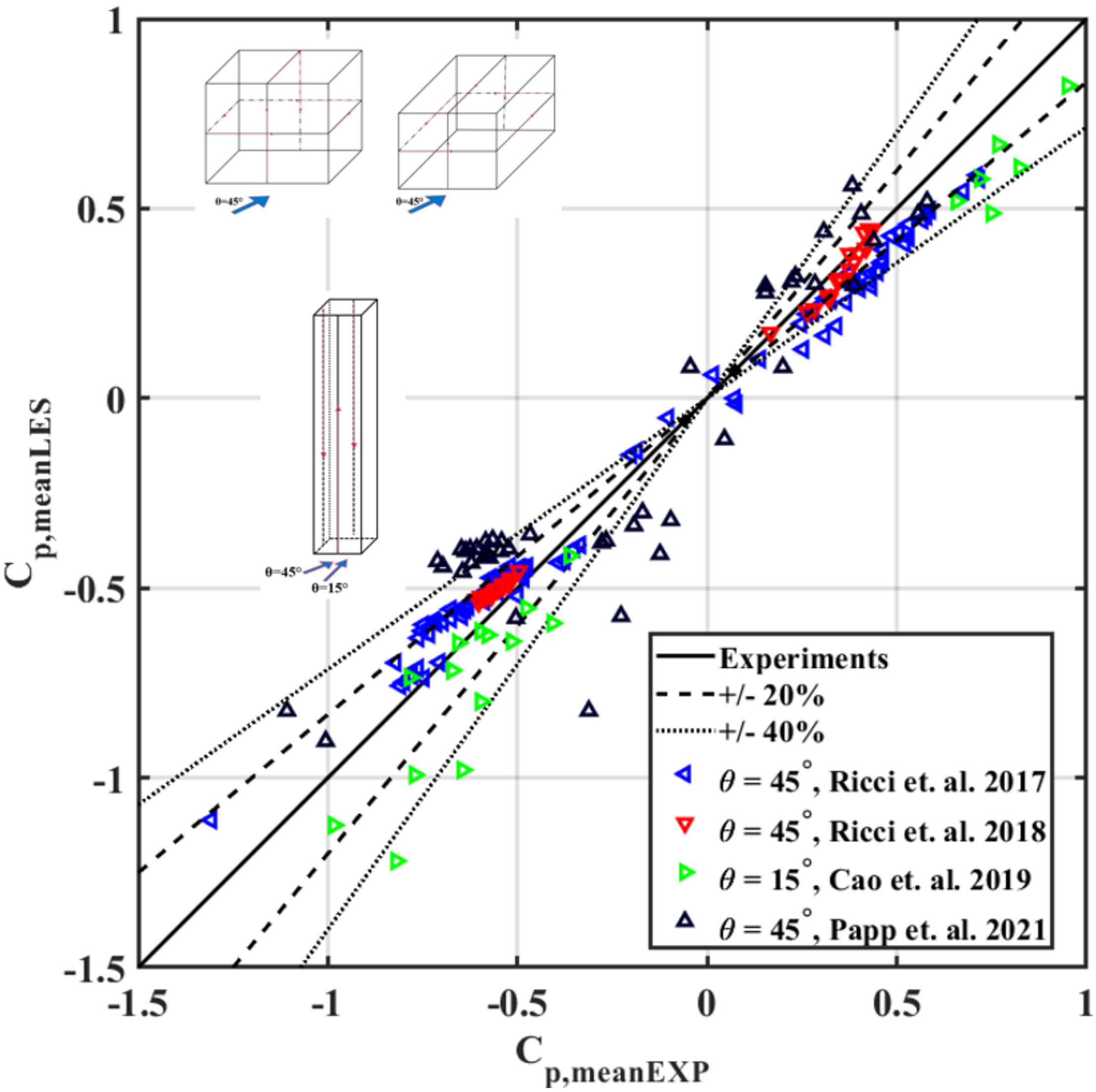

Figure 2.7: Correlation between LES and experiments for the mean pressure coefficient at vertical and horizontal center lines of the 1:1.5:0.5 building (Ricci et al., 2017) for 45°, 1:2:5 (Ricci et al., 2018) for 45°, 1:1:4 (Cao et al., 2019) for 15° and cube (Papp et al., 2021) for 45°.

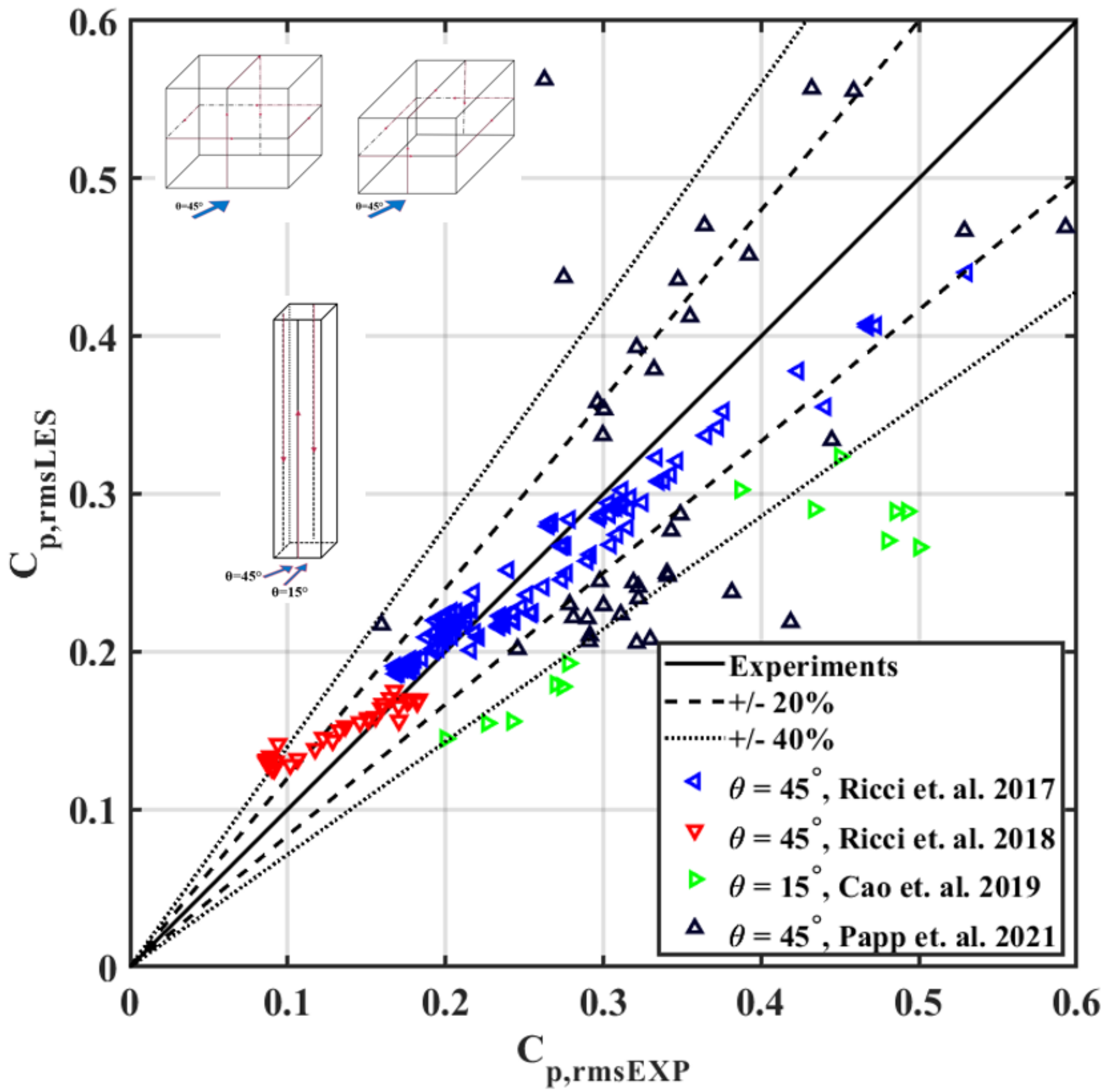

Figure 2.8: Correlation between LES and experiments for rms pressure coefficient at vertical and horizontal center lines of the 1:1.5:0.5 building (Ricci et al., 2017) for 45°, 1:2:5 (Ricci et al., 2018) for 45°, 1:1:4 (Cao et al., 2019) for 15° and cube (Papp et al., 2021) for 45°.

2.4 Future perspectives on CFD application to structural problems

Reviewing the contributions in structural CWE since 1992, the computational methodologies to model wind effects in the ABL show a clear improvement with time. In the future, many unexplored paths will be studied by the scientific community. Some of these paths from the structural point of view are outlined in this section.

Since 1992, the field has seen great improvements in terms of matching computational and experimental procedures. Regarding the pressure statistics: mean values have been accurately introduced since the beginning, while the rms and peak values are still being improved. The target level of accuracy has been reached in the last decade, although a generalized, consistent, and conservative process is yet to be established.

Comparisons of CFD and code provisions are rarely found in the literature since usually the validation is done by wind tunnel tests for the velocity and pressure regime and some empirical models for the turbulence features. These models consist of mean profile, turbulence intensity, integral length scale and spectral representation (von Karman, 1948, Davenport, 1961, ASCE/SEI 49-21, ESDU, 1993). Results of the most representative papers from 2010-2023 prove that the first three categories are well captured.

Empirical models have been researched regarding fluctuating pressures. These models were based on the mean pressure values and flow parameters such as mean velocity and turbulent kinetic energy to estimate the rms pressure distribution. This procedure proved an adequate fit for the Texas Tech University model (Selvam, 1992, Paterson, 1993). Although, such an approach is difficult to be generalized for more diverse building configurations, and pressure taps in non-symmetrical lines. Machine learning techniques have surfaced in the field to close this gap. Recently, a framework was proposed that uses results of a computationally efficient steady-RANS approach to estimate rms values of a more computationally demanding LES (Lamberti and Gorlé, 2021). Results proved that the above correlation was better than what empirical equations proposed for the rms values on a high-rise building. It is clear that a large database that provides accurate results can benefit practitioners and future research applications for comparison.

Few studies have focused on pressure results in non-symmetrical lines, which indicates that there has been little improvement in this area. One more issue that can easily be spotted is the lack of uniformity in the calculation of peak values by various studies when compared with experiments. Some works use the quasi-static approach (Nozawa and Tamura, 2002, Thordal et al., 2020c), some compare maximum and minimum values (Lim et al., 2009, Nozu et al., 2015, Hu et al., 2018, Ong et al., 2020) and some others turn their attention to higher order statistics (Ong et al., 2020, Wang et al.., 2020). In all those efforts, a common theme is the similar behavior of the peak data with the rms values. The correlation of the higher order statistics with peak value distribution should be sought first in the wind tunnel and then via computational approaches. The non-Gaussian nature of the distribution that relates with wind induced pressures should be researched in computational procedures as well. Spectral content of the pressure time series should be compared with wind tunnel results in local taps and area averaged loads, to validate the capacity of the methods used. This makes clear that both wind tunnel and CFD need to cooperate and work by substituting each other, as to understand more about the complex wind structures that exist in the atmosphere and interact with building envelopes.

LES has proven its capabilities and it is used in most of the studies found for structural applications. In order to evolve the current state-of-the-art, there are many parameters worth investigating deeper. Something that seems to be missing from most of the referenced studies is oblique wind directions. This comparison with experimental results is necessary to establish the capacity of each approach to capture the envelope peak values. After all, that's a key factor for any building design against wind loads. More studies should focus on the impact of oblique winds to the mesh size and its configuration and quantify the increase in computational cost. The field would benefit from such comprehensive works on this topic that can be generalized for various aspect ratios of buildings.

A topic emerging in the recent past is downburst modelling. Kim and Hangan (2007) conducted steady-RANS simulations for vortex type downbursts by using an inlet jet. Results for the velocity regime tended to agree with full-scale data, to an acceptable extent. Later, the LES approach was used to model downbursts for various exposure conditions and the evaluated instantaneous radial velocities, and their peaks were in good match with field measurements (Aboshosha et al., 2015a). Full-scale measurements are the most appropriate way to validate numerical and experimental data. The THUNDERR project opened new prospects of research and combined various field data, in an effort to create a uniform framework to design safe and cost-efficient structures against extreme wind loads (Solari et al., 2020). CFD simulations have been carried out since then and velocity results match the acquired data (e.g. Yan et al., 2022). Future research will focus on measuring field data for the pressure regime in order to simulate and validate them in computational procedures.

One more fundamental issue that is rarely found in previous studies is the Reynolds number effect, e.g. on peak surface pressures. In wind tunnel tests, these issues have been addressed by ASCE 49-21. Usually, similar conditions are chosen for CFD. For example, in computational procedures small scales can be modeled since there is no limitation for the pressure tap configuration, and larger scales are not restricted by the wind tunnel dimensions and blockage ratio issues. These issues should be addressed more comprehensively in computational procedures in the future, as to quantify the similarities of the results of different scales. The Jensen number (ratio of building height to roughness height) affects dramatically the pressure distribution of building surfaces, and it is an important parameter to match data from different scales. These types of effects should also be examined, especially when considering loads on low-rise buildings, where the surrounding roughness plays a key role in the turbulence intensity at roof height.

Many approaches have been used regarding the domain selection for LES, and one aspect is of great importance to highlight. Despite the method, the turbulent statistics that will interact with the obstacle should be first established in an empty computational domain (Blocken et al., 2007). This is similar to the experimental procedure in the wind tunnel. These values should be compared with experimental results or corresponding empirical models. The virtual wind tunnel method is based on precisely depicting the wind tunnel (roughness elements, spires, etc.) in computationally demanding domains and results have proven adequate for the velocity regime, despite the time-demanding procedures (Ricci et al., 2017, Vranešević et al., 2022). Studies based on recycling and synthetic techniques have proven adequate in that perspective (Yan and Li, 2015, Ricci et al., 2018, Wang et al.., 2020). These parameters need to be checked in all cases, as to establish the level of accuracy of the interaction between the building and the wind flows in wind tunnel and the one in the computational domain. Key points for this interaction to be constructive for peak value estimation is the turbulence intensity at roof height (Tieleman et al., 1997) and the spectral content of the streamwise velocity in the high frequency region (Potsis and Stathopoulos, 2022). The first point has been taken care of by solving the turbulence decay issue by using various approaches (Lamberti et al., 2018, Guichard, 2019, Melaku et al., 2022), but the second point has troubled the state-of-the-art in the last decade. In order to correctly express energy level in all turbulent lengths and wavenumbers, theoretically, DNS approach is necessary, thus most of the studies assume that the misrepresentation of the spectral content at the high frequency range is acceptable. There is no question that by following the DNS approach, the resulting peak values will be very well correlated with experiments, but this is accompanied by a computational burden that makes it non-pragmatic for engineering applications at the moment.

Inlet conditions, if optimized, can reduce the computational time from several months to a matter of days (depending naturally on user's access to resources). Indeed, these inlet conditions play the most influential role in expressing correctly the spectral content of the velocity fluctuations and will determine the peak values on the building envelope. Recently, a procedure was proposed that is based on using inlet data from wind tunnel measurements (Potsis and Stathopoulos, 2022). The results of the so-called *Dynamic Terrain* method proved that the inlet frequency of the time series plays a key role in grasping the spectral content of the velocity, in the entire frequency domain. The approach seemed to increase the ability of the coarse domain to express the high-frequency fluctuations above the filter limit and relieve the sub-grid model. This expression might improve the pressure fluctuations in the building envelope and the equivalent spectral content in points of interest, thus providing accurate peak values in a conservative and consistent manner, with minimized complexity for practitioners and reduced computational cost. This methodology consists of the main contribution of this thesis and it is further explored at Chapter 4.

2.5 Summary and Conclusions

This Chapter summarizes the most seminal advancements of CWE in building structures and environment since 1992. As a groundwork for the application of CFD to various environmental issues, the importance of accurate modeling of ABL/UBL/UCL is pronounced. Turbulence inflow generation techniques were discussed and some aspects of validation and verification were presented.

Structural loads calculated by CFD for low-rise and high-rise buildings have been addressed. The future research paths refer to comparisons with empirical models, machine learning techniques, non-symmetrically located pressure taps, peak values, non-gaussian distributions, wind directionality, envelope peak loads, Reynolds number effects, and the importance of inlet conditions. It is clear that the engineering community has gained more benefits from environmental than structural applications (Potsis et al.., 2023). Future research will focus on capturing the essential parameters of the turbulent flow field, for the development of models that respect the interaction between buildings and the actual wind flow. Modeling procedures should become clearer and more relevant to practical use, as to compose a structured design tool.

Considering the future development of computers, there is no doubt that the turbulence modeling used for CWE will shift from RANS to LES in the future. In this sense, the differences in the numerical methods between the environmental and structural fields may diminish. However, the computational cost of LES is still too large for practical applications that require a large number of different analysis cases in a short time period. Also, conducting reliable LES requires more knowledge and experience than RANS. It is of utmost importance to correctly understand the information obtained from each modeling approach and how to efficiently utilize them for structural and environmental design of buildings. After all, it will be prudent to recall the original definition of wind engineering (Cermak, 1975) and continue to carefully observe the interactions between wind in the ABL and buildings computationally and experimentally.

CHAPTER 3: ENGINEERING NEEDS, COMPUTATIONAL TARGETS, VERIFICATION AND VALIDATION

3.1 Introduction

Considering the state-of-the-art as presented in Chapter 2, this Chapter focuses on establishing the engineering needs, which coincide with the computational targets of the novel research and contributions of this thesis. Also, it discusses Validation and Verification techniques of CWE for structural applications. It is subdivided in two subsections where these topics are thoroughly discussed and a concluding subsection as to smoothly introduce the reader to the main ideas and findings of this thesis in Chapters 4 and 5.

3.2 Engineering needs and computational targets

As established in Chapter 2, the complexity of computational methodologies available in order to model wind-induced peak loads has increased significantly throughout the years. One aspect that contributes to that is the chaotic nature of turbulence flow field in the ABL. For example, experimental results from various wind tunnels seem to provide large variations when it comes to peak wind-induced pressures. A representative example of this issue is presented in Figure 3.1., where a recent study was carried out to establish the level of reliability of NBCC (2020) code provisions for low-rise buildings (Chavez et al., 2022). In this study, a low-rise building with full-scale dimensions of 73 m x 73 m x 7 m was selected and field measurements were recorded. Two wind tunnel experimental studies were carried out, one in Western and one at Concordia University. Area-averaged wind load on three zones of the roof, as defined in NBCC 2020 (corner, edge, and interior) were calculated and presented in Figure 3.1 (c), (d), and (e) respectively. Field data are also displayed for this comparison. The pressure tap configuration of the model in Concordia and Western wind tunnels are presented in Figure 3.1 (a) and (b) respectively. Clearly, there are significant deviations between the two experimental campaigns, for all three zones, ranging from 25% to 50%. Field data seem to be within this discrepancy, by underestimating the experimental values of Concordia and overestimating the experimental values from Western. It is important to mention that these values are calculated as the envelope peaks, based on wind flow directions from 0° to 360°.

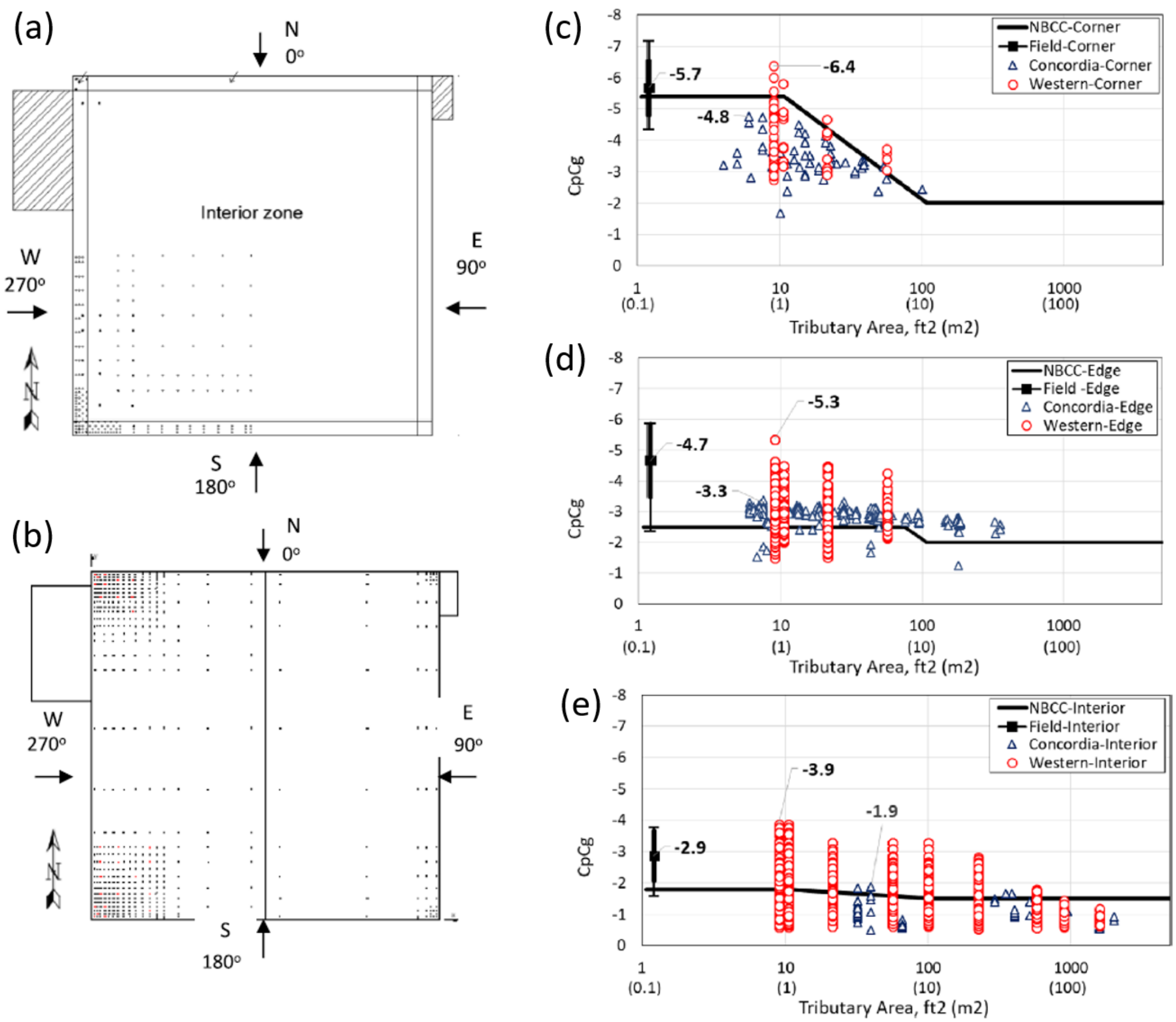

Figure 3.1: Pressure tap configuration in (a) Concordia and (b) Western models and comparison of peak area averaged pressures at (c) corner, (d) edge and (e) interior of the roof. (Figures are taken from Chavez et al.., 2022 slightly modified).

Local peak pressures are also of high significance for the design of cladding elements. In Figure 3.2 peak pressures are displayed along the lines in the edge zone of the building with full-scale dimensions of 16 m x 24 m x 4m, from TPU and NIST databases. These data were presented in Shelley, et al.., 2023. As can be seen, significant differences are noticed at this location ranging up to 60%. The study mentions that these differences cannot be explained by the measurement uncertainty but may be related to the inflow conditions of mean speed and turbulence intensity profiles and Jensen number effects.

Similar results are presented in Figure 3.3 (a) and (b) for perpendicular and 45° wind direction for a low-rise building of 16 m x 24 m x 8 m. The figure correlates the peak values in 192 locations on the roof (also included in the figure) for open exposure. Data seem to generally agree more for the perpendicular wind direction, but still significant differences can be found. The Percentage of Root Mean Square Error (PRMSE) is also displayed for these data and is measured close to 10 %. The definition of PRMSE can be found in Equation 3.1, where $C_{p,a,i}$ and $C_{p,b,i}$ are two different sets of pressure coefficients from two different experiments, and $C_{p,max}$ and $C_{p,min}$ are the maximum and minimum values of the entire set. Similar to PRMSE of peaks presented in Figure 3.3, the same metric can be calculated for mean and standard deviation (hereafter std) to see their accuracy as well. Although these metrics are also critical, in this subsection focus is given only to peaks, but later in the thesis PRMSE of mean and std will also be presented.

$$PRMSE = \frac{RMSE}{\left|C_{p,max} - C_{p,min}\right|} = \frac{1}{\left|C_{p,max} - C_{p,min}\right|} \cdot \sum_{1}^{N} \sqrt{\frac{(C_{p,a,i} - C_{p,b,i})^2}{N}} \qquad \textit{Equation 3.1}$$

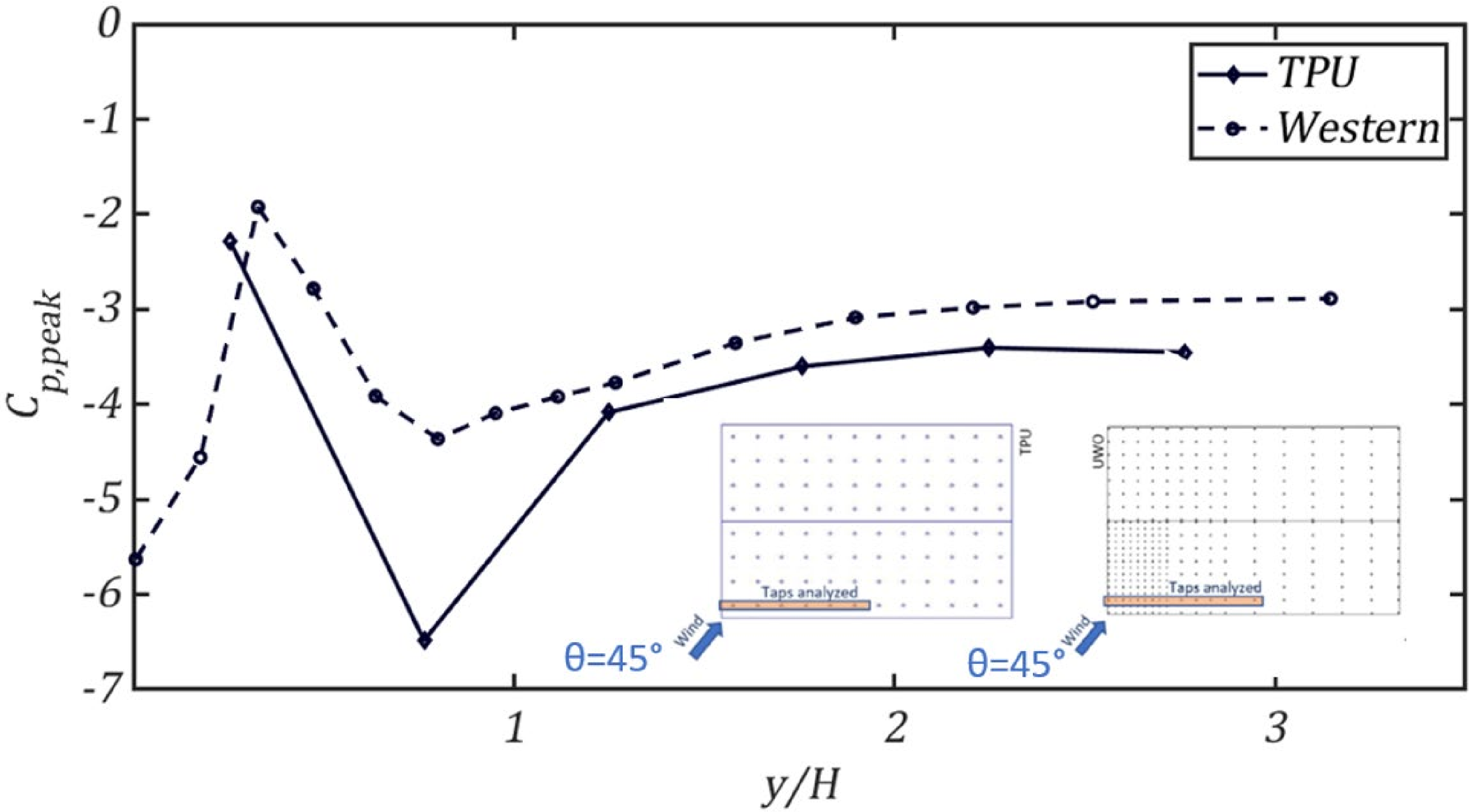

Figure 3.2:Peak pressure coefficient on the edge of the roof between TPU and Western WT for 45° wind direction (results are taken from Shelley et al.., 2023, slightly modified)

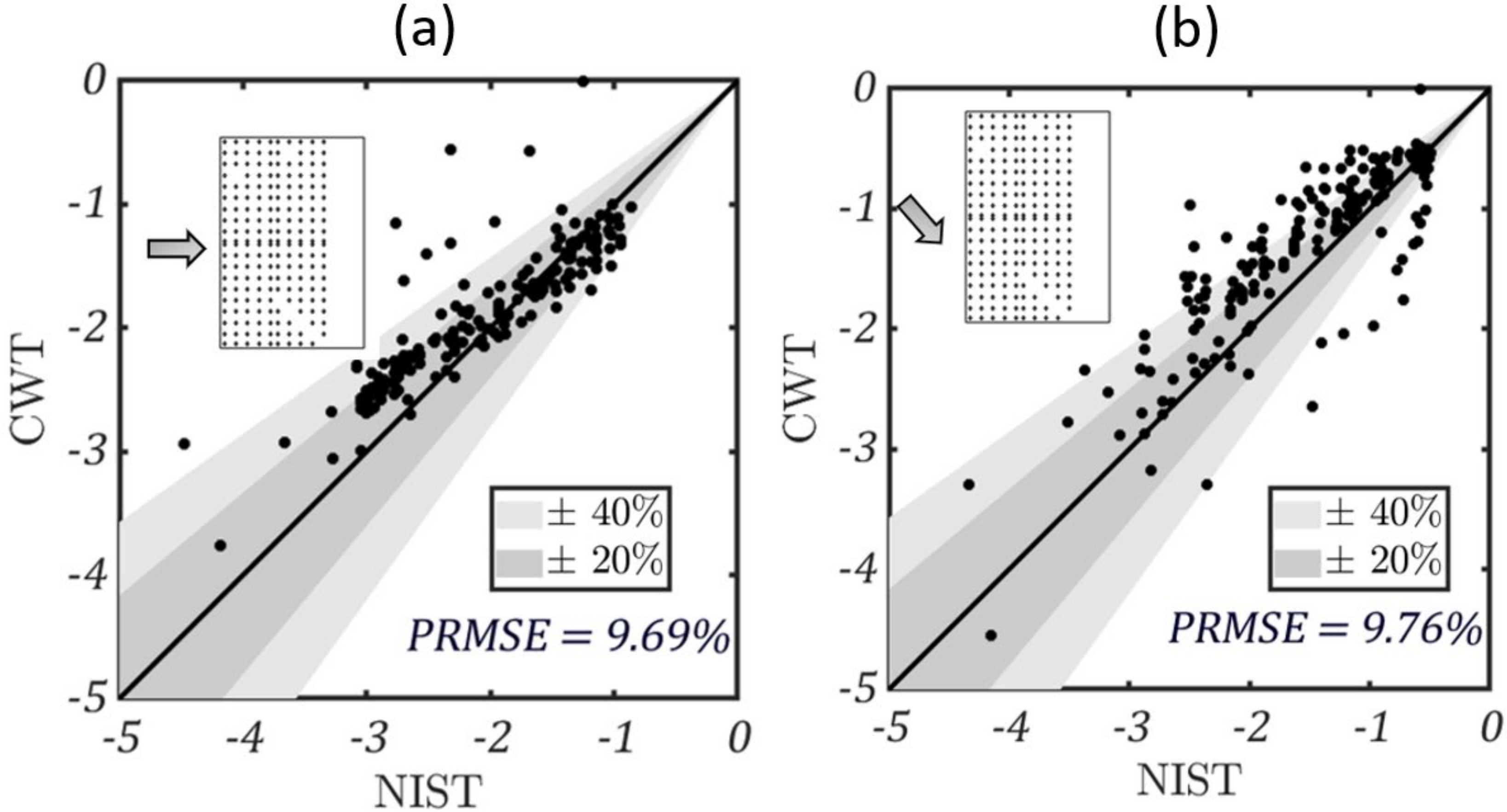

Figure 3.3:Peak pressure coefficient on the entire roof between Concordia Wind Tunnel (CWT) and NIST for (a) perpendicular and (c) 45° wind direction

The results presented in Figure 3.3 relate to a case study of peak wind-induced loads on roofs, conducted to develop the LES-DT method that will be displayed in Chapter 4. Besides the PRMSE as a metric to compare the two experimental sets of results the Percentage of Accuracy (PoA) is also used which is defined in Equation 3.2. It is calculated for tolerance values from 0 to 1 (or 0 to 100%) with small time steps as not to miss valuable information (usually 1%). For example, for tolerance 10%, if the number of pressure taps whose absolute error of peak (or mean or std) is 10 or less and there are 100 pressure taps in total, the PoA (10) = 0.1.

$$PoA\ (tolerance) = \frac{Number\ of\ pressure\ taps\ with\ absolute\ error\ less\ than\ the\ tolerance}{Total\ numer\ of\ pressure\ taps} \qquad \textit{Equation 3.2}$$

This is important because in many cases peak values have relatively small values (even if they are the peak) and linear regression metrics (such as PRMSE) perform poorly. Nonetheless, the peak values might have very high PoA, which proves that the absolute error between the two sets is low. On the other hand, there are certain cases where the linear regression metrics show very good comparison, but the PoA metric is low, which means that there is larger error between the two sets. In such cases, usually the basic aerodynamics trends are captured similarly between the two cases.

Besides roof loads, wall loads are also of critical importance. In Figure 3.4 results from NIST and TPU databases are presented for the same building as the one in Figure 3.3, but for suburban exposure. The building envelope is divided into 5 separate sections: roof, and four sides and results are presented for perpendicular (Figure 3.4a) and oblique wind direction of 45° (Figure 3.4b). Besides the PRMSE metric, the coefficient of determination R^2 is also presented, by linearly relating the two datasets. The differences between the two experimental results are significant for this example too, especially for the oblique wind direction, as seen from PRMSE and R2 metrics. In many taps the absolute error is above 40 %, as also seen in Figure 3.3

Comparing all the above results from various wind tunnel experimental facilities, it becomes clear that wind tunnel procedures, although they consist of the most reliable tool for wind loading estimation, they also have some drawbacks. Due to the physical complexity of fluid dynamics, wind is characterized by high turbulence and even the inherent small differences in the incoming flow can create large deviations in peak pressures. This proves that even by following the provisions of ASCE 49-21 wind tunnel results may lead to significant deviations from one facility to the other. This highlights the importance of establishing a threshold of accuracy for wind-induced peak pressures estimation, which is closely related to the engineering needs of computational tools in CWE.

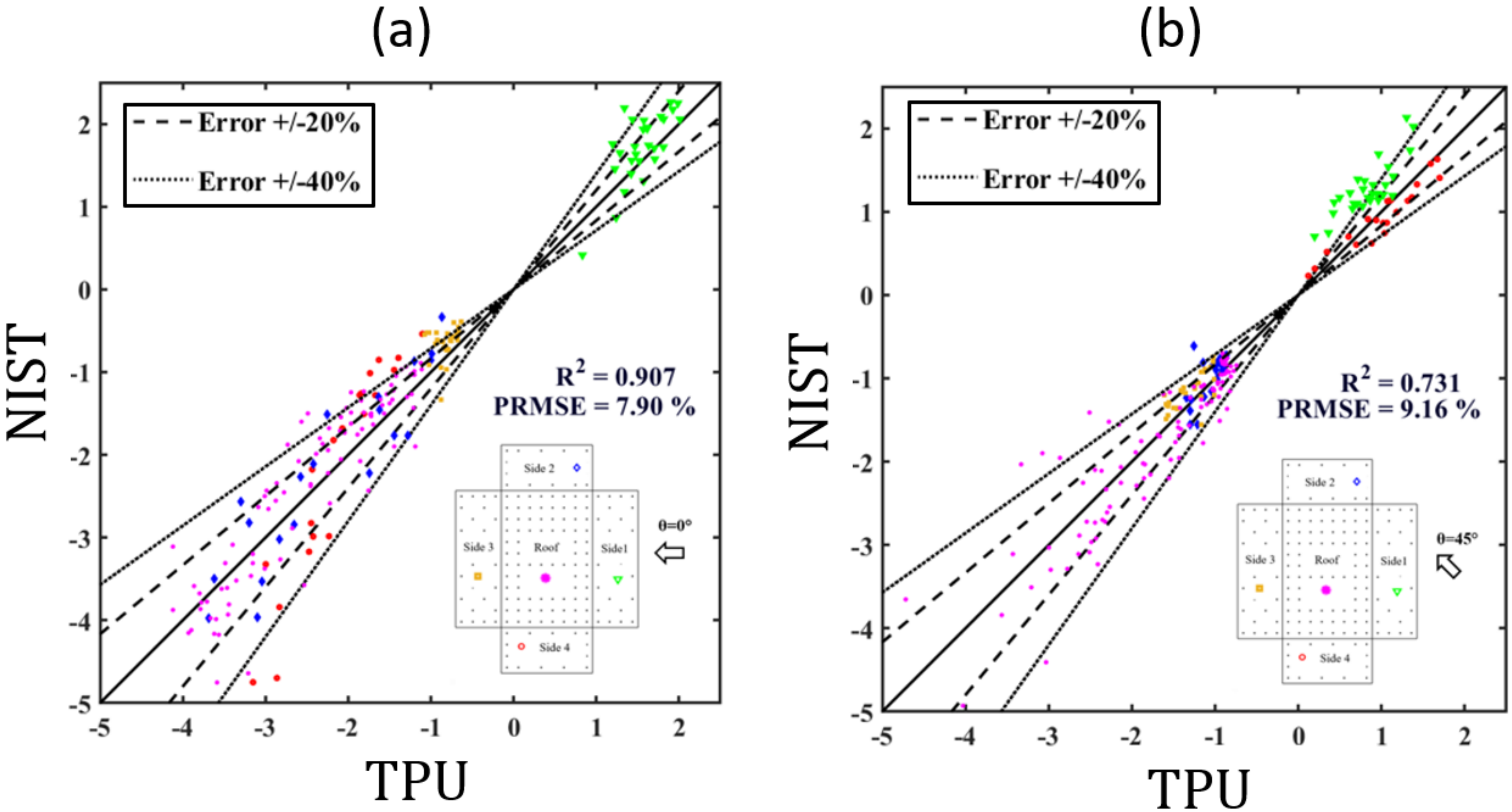

Figure 3.4: Peak pressure coefficient on the entire envelope between NIST) and TPU for (a) perpendicular and (c) 45° wind direction

Another important need is computational efficiency. This means the analysis should produce acceptable and reliable results within a reasonable time frame. Especially, by considering the need to model various wind directions in wind engineering. This is hard to achieve with the current methodologies in the state-of-the-art as explained in Chapter 2. Optimization of inlet conditions can be beneficial to address this issue, and they are the basis of this thesis's research contributions. Besides that, an efficient computational methodology should also combine the minimum level of complexity for its application. Also, thorough documentation and guidelines are key to generating methodologies that are accessible and applicable by other parties of interest. These consist of two particularly important computational targets of the research in this thesis.

One more aspect of an efficient tool is to include in the procedure the extraction process of the pressure time series and the necessary post processing tools. In wind engineering, Extreme Value Analysis (EVA) is necessary to estimate the peak pressures needed for design. The basic concept of EVA is to divide time-depending pressure signals into several segments and extract the peak value from each segment. Then the peak values are distributed based on Gumbel (or similar) Probability Density Function, and a characteristic peak value is defined based on the selected probability of non-exceedance. The number of segments, the choice of PDF distribution and the selected probability of non-exceedance are all particularly important choices to extract meaningful peak values (Peng et al.., 2014 and Gavanski et al.., 2016). In all results presented in this thesis, the number of segments is selected as 10, the distribution is Gumbel distribution (Type 1), the Best Linear Unbiased Estimator (BLUE) was used to calculate the necessary fitting parameters and the percentage of non-exceedance was chosen as 78%. More information on these choices can also be found in Chapter 4, Simiu and Yeo, (2019) and ASCE 49-21.

Furthermore, it is vital to keep in mind the physical interpretation of the interaction between natural wind and structures in the ABL. The computational targets should be to capture this interaction as accurately as possible, as also done in wind tunnels, in order to have reliable design (peak) values. One important aspect of this is the total duration of the numerical analysis to provide representative results in full-scale. The usual practice in wind tunnel testing is full-scale duration of 10 minutes to 1 hour, and this was set as a computational target. More information regarding this can be found in Gavanski et al.., (2016), Geleta and Bitsuamlak, (2022), Vranešević and Glumac, (2024).

Besides the total duration of the modeling, the physical interpretation of the interaction between wind and structures should also be considered in the frequency domain. The most important part is the spectral content of the velocity fluctuations at the incident flow. As also mentioned in Morris and Kopp, (2018), modeling properly the small-scale (high frequency) velocity fluctuations is necessary for capturing peak values on building envelopes. This is easier said than done, especially because with LES modeling, the spectral content tends to be radically reduced after the cut-off frequency of the filter (Figure 1.5). Improving the spectral content at the incident flow consists of the most important computational target of the tool that was developed for this thesis and a big part of the results and discussions in Chapters 4 and 5. More details about how this improvement is achieved in this thesis can be found in Sections 4.2.2 and 5.2.2.

3.3 Validation and Verification of CWE for structural applications

Another very important aspect is the comprehensive Validation and Verification (V&V) procedure for the usage of LES in structural computational wind engineering. In the literature there are various definitions of V&V of CFD, based on the realm of application. For example, according to Oberkampf et al., (2002) *Model Verification* is the substantiation that a computerized model represents a conceptual model within specified limits of accuracy and *Model Validation* is the substantiation that a computerized model within its domain of applicability possesses a satisfactory range of accuracy consistent with the intended application of the model. According to ASME (2006), *verification* is the process of determining that a computational model accurately represents the underlying mathematical models and its solution., while in AIAA (1988) validation is defined as the process of determining the degree to which a model is an accurate representation of the real world from the perspective of the intended uses of the model. Unfortunately, at the moment there is no consensus from the scientific and practice communities as to what exactly the V&V of LES for structural CWE should be, as discussed also in Chapter 2. Similar discussion can be found in Daniels and Xie, (2022) and Tominaga et al.., (2023).

Some of the basic concepts and ideas for a consensus-based V&V process for LES in CWE can be found in Scott et al.., (2023). They can be summarized as follows:

- Validation of incident flow in terms mean, turbulence intensity profiles and spectral content in various heights.
- Validation of local mean, standard deviation and peak pressures on the entire building envelope.
- Uncertainty quantification of experimental results based on various experimental facilities
- Uncertainty quantification of numerical results based on incident flow, mesh and numerical setup.

Of course, some metrics should be established to estimate if and how much a computational tool is validated and verified. Validation metrics are usually statistical correlation metrics (e.g., PRMSE and R^2, PoA, absolute error, etc.) between numerical and experimental results, such as the ones presented in Section 3.2. If they are within the accuracy threshold discussed in Section 3.2, the computational tool can be considered validated. Depending on each case the threshold of accuracy and the specific critical validation metrics might be different, something that complicates matters a lot. Verification metrics are closely related to the uncertainty quantification criteria discussed earlier as also seen in Chapter 2. Given that the CFD code used is commercial, it can already be considered verified as discussed in Tominaga et al.., (2023), while in-house codes that solve the NS system of equations have to pass more verification metrics.

In this way, a specific computational setup that has been scrutinized by a guided V&V process can be eventually used to determine wind-induced peak pressures, independently of wind tunnel testing. These data can be considered acceptable for structural design decisions and used for more detailed static or dynamic structural analysis. According to code provisions and standards the practice of CFD for structural wind engineering is still forbidden. For example, in NBCC (2020) it is stated that: "It is not currently possible to verify the reliability and accuracy of CFD and no standards address it; as such, this method is ***not permitted*** to be used to determine specified wind loads". Recently there are some endeavors from the Eurocode (Bruno et al.., 2023) and the Architectural Institute of Japan (AIJ, 2019) that target to create guidelines for the usage of LES for this purpose, but there are no final recommendations available.

3.4 Summary and Conclusions

In this Chapter the engineering needs and computational targets of CWE for structural applications with LES were discussed. They can be summarized as follows:

1. Threshold of accuracy based on comparing various wind tunnel experiments
2. Computational efficiency
3. Minimum complexity and thorough documentation that can be replicated for practical applications
4. Reliability of results for structural design
5. Peak values (EVA) and post-processing tools
6. Modelling of high frequency (small length) eddies with the proper physical energy content since they relate more with the peak values

Furthermore, a discussion regarding the lack of consensus on V&V in LES structural CWE application was presented. V&V metrics of the proposed methodology in this thesis were presented and are further elaborated in Chapters 4 and 5.

CHAPTER 4: DYNAMIC TERRAIN METHODOLOGY VIA LES (LES-DT)

This Chapter is based on material from Potsis and Stathopoulos, (2024). Some modifications of the published paper were made for uniformity reasons.

4.1 Introduction

Buildings and bridges in the atmospheric boundary layer (ABL) are exposed to wind loads, and design criteria need to be addressed to establish safe and economical structural systems. Computational Fluid Dynamics (CFD) is an innovative tool, recently added to the toolbox of modern practitioners, that expands the abilities of the structural design practice for wind loads. Although a uniform procedure in order to calculate peak (design) values with confidence is yet to be defined, important steps have been made towards this goal in the last decades. The present Chapter provides an overview of the established procedures and proposes a new approach that can evolve the current state-of-the-art.

Computational wind engineering was formally born as a scientific field due to the inaugural conference of CWE 1992, in Tokyo. In the first years, most of the studies focused on mean wind flow representation and mean pressures on building envelopes. For example, Murakami et al., (1992) and Delaunay et al., (1995), captured the mean pressures on a symmetry line of a cubic building, with good agreement compared to wind tunnel experimental results. Mean pressures on a similar low-rise building were captured accurately in Mochida et al., (1993), Selvam, (1997), Richards and Hoxey, (1992). During that time the complexities of modeling oblique wind directions and mean pressure in non-symmetrical locations were presented in Stathopoulos and Zhou (1993). Stathopoulos (1997) was one of the first endeavors to define the evolution of CFD practice, based on structural wind engineering applications. The study concluded that attention needs to be given to expressing accurately the turbulence features in the ABL and that experimental procedures and CFD should work together, but the final decisions should be based on the former.

A review of computational wind engineering was conducted that included environmental and structural application of CFD, during the last three decades of research (Potsis et al., 2023). Among the conclusions it is stated that the environmental field has gained more focus from the research and industrial community in the last three decades, usually due to the lower computational burden and the simplicity of the procedures. A fundamental difference between the environmental and structural field is that for the latter time series of the values of interest are indispensable, which has a direct impact on the turbulence modeling selection. For example, usually the RANS approach is selected for environmental applications and LES for structural. Comparison studies between the two modeling procedures of RANS and LES can be found that highlight their differences (Tominaga et al., 2008a, Khaled and Aly, 2022). LES modeling is accompanied by more complicated procedures and necessitates numerically expensive computational domains for calculating peak (design) wind loads on buildings. During the last decades, the modeling techniques have become more complex, and the results of the fluctuating wind pressures have reached the target accuracy in many cases (Potsis et al., 2023), mostly of it due to the use High Performance Computations (HPC) that have rapidly expanded in the field.

A fundamental difference between various seminal works in the last decades that were able to model accurately peak pressures, are the inlet conditions that the authors used to express the turbulence that interacts with the building of interest. Detailed overview of the inlet conditions that have been utilized and their evolution through the years can be found in (Dhamankar et al., 2018, Wang, et al., 2022, Potsis and Stathopoulos, 2022). For example, Nozawa and Tamura, (2002) and Ono et al., (2008), used the recycling technique established by Lund (1998) to evaluate the fluctuating loads on low-rise buildings. In both cases, the results correlated well with experimental measurements. Huang et al., (2010) utilized the Random Flow Generator (RFG) method, first introduced by Kondo et al.., (1997), to evaluate the overall wind loads on a high-rise building. Results correlated well with experiments at the time, while the RFG method was further developed by Smirnov et al., (2001), Castro and Paz, (2013), Aboshosha et al., (2015b), Yu et al., (2018), Patruno and Ricci, (2018), Bervida et al., (2020) and Melaku and Bitsuamlak, (2021). Daniels et al. (2013) utilized the Digital Filtering method, first presented by Klein et al.., (2003) and further developed by Kim et al., (2013) and Lamberti et al., (2018), to calculate the fluctuating loads on a similar high-rise structure. Local fluctuating pressures were estimated within an acceptable range from experiments, while of great interest is the non-gaussian nature of these pressures on the sides of the building. Yan and Li (2015) used various synthetic methods to calculate the fluctuating loads on the CAARC benchmark building, Among the methods is the synthetic vortex method, fist established by Jarrin et al. (2006) and further developed by Polleto et al., (2013) and Luo et al., (2017).

Ricci et al., (2017), used the Modified Discretizing Synthetic Random Flow Generator Technique to reproduce the flow field of a suburban terrain and model the mean and fluctuating loads on a low-rise building for perpendicular and 45° wind angle. Results correlated well with experiments, although the tuning of the inlet conditions needs accurate modeling of the entire wind tunnel, which leads to an expensive computational procedure. Guichard (2019) used an improved version of the Random Flow Generator of Yan and Li 2015, by modeling more efficiently the turbulence decay in the domain from inlet until the building, which was selected as a cube, a typical high-rise and low-rise. Comparisons were made according to TPU (2013) and full-scale data from the Silsoe Cube (Richards and Norris, 2012). Results correlated well with the target experiments for mean, standard deviation (hereafter std), min and max values. Wind loads on a low-rise cube were studied, by using a precursor domain with periodic inlet (Ong et al., 2020). Various sub-grid models of LES produced similar errors compared with experimental results of TPU (2013). A similar building was included in a computational domain with rectangular and circular holes to generate vortices at the inlet (Papp et al. 2021). Pressure coefficients for perpendicular and oblique wind direction of 45° correlated well with experimental and full-scale data.

Melaku et al., (2022) concluded a study for the fluctuating wind loads on a roof-mounted cube on a low-rise building. Mean, std, skewness and kurtosis of pressure coefficients for various wind directions were examined, by using a synthetic inlet already tuned previously by the authors (Melaku and Bitsuamlak, 2021). Local and total loads were found to be within the marginal error of 20%. Geleta and Bitsuamlak, (2022), used the virtual wind tunnel technique to model the wind flow and pressures on a low-rise building, with similar dimensions as the one that is presented in this Chapter. They modeled mean, std, and peak local loads for two perpendicular and one oblique wind direction of 45°. Comparisons of the pressure results for symmetric taps, proved the validity of the proposed technique.

Monitoring closely the field of inlet conditions in LES and peak pressure evaluation since 1992, and especially since 2017, results in the following conclusions from the authors' perspective: first, a simple computational procedure should be created, that practitioners can easily apply in order to extract accurate peak pressure values on the building envelope. Second, as concluded in (Potsis et al., 2023), existing synthetic inlet methods are too complex and the resulting fluctuating pressures are very sensitive to the numerical set-up – optimization of the important parameters is still an issue. Third the virtual wind tunnel technique, although accurate, is computationally expensive and non-easy to implement for practical use, where various wind directions are of design interest. This means that the procedure should be applicable for coarse computational domains and the level of accuracy should be similar to the accuracy achieved in the well-established experimental results. Similar to what was stated in Blocken, (2014); utilizing LES modeling with coarse computational domain in a precise way, might evolve the current capabilities of structural engineers to calculate wind design loads.

To achieve the above goals the Dynamic Terrain (hereafter LES-DT) method has been developed (Potsis and Stathopoulos, 2022), a technique that regards coarse mesh and LES modeling, with a novel approach for the inlet conditions. Definition of the methodology and assumptions are mentioned in Section 4.2, where the main procedure is divided into four steps. First is the inlet data acquisition and second is the spectral tuning process, with the target to correctly express the spectral content of the longitudinal velocity fluctuations that will interact with the building of interest. Third step is the turbulence modeling of the incident flow as to express the mean and turbulence intensity profiles according to the target ones, based on the exposure of the building under discussion. The final step regards the pressure time series acquisition from selected locations on the building envelope. In the present work, a low-rise building was selected as a case study, and roof loads were examined for perpendicular and oblique wind direction of 45°. Experimental conditions in wind tunnel, computational details regarding the set-up of LES, characteristics of the turbulence flow field and flow visualization figures are presented in Section 4.3. Comparison of pressures in terms of mean, std, and peak values are presented in Section 4, with contours that specify the spatial distribution of the pressures. In Section 4.5, the benefits of the method are provided, and the Chapter concludes with final comments in Section 4.6.

4.2. Process description

Wind flow patterns interact with solid surfaces and expose structural systems to wind loads. In this process, the effects of high turbulence intensity may be critical for calculating design values. In Figure 4.1 a collection of velocity profiles obtained with successive data from the Concordia Wind tunnel (Stathopoulos, 1984) are presented. These are instantaneous profiles measured every 1000 Hz including their corresponding mean profile, during 23 seconds of experiments. This duration is long enough to assume stationarity of the flow, appropriate for full-scale representation. Clearly, during this time window the building is exposed to velocity profiles that differ significantly in terms of vertical distribution. It is expected that these variations will impact the corresponding variations of the local pressure coefficients and overall loads on the building envelope.

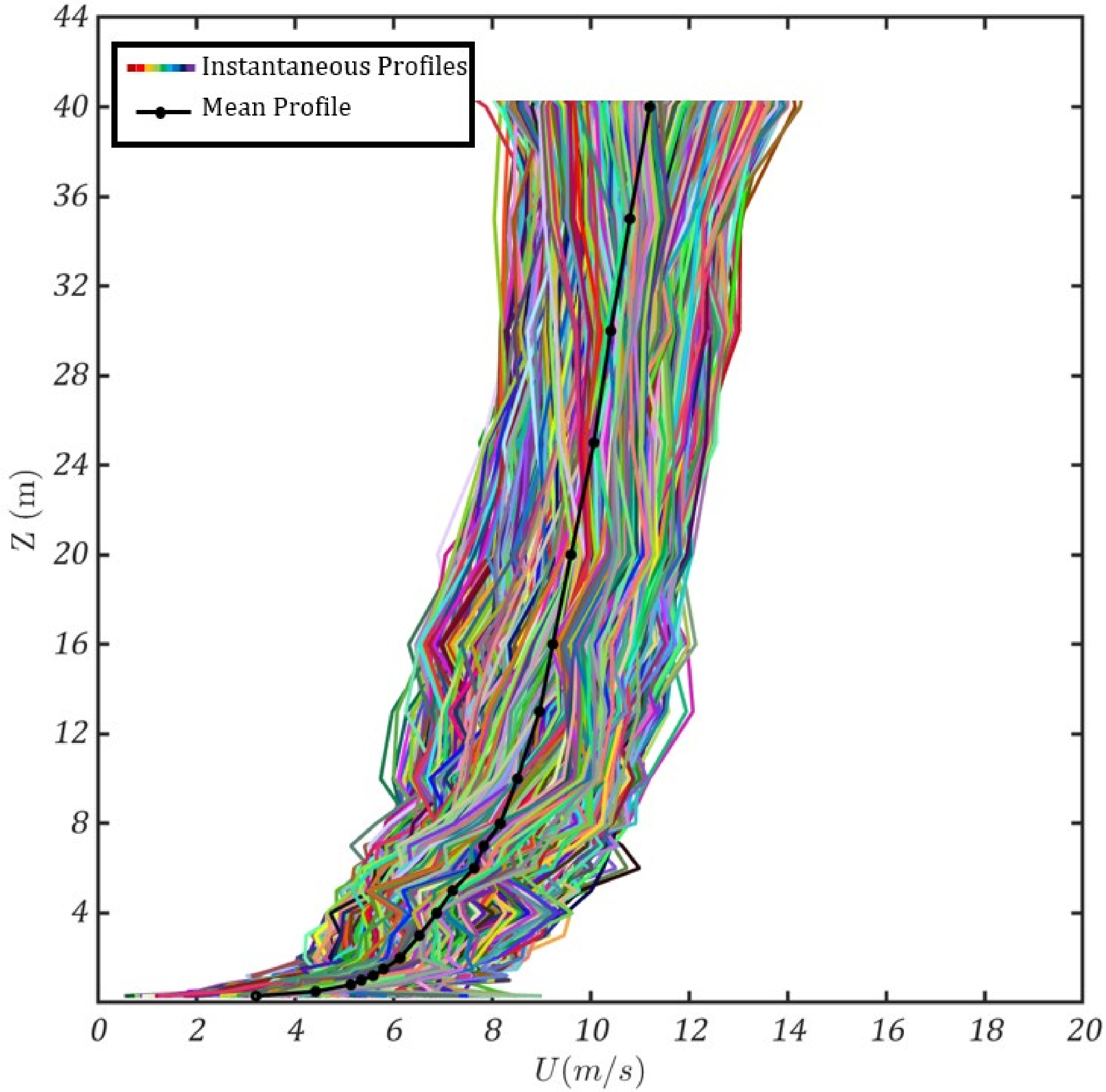

Figure 4.1: Instantaneous profiles and corresponding mean profile of successively derived experimental data with frequency 1000 Hz for a total duration of 23 s in Concordia Wind Tunnel.

The LES-DT method reformulates the character of these turbulence features. In a fictitious way, it is assumed that these instantaneous profiles are generated by virtually changing the actual terrain roughness respectively. These profiles are introduced successively at the inlet plane of the computational domain, as if they were the acting mean profiles, for each instantaneous terrain assumed. Each profile is modeled in a quasi-steady way and propagates inside the domain to interact with the building envelope. The duration for which each profile is introduced and how frequently this fictitious terrain is changed (inlet frequency hereafter), has proven to be a critical parameter to represent the energy of the small temporal (high frequency) and length scales of turbulence (Potsis and Stathopoulos, 2022). For this duration, an individual pressure value is extracted from locations of interest, to construct the final pressure time series that are used to calculate peak values by Extreme Value Analysis. The methodology was developed in OpenFOAM v2012, based on the Pressure-Implicit with Splitting Operators (PISO) algorithm and turbulence modeling with LES, by utilizing the WALE subgrid model (Nicoud and Ducros, 1999).

4.2.1 Wind tunnel database – Velocity time series

Experimental velocity time series are a vital part of constructing the inlet data for the LES-DT method and consist of the first stage of the process. Instead of using synthetic methods, or recycling techniques, the LES-DT method utilizes velocity time series from wind tunnel measurements. The velocity data are introduced in a quasi-steady manner at the inlet plane of the computational domain by using the *timeVaryingMappedFixedValue* function of OpenFOAM. The locations are identical to the heights for which the velocity time series are extracted from the wind tunnel, while linear interpolation techniques are adopted spatially, in the vertical and horizontal direction of the inlet plane. The velocity data were extracted from Concordia Wind Tunnel (Stathopoulos, 1984) and more information regarding the wind tunnel procedure can be found in Potsis and Stathopoulos, (2022). The extracted time series have an output frequency of 1000 Hz that matches the higher efficiency of cobra probe that was used. Output frequencies higher than 2000 Hz were also tested, but the corresponding velocity time series were not as stable and precise, thus were not used. In

Figure 4.2 the statistical parameters of the velocity time series are presented in terms of mean velocity, turbulence intensity and integral length scale.

The pressures that will be developed on the building envelope are closely related with the wind velocity profile that interacts with it. The fluctuations of the incoming velocity profile are more influential than the mean values when modeling pressures on low-rise buildings (Tieleman et al., 1997). The energy of those fluctuations in the frequency domain should also be considered, and match with theoretical spectrum distribution. This energy is usually expressed based on the normalized spectral density function versus the normalized frequency and is presented in Figure 4.3 for the along wind direction of the velocity. The theoretical von Karman spectrum (von Karman, 1948) is also displayed for comparison.

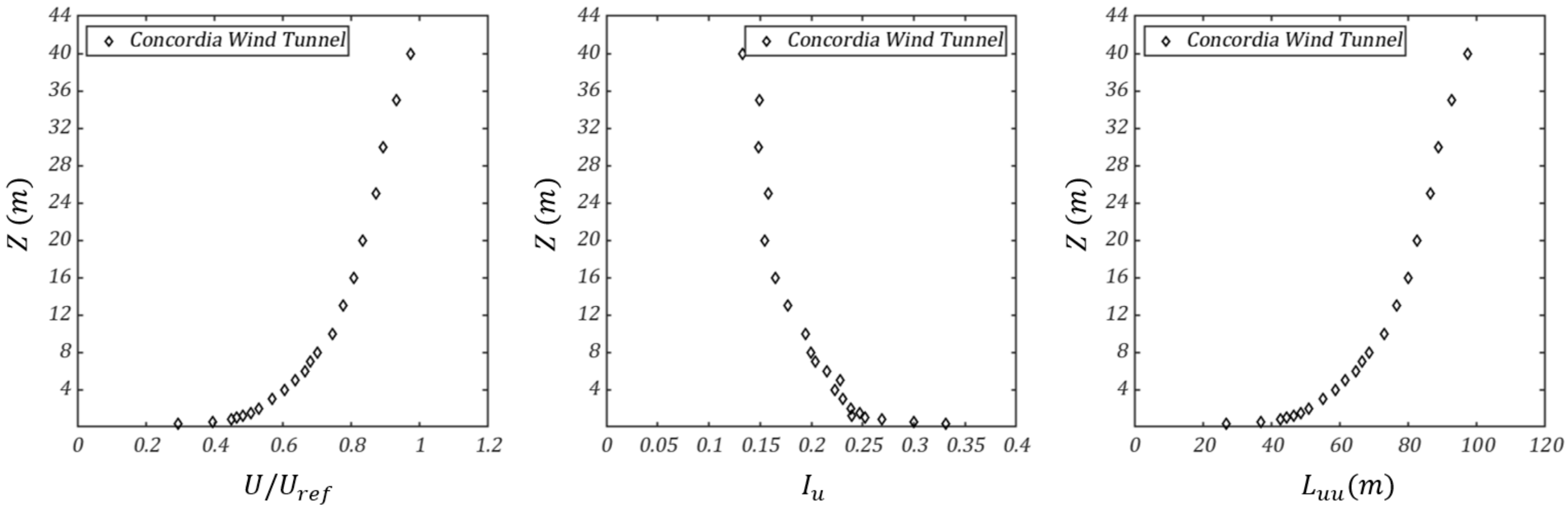

Figure 4.2: Mean (left), turbulence intensity (middle) and integral length scale (right) profiles of the experimental procedure.

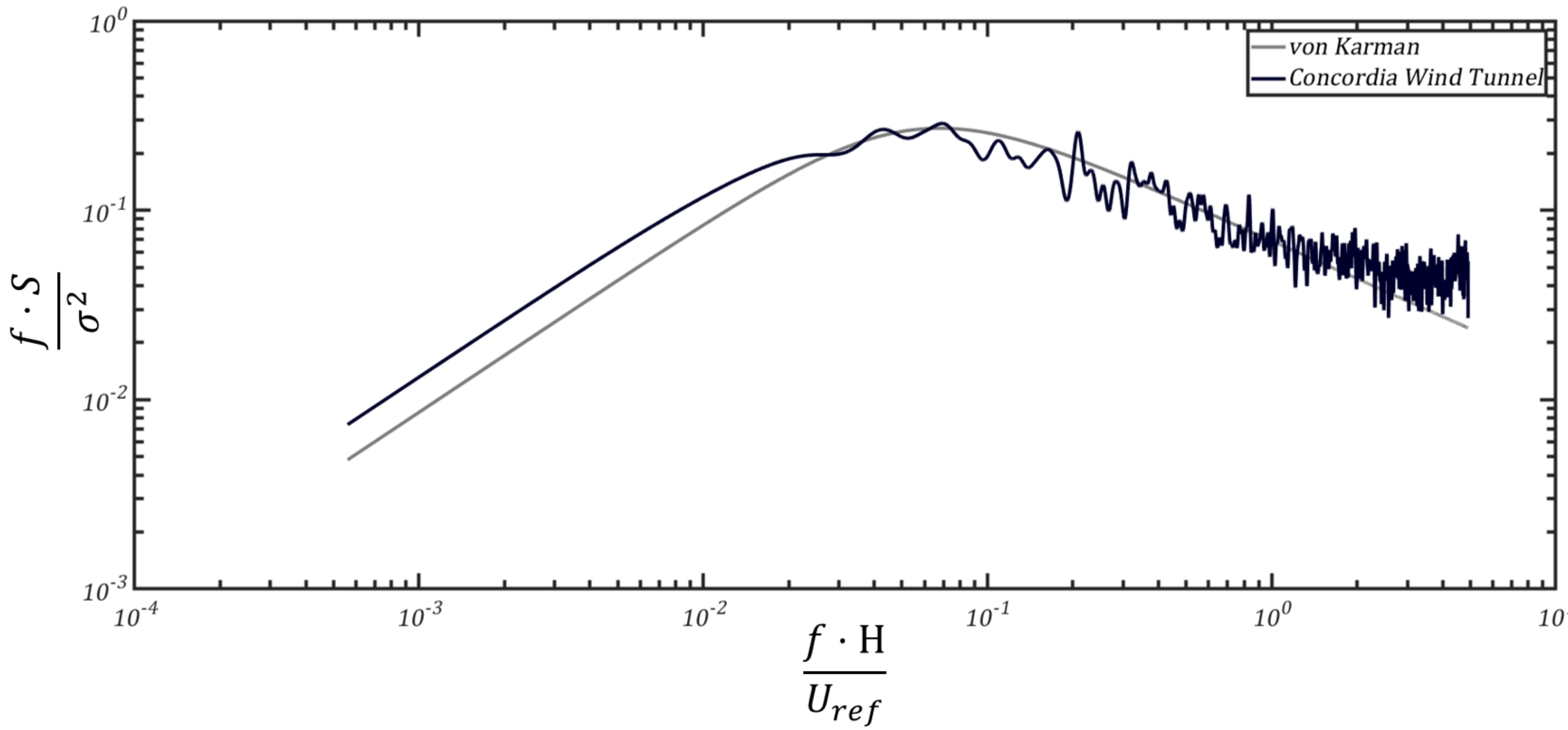

Figure 4.3: Normalized spectral content for z = 8 m in full scale

4.2.2 Spectral tuning

The spectral tuning process is the second stage of the LES-DT method, in order to express the energy content of the high-frequency (small-size) eddies that interact with the target building. Focus is given on the streamwise component of the velocity since it is the dominant direction of the wind flow. As established by initial parametric studies presented in Potsis and Stathopoulos (2022), the inlet frequency of the velocity data relates closely with the energy content in the high frequency range in the longitudinal velocity, even after the normalized cut-off frequency limit of LES (n_c). For example, two uniformly meshed computational domains were used, a fine domain with 28 million elements and $n_{c,f} = 1.05$ and a coarse domain with 0.9 million elements and $n_{c,c} = 0.49$. The normalized cut-off frequency was calculated based on procedures proposed in Pope, (2006). In Figure 4.4, the normalized spectrum is presented for both fine and coarse computational domains, with inlet frequency 1000 Hz ($\sim 20 \cdot n_{c,c}$) which is the same as the frequency which the time series were extracted from Concordia Wind Tunnel. In both cases the drop of energy is observed after n_c, similar to what is seen by using other inlet conditions (recycling, synthetic or virtual wind tunnel) (Yan and Li 2015, Ricci et al., 201, Lamberti et al., 2018, Melaku and Bitsuamlak, 2021, Vranešević et al., 2022, Geleta and Bitsuamlak, 2022). In contrast, when using inlet frequency of 5000 Hz ($\sim 100 \cdot n_{c,c}$), even by using the coarse computational domain, the spectrum of the longitudinal velocity agrees more with the experimental measurements and the theoretical von Karnam spectrum.

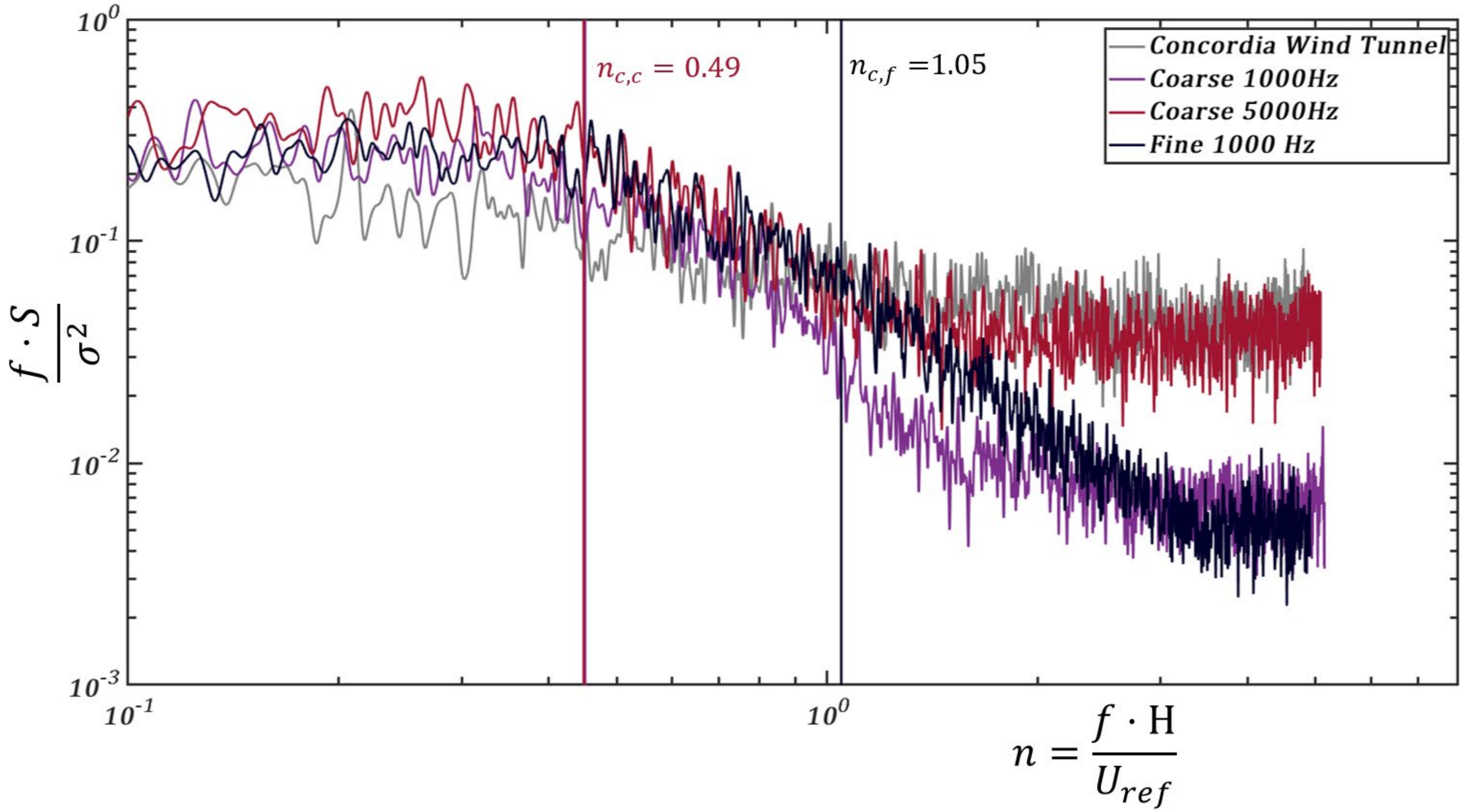

Figure 4.4:Normalized spectrum at z = 8 m in full-scale, after the cut-off frequency, by using coarse and fine mesh and inlet frequency of 1000 Hz and 5000 Hz, at the location of the building in the computational domain

Choosing the appropriate inlet frequency depends on the mesh formulation, the target building that is going to be modeled and the range of frequencies that targeted to be validated from experimental results and numerical schemes. At this moment, creating a generalized approach to evaluate this parameter a priori might introduce a level of complexity in the method that is undesirable. Thus, an empirical iteration process is more favorable to estimate the most suitable inlet frequency depending on the numerical setup. It should be noted that the target is not to model all the length scales until Kolmogorov, but the small scales that are relevant with the experimental instrumentation used in the wind tunnels. Different mesh configurations and numerical schemes were also tested, and the same qualitative outcome was noticed: coarser domains need larger inlet frequencies, to express the small turbulence scales accurately. Also, it is important to stress out that the spectral content is measured inside the computational domain, at the incident flow and not at the inlet plane. In this way, the small turbulence vortices in the region of n = 0.1 – 5 interact with the building at the correct energy level. As mentioned in Morrison and Kopp, (2018) modeling the length scales in the region n > 0.1 correctly is the minimum requirement, for accurate prediction of peak loads on building envelopes. This highlights the importance of this step, and the big difference between the LES-DT method and the methods found in the current state-of-art.

4.2.3 Incident flow modification

Third step of the process is to match the first and second statistical moments (mean and root-mean-square) of the longitudinal velocity profile that interacts with the building of interest. This step is vital since the turbulence features tend to decay rapidly in the computational domain form inlet until the building location and the mean speed and turbulence intensity profiles need to be matched with the target values measured in the wind tunnel for validation. Various approaches have been used through the years from different authors to address this issue. Ricci et al., (2017; 2018), modeled roughness elements based on Lettau, (1969), to keep the turbulence features in the distance from inlet to the building. This leads to an increased computational cost, that usually exceeds the capacity of practical use. Lamberti et al., (2018), optimized the inlet conditions of the SDFM method, based on Kim et al., (2013) in order to sustain the turbulence features. Although the final results were satisfactory, the procedure can not be generalized that easily for every type of inlet, or any target exposure. In the modeling procedure of Guichard (2019), a different approach was considered, based on augmenting the fluctuations on the inlet plane, so the turbulence decay inside the domain leads to the target profile. This trend has been followed ever since, with authors augmenting the velocity fluctuations uniformly by a specific percentage at the inlet (Melaku et al., 2022, Xing, 2023). Abu-Zidan and Nguyen (2023) highlighted the complexity of scaling inlet data as to capture the target turbulence intensity at the location of interest and used machine-learning approach to optimize the inlet time series based on the synthetic technique of Yu et al., (2018).

Turbulence decay is sensitive to the computational set-up (e.g., mesh size, wall boundary conditions, solution schemes). All approaches dealing with turbulence decay in the state-of-the-art are efficient according to the specified set-up of various parameters that the authors chose in their studies. To define a more generalized (and simple) approach that is insensitive to those parameters a scaling technique is applied to the average speed of the entire series and the amplitude of the velocity at each time step, for each vertical location under control. This way the user can modify the mean and standard deviation profiles based on the vertical control points. The procedure starts by introducing the tuned time series at the inlet of the computational domain that has identical configuration to the one with the building, but without it, so not to alter the flow. The steps of the procedure are as follows:

1. The mean and std deviation values of the control points are extracted from the location of interest, as seen in Figure 4.5, define as $I_{B,1}$. In this way the degree of turbulence decay is defined.

2. The mean values are subtracted from the time series.

3. The velocity values are increased (or decreased) based on $\acute{u}_{inlet,2}(z) = \frac{\acute{u}_{target(z)}}{\acute{u}_{inlet,1(z)}}$ for the suburban exposure and based on $\acute{u}_{inlet,2}(z) = (\frac{\acute{u}_{target(z)}}{\acute{u}_{inlet,1(z)}})^2$ for the open exposure.

4. The new mean speed calculated from $\overline{U}_{inlet,2}(z) = \frac{\overline{U}_{target(z)}}{\overline{U}_{inlet,1(z)}}$ is added to the time series.

This very simple scaling technique allows the user to gain control of the mean speed and turbulence intensity profile at the location of interest, based on the selected set-up conditions, but not affected by them. For example, if a less dissipative numerical scheme is selected, the same technique can be used to correctly adjust the mean and turbulence intensity, since the degree of influence of the scheme is defined in the turbulence decay measured at step 1. Figure 4.6 shows the above technique can adapt the mean, std, and turbulence intensity profile according to the target one. For the purposes of this study this technique was applied twice, in order to define an open and a suburban terrain.

During the sensitivity studies as to define the linearity of the turbulence decay parameters (mean and std) in the scaling technique of the inlet data, two main conclusions can be drawn: first, the linearity of the decay of the mean speed (step 4) was evident besides the target mean profile (open or suburban) or the specific numerical set-up (mesh size and numerical schemes). Second, the turbulence decay of the std deviation is more sensitive to the mesh size and the target std deviation profile, and it was noticed that for suburban exposures the linear expression of Step 2 is appropriate, while for the open exposure the nonlinear equation fits the parameters more accurately. It should be noted that other types of equations were tested, but the data did not give desirable outcomes. Although, the dissipation of velocity fluctuations is complex, the nature of the above procedure ensures that the target mean and std deviation profiles can be achieved within the target level of accuracy.

Another important aspect of the above procedure is that it provides the ability to stochastically change mean or std deviation profiles independently, for each vertical control point individually. In this way, parametric studies that consider the consequences of the turbulence incoming wind flow to the pressures that are developed in the building envelope can be conducted easier. Also, it has the potential to model more realistic exposure conditions, based on the actual exposure of buildings in urban areas for extreme synoptic or non-synoptic events.

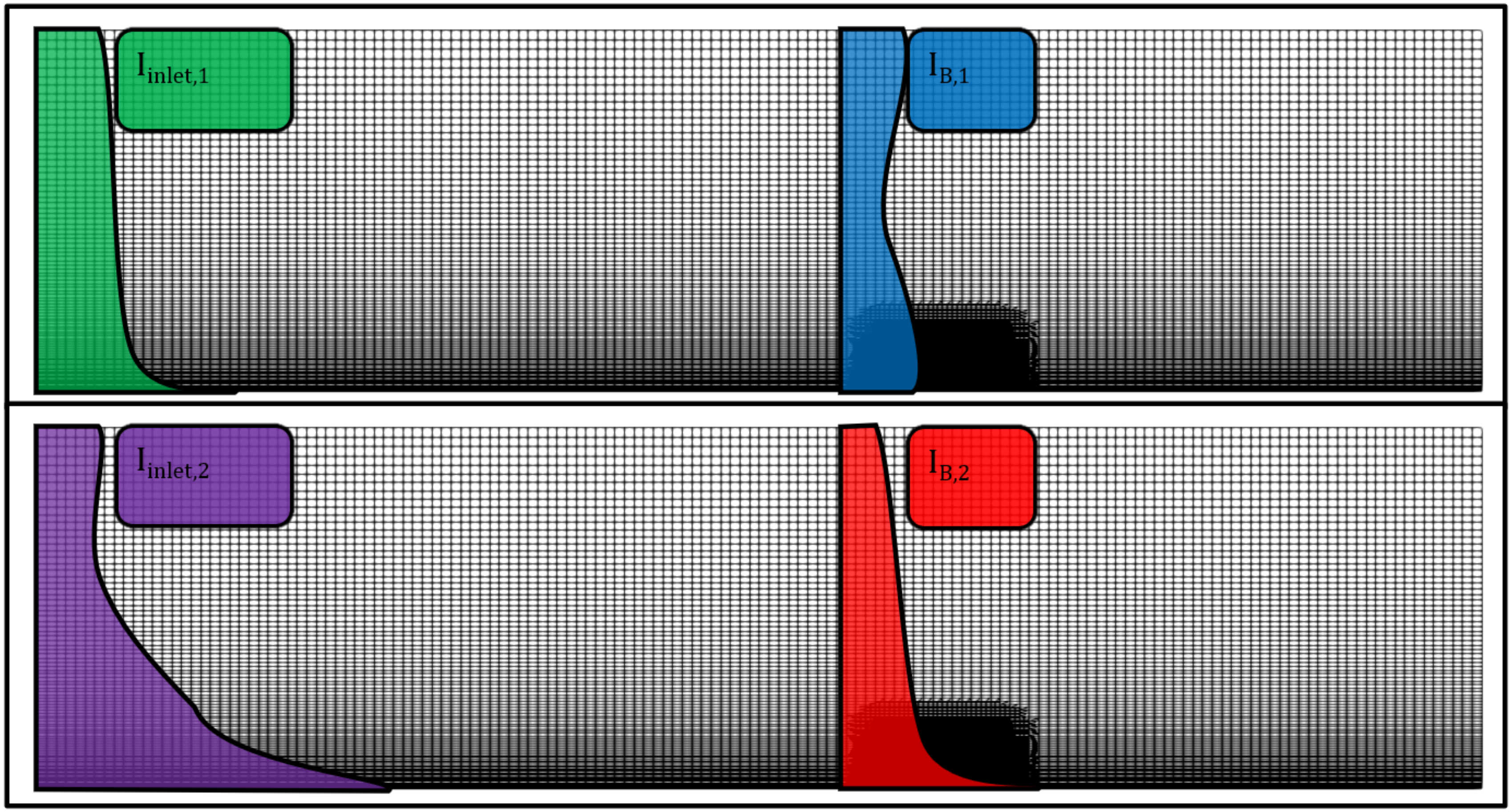

Figure 4.5: Turbulence intensity at the first (top) and final steps (bottom) of the procedure

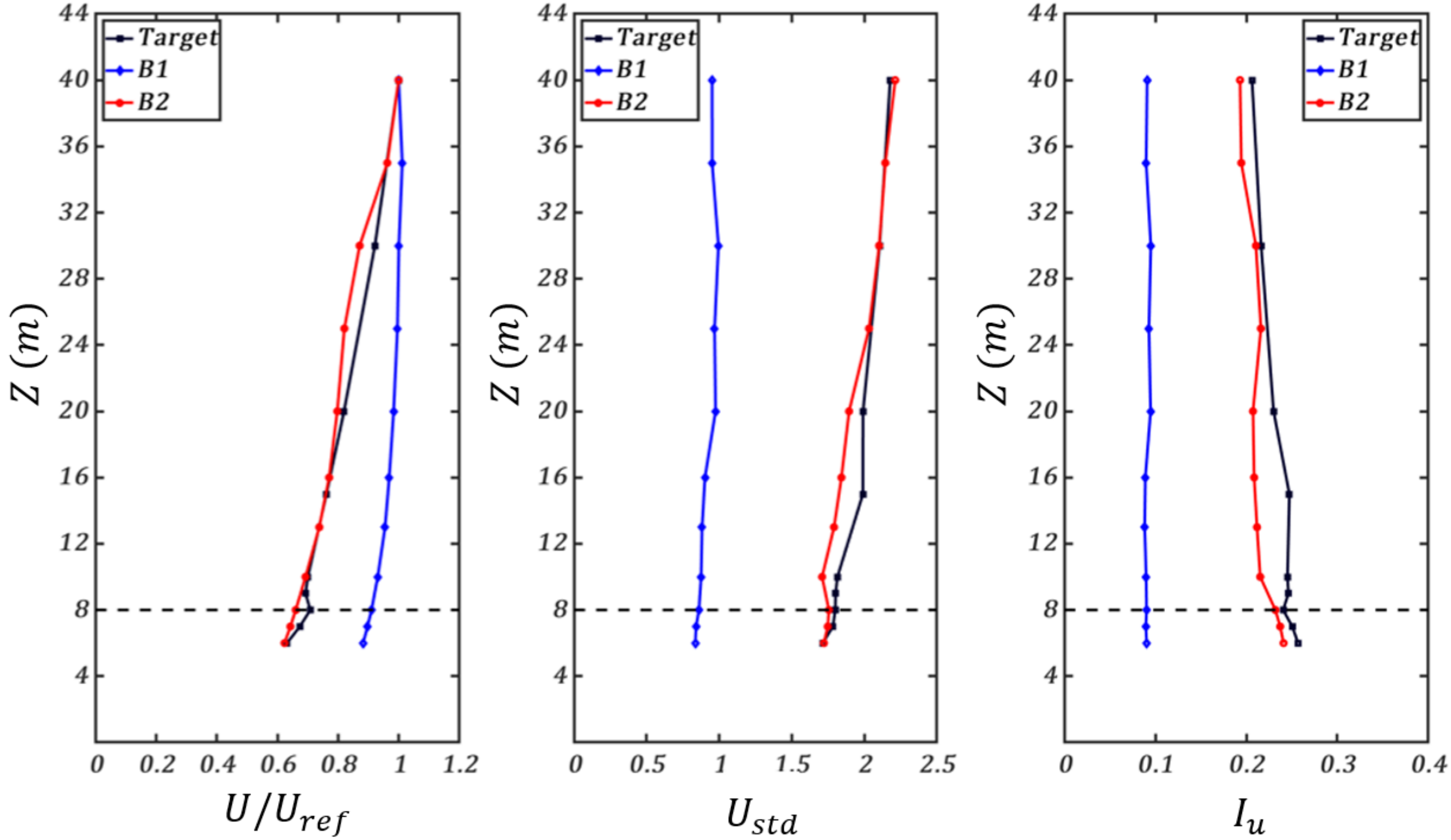

Figure 4.6: Scaling technique as displayed in Figure 4, for mean (left), std deviation (middle) and turbulence intensity (right) velocity profiles.

4.2.4 Pressure time series acquisition

The final step of the method is to remove the corresponding computational cells and to create an obstacle in the flow field, that represents the building of interest, by using exactly the same mesh formulation. Numerical pressure taps are inserted in the computational domain and pressures are extracted for each time step of the computational procedure. Due to the quasi-steady alternation of the inflow between the successive profiles, time discontinuity is inherently introduced into the computation. For this reason, the algorithm needs a couple of time steps to converge into the new conditions. As to extract meaningful pressure time series, the data during those time steps are discarded, and *one* averaged pressure value is extracted for the duration which the inflow is at a steady state. Finally, the extracted time series is treated by a second average, based on the target output frequency. In the present study, the output frequency was based on the experimental data and selected as 500 Hz for the validation of TPU (TPU Aerodynamic Database, 2013) and NIST (NIST, 2003) and 300 Hz for validation of Concordia Wind Tunnel (hereafter CWT). For computational results the abbreviation "Dynamic Terrain" will be used hereafter as to keep the original terminology of Potsis and Stathopoulos, (2024). The abbreviation also used for the Dynamic Terrain method is LES-DT throughout this Chapter.

Pressure coefficients are calculated by normalizing the instantaneous pressures based on the dynamic pressure at roof height based on $C_p = \frac{p-p_0}{0.5\cdot\rho\cdot\bar{U}^2}$. Extreme value analysis was conducted to calculate the peak values of the pressure coefficient by using the Gumbel distribution (Type 1). The Best Linear Unbiased Estimator (BLUE) was used to calculate the necessary fitting parameters and the percentage of non-exceedance was chosen as 78% (TPU Aerodynamic Database, 2013).

4.3. Wind loads on buildings

4.3.1 Wind tunnel experimentation

Wind loads for design of low-rise buildings are usually based on code provisions or wind tunnel results, depending on the complexity of the exposure conditions. In this sense, codes define various exposures that isolated buildings should be designed against. In the National Building Code of Canada 2020 the open and urban exposures are selected as the most representative conditions for the interaction between natural wind and buildings. In the present study, an isolated building was chosen with full-scale dimensions 8 m x 16 m x 24 m (H x B x D), for open and suburban exposures for perpendicular and 45 wind angles of attack. Focus is given to the roof loads since those are the most influential in the final design decisions.

Experimental results are available from three different wind tunnels for the selected building and their modeling parameters are presented in *Table 4.1*. First, for the open exposure results can be found from NIST database with a pressure tap formulation presented in Figure 4.7a. In total 336 pressure taps were placed in the model, with more dense formation on the top left corner. The length scaling factor for the building of the study is 1:65 (SF_L in *Table 4. 1*), which falls in line with geometric scale criteria to ensure compatibility with lengths associated with the approaching flow (ASCE/SEI 49-21, 2022). Second, experimental results were conducted in CWT with 192 pressure taps, whose location is presented in Figure 4.7b. The scaling for the building length was chosen as 1:160. Regarding the suburban exposure, similar experimental results are found in NIST and in TPU (with taps formulation in Figure 4.7c). In the experimental procedure of TPU the scaling is 1:100, with 96 pressure taps on the roof of the model. The scaling differences from each experimental procedure are expected to affect the resulting pressures, although all of them respect provisions established by ASCE (ASCE/SEI 49-21, 2022).

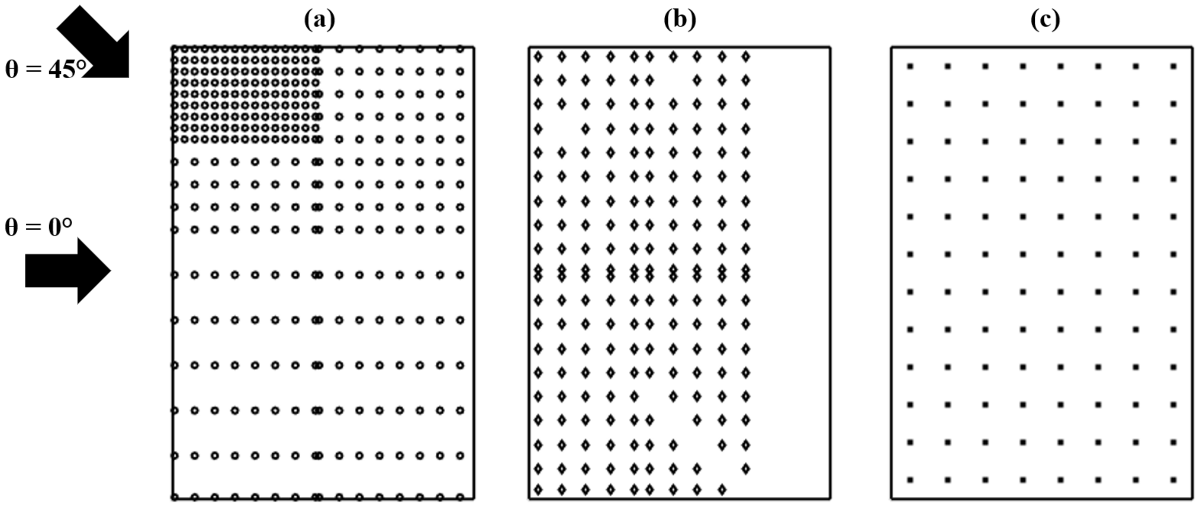

Figure 4.7: Pressure taps locations of the roof of the three models.

Scaling studies are limited in the literature, due to the complexity and the difficulty to generalize the experimental results. The relaxation of the scale between NIST and CWT, and NIST and TPU for the given configuration is expected to be negligible for the mean values, although it should be more impactful for the peak values, since the relaxation factors correspond to 1.6 and 2.2 (Stathopoulos and Surry, 1983, Jayakumari et al.., 2023).

4.3.2 Computational approach

An advantage of the LES-DT method is that the mesh can be coarser compared to similar modeling approaches, in terms of total number of cells, refinement near the building and mesh at the approaching flow region. Besides that, larger mesh sizes have proven beneficial in these types of modeling (Gousseau et al., 2013, Xing, 2023). Interested readers are referred to Celik et al., (2005), where the authors discussed this "counter-intuitive" result. For both open and suburban exposures, the same mesh was used for perpendicular and oblique wind direction of 45° (mesh for the oblique wind direction is exactly the same as the perpendicular but rotated). The mesh was generated with the snappyHexMesh function of OpenFOAM. The computational domain has similar dimensions as the Concordia Wind Tunnel testing section, L_x = 2 m x L_y = 1.8 m x L_z = 0.5 m. The location of the outlet was also considered to be further downstream, and the results provided negligible deviations on the incident flow and the pressures on the building envelope. First, the domain is divided by 150 in the x-axis, 180 in the y-axis and 100 in the z-axis., thus a meshed box of elements is created. Inflation of the mesh is applied in the z-axis, close to the ground. A box of 0.16 m x 0.24 m x 0.08 m is inserted 1.25 m after the inlet. In a region of H/2 outside of the box the mesh size was selected as H/32, and in a region of H/4 as H/64. Finally, the mesh near the building in a region of H/16 was H/128. This leads to a total number of almost 4 million cells, the formulation is consistent with the seminal guidelines in Tominaga et al., 2008b - see Figure 4.8.

Table 4.1: Modeling parameters from experiments of TPU, NIST and CWT and LES-DT computational method

	TPU	**NIST**		**CWT**	LES-DT	
H (m)	0.08	0.12		0.05	0.08	
B (m)	0.16	0.24		0.10	0.16	
D (m)	0.24	0.38		0.15	0.24	
H:B:D	1:2:3	1:2:3.16		1:2:3	1:2:3	
Uh (m/s)	7.65	Suburban	Open	9.41	Suburban	Open
		7.66	10.65		7.65	10.65
Iu,h (%)	24.5	28.5	16.9	15.1	23.8	14.1
SFL	100	65		160	100	
Pressure Output Frequency	500	500		300	500/300	

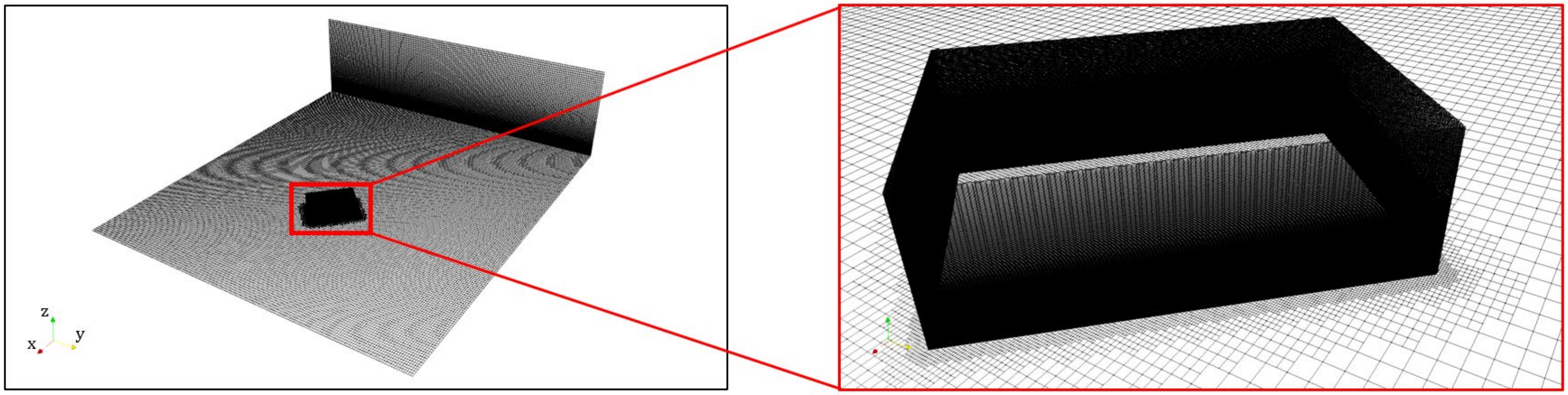

Figure 4.8: Mesh configuration of the computational domain for 45° wind angle of attack

During the tuning and turbulence modeling process presented in Section 4.2, the computational domain is empty and then the mesh is removed to create the building that will obstruct the flow. This is done as to not alter the flow in the initial steps and at the same time to create a computational domain with exactly the same conditions in the inflow region, with and without the building. As suggested in Blocken et al., (2007), an empty domain needs to be tested initially to validate the flow conditions before obstacles of interest are inserted. After the flow is validated, the mesh near the building needs to be fine enough as to be able to capture the shear stresses at the first computational cells – a condition that relate with the y^+ values. The resulting mean y^+ values on the building envelope are below 5, for all results presented in the paper.

Regarding the velocity boundary conditions: at the inlet the *timeVaryingMappedFixedValue* function is used, at the left, right and top sides the *symmetry* function, at the ground and at the building surface the *no-slip* condition and at the outlet the *zeroGradient* condition. Regarding the pressure boundary conditions: a *zeroGradien*t condition is used at the inlet and at the ground, the *symmetry* condition at the left, right and top wall, and a value of 0 is set at the outlet plane. The time step of the analysis was chosen based on a maximum *CFL* number of 0.4. Regarding the solution schemes: for the pressure the *GAMG* solver and for the velocity the *smoothSolver*. Regarding the discretization schemes: for the time dependent term the *backward* scheme, for the gradient and divergence terms the *Gauss linear* scheme, for the Laplacian term the *Gauss linear corrected scheme,* the interpolation scheme was chosen as *linear* and for the snGradient (normal) *the corrected scheme*. As already mentioned, the turbulence model used was the WALE model (Nicoud and Ducros, 1999). All analyses were run in parallel in the Beluga Cluster of the Digital Research Alliance of Canada, by using OpenFOAM v2012.

4.3.3 Turbulence flow field characteristics and visualization

- Empty computational domain

Calibration of the incident flow is done in an empty computational domain, similar to the one presented in Figure 4.8, but without the building. It is important to initially estimate the vortical structures of the wind flow at the empty computational domain to evaluate how they evolve inside the domain. In Figure 4.9 the vorticity in the streamwise direction (XZ plane) at the middle of the computational domain is visualized for 4 different snapshots of the analysis. The vortices are presented for t^*=0.2, 0.8, 1.98 and 19.8, where $t^* = \frac{t \cdot U_\infty}{L_x}$ is the time of the analysis normalized with the length of the computational domain (L_x) and the mean speed at the top of the ABL (U_∞). In this way, for one unit of normalized time the inflow has moved from inlet to outlet one time. Vortical structures, which vary in terms of size and magnitude, are introduced in the computational domain from the beginning of the analysis – see Figure 4.9. Thus, they are introduced immediately from the inlet plane and eventually fill up the entire computational domain. Vortices are not simply convected, but mixed and un-stabilized as they move downstream. Length and time scales of vortical structures that are generated in this way are sensitive to the adopted parameters defined by the inlet conditions. The ABL that is generated is uniform in the vertical direction (Y-axis) of the flow.

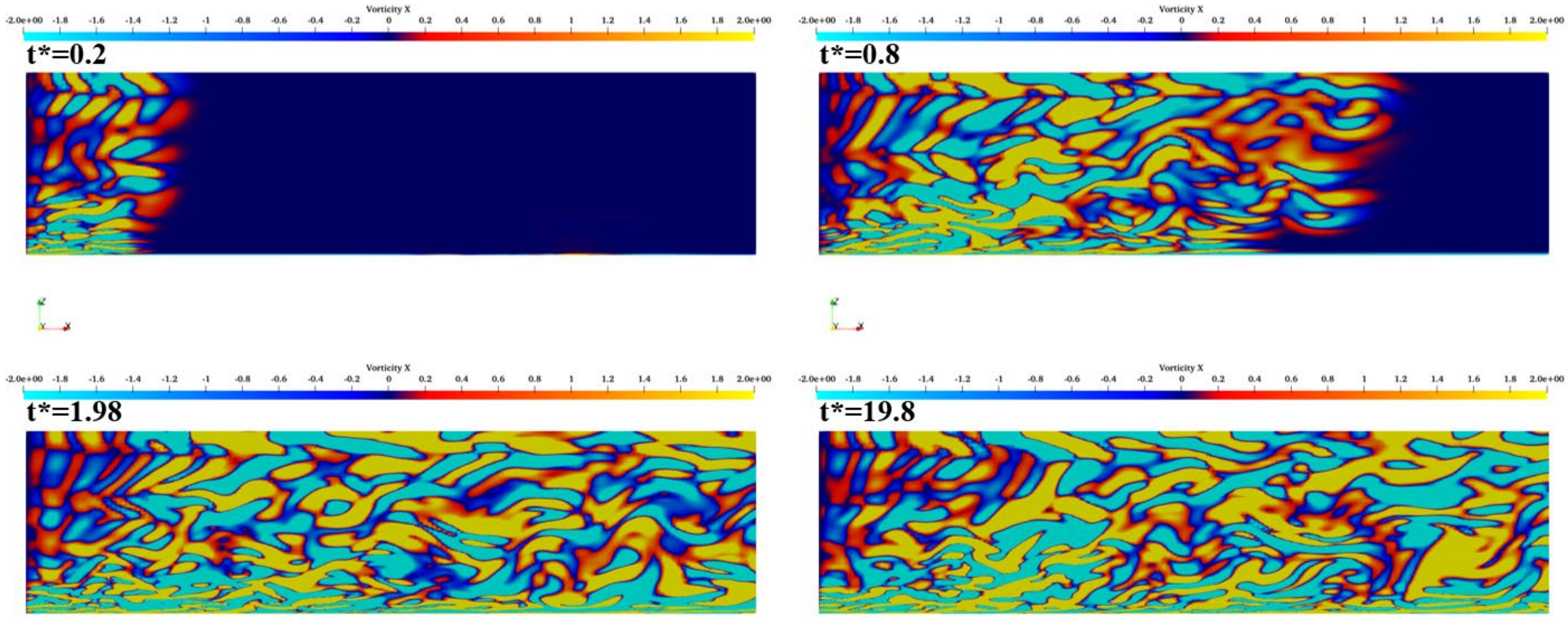

Figure 4.9: Vorticity X in 1/s at the middle of the empty computational domain at the XZ plane.

The spectral content of the longitudinal velocity at the incident flow (building location and height) in the empty computational domain is presented in Figure 4.10. As can be seen, the high range of the frequency fluctuations is expressed similarly to what is measured experimentally and to the theoretical von Karman spectrum. It is also interesting to notice that the energy of the high frequency fluctuations is sustained at similar levels, while they propagate inside the domain, from inlet until outlet. This was noticed by comparing the velocity spectrum in more than 10 locations speed out evenly in the streamwise direction, in different heights. The results are not presented for simplicity, since all the lines are very similar.

Pressure fluctuations in the computational domain are also of great interest since it is important to verify the physical aspect of the flow. The spectrum of the pressures was calculated and agreed to the theoretical distribution according to the corresponding velocity spectrum at each location by considering the Bernoulli Equation. It is important to ensure that the pressure fluctuations stabilize into small values as the flow propagates inside the computational domain. In Figure 4.11 the std of the pressure coefficient is presented for height of 8 m in full-scale, that corresponds to the height of the building that is studied, in 10 different locations in the streamwise direction. As can be seen, within a distance of $0.1 \cdot Lx$ from the inlet boundary the pressure fluctuations stabilize. Similar results have been reported in Bervida et al., (2020). The mean and turbulence intensity profiles of the velocity for the two exposures are presented in Figure 4.12, as calculated experimentally from each facility, and modeled by the LES-DT method. The exposures of the different facilities are similar enough, as to assume almost identical conditions for these experiments

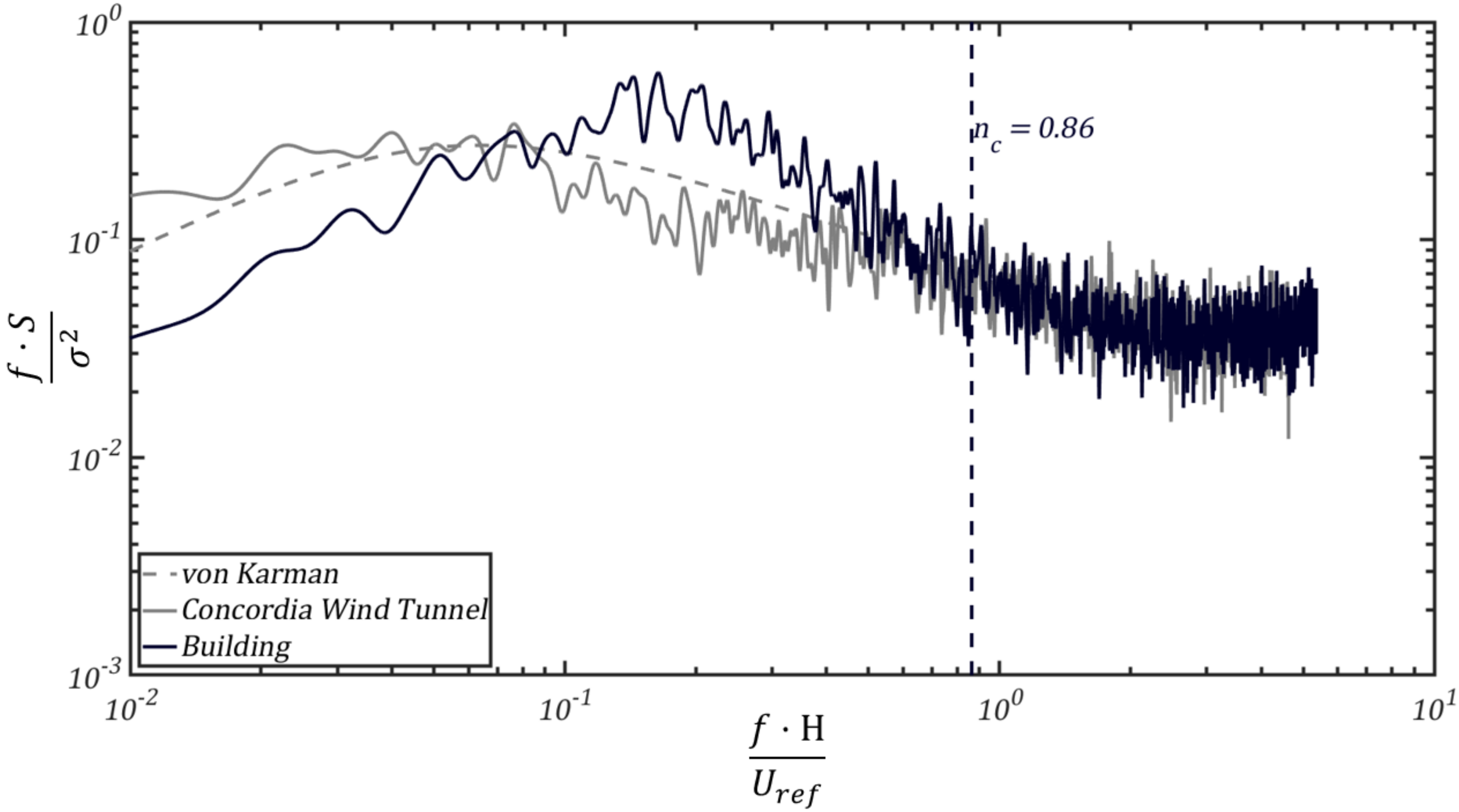

Figure 4.10: Spectral content of the longitudinal component of the velocity at the incident flow for z = 8 m full-scale.

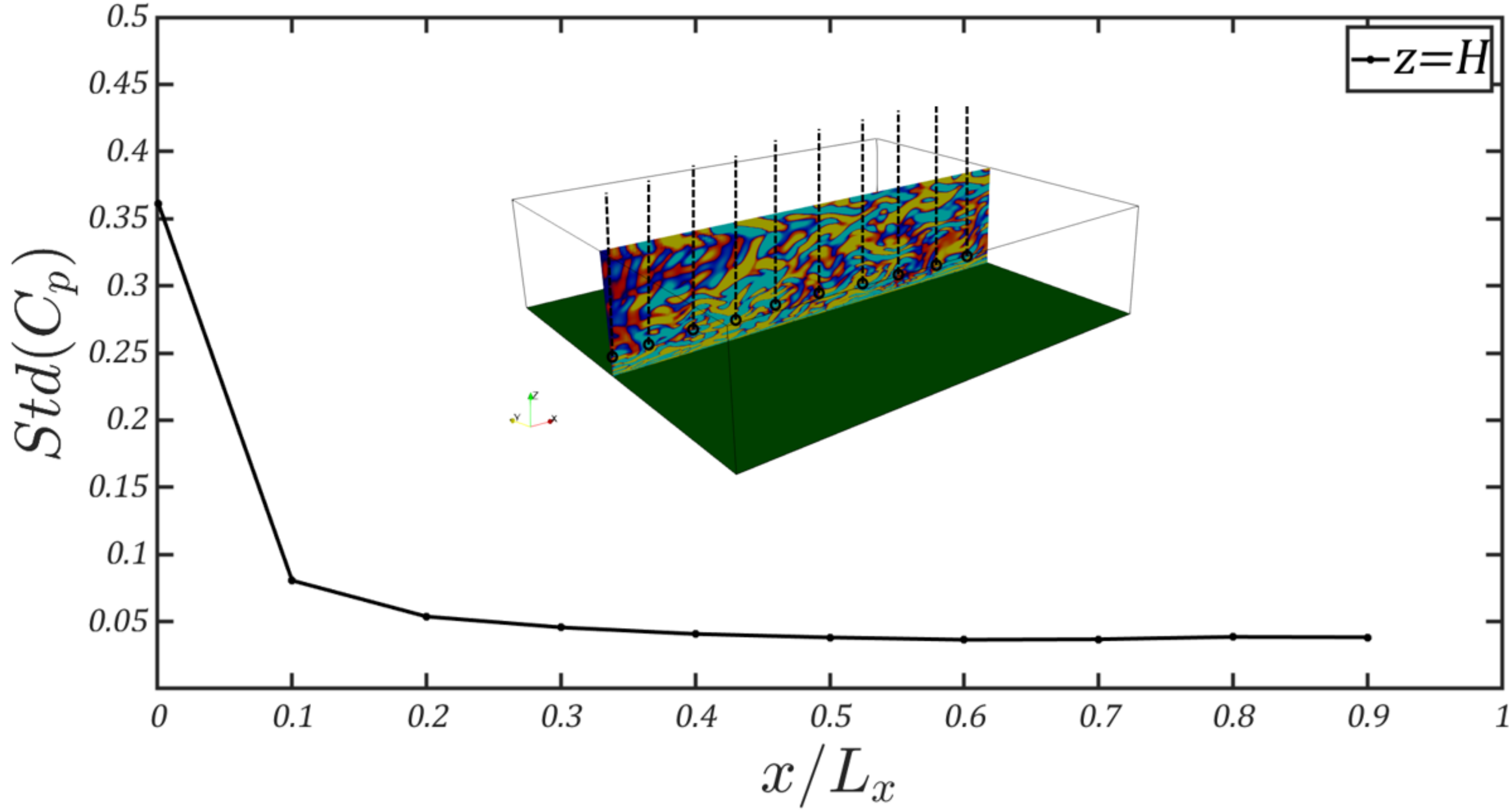

Figure 4.11: Standard deviation (std) of the pressure coefficient at height z = 8 m in full scale at the middle plane of the empty computational domain

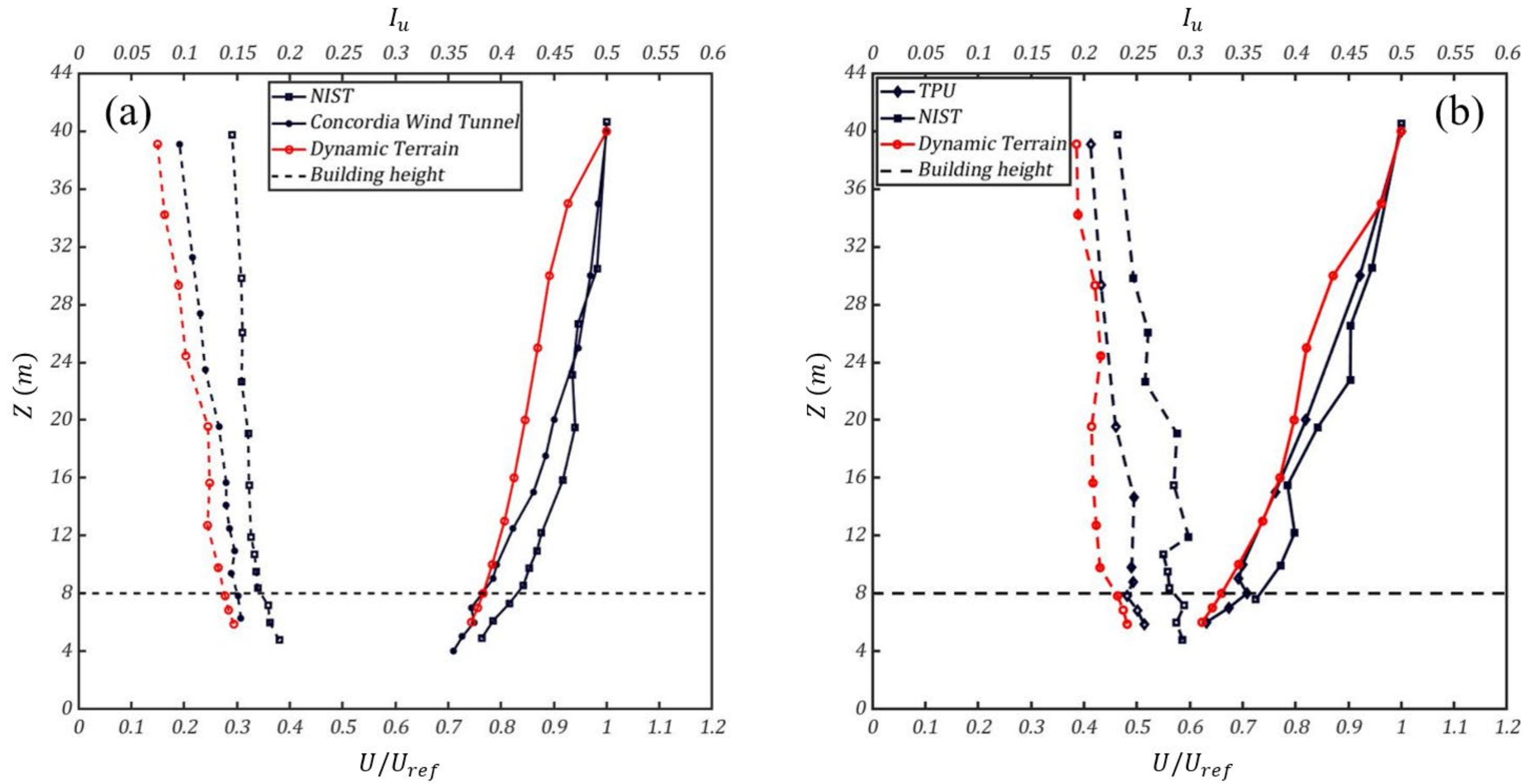

Figure 4.12: Mean velocity and turbulence intensity profiles for open exposure (a) and suburban exposure (b).

- Computational domain with building

Visualizing the flow field in the computational domain with the building located at the incident flow, is of equal importance. Utilizing the ParaView Software, streamlines are generated for specific snapshots of the computational analysis. In Figure 4.13 the streamlines are presented for t*=72.6 for the perpendicular wind to the building envelope at the XZ plane. The lines are colored with the magnitude of the velocity at this instant. It is interesting to notice the variety of the vertical distribution of the magnitude of the velocity for the incoming flow. This is expected to be the case, since the incoming flow field is in accordance with the turbulence characteristics that were presented in Figure 4.9 and 4.12. Thus, the evolution of the flow field in this part of the computational domain consists of various vortical structures, and instantaneous velocity values that are nonuniform in the stream wise direction, that are generated due to the inlet conditions of the LES-DT methodology. The flow around the structure seems to agree in qualitative terms with what is expected to be observed in the real interaction between ABL and low-rise buildings. A stagnation vortex is present in front of the building, the flow is detached at the roof and lee ward side, and in the wake region the inflow field is still disturbed by the existence of the building. Environmental studies focus on quantitative comparisons regarding these types of data, but this is not the scope of the present work.

Similar results are displayed in the XY plane for the oblique wind direction at t*=75.9 in Figure 4.14. The plane presented in the figure is at the mid-height of the building. Similar to what is observed in Figure 4.13, the flow field around the structure can be considered qualitatively accurate. Furthermore, in the Y-direction the magnitude of the velocity is more or less constant.

This is due to the uniformity of the inlet data at the inlet plane that propagate in a similar way inside the computational domain.

Expanding on the results of the flow for the oblique wind direction, it is interesting to visualize the theoretical conical vortex that should be generated in the roof of the building. This is a difficult task by just displaying the vorticity, since a large range of vortices interacts with the building, which results in incomprehensible contours. For this reason, the q-criterion was utilized for that purpose and calculated by using ParaView. This is defined as $Q = 0.5 * (\|\Omega\|^2 - \|S\|^2)$, where Ω is the vorticity tensor and S the strain rate tensor of the velocity. More information can be found in (Jeong and Hussain, 1995). Although, to the authors knowledge there is no consensus on which values of the Q-Criterion should be displayed, the values were parameterized and finally a value of $10 \cdot (\frac{U_{\mathrm{h}}}{\mathrm{H}})^2$ was chosen empirically. This result is presented in Figure 4.15, where the contour is colored again with magnitude of the velocity for t*=75.9. It is interesting to see that for this value of the Q-Criterion, the conical vortex is generated at the edge of the roof and propagates further downstream with this “irregular” shape. Similar findings have been presented in Ricci et al.., (2017), for the same building dimensions, but with a small slope at the roof.

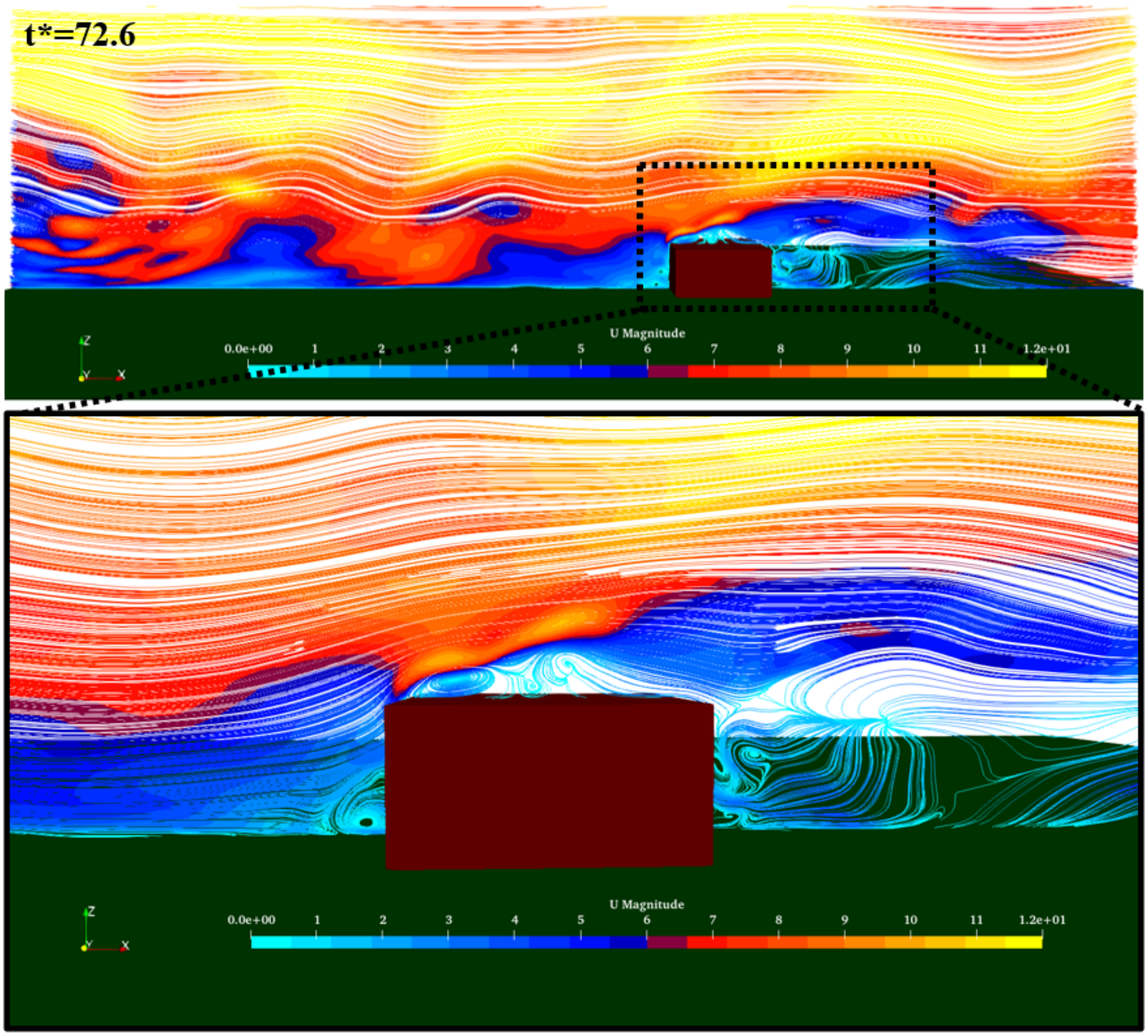

Figure 4.13: Velocity streamlines colored with the velocity magnitude in the XZ plane for flow perpendicular to the building.

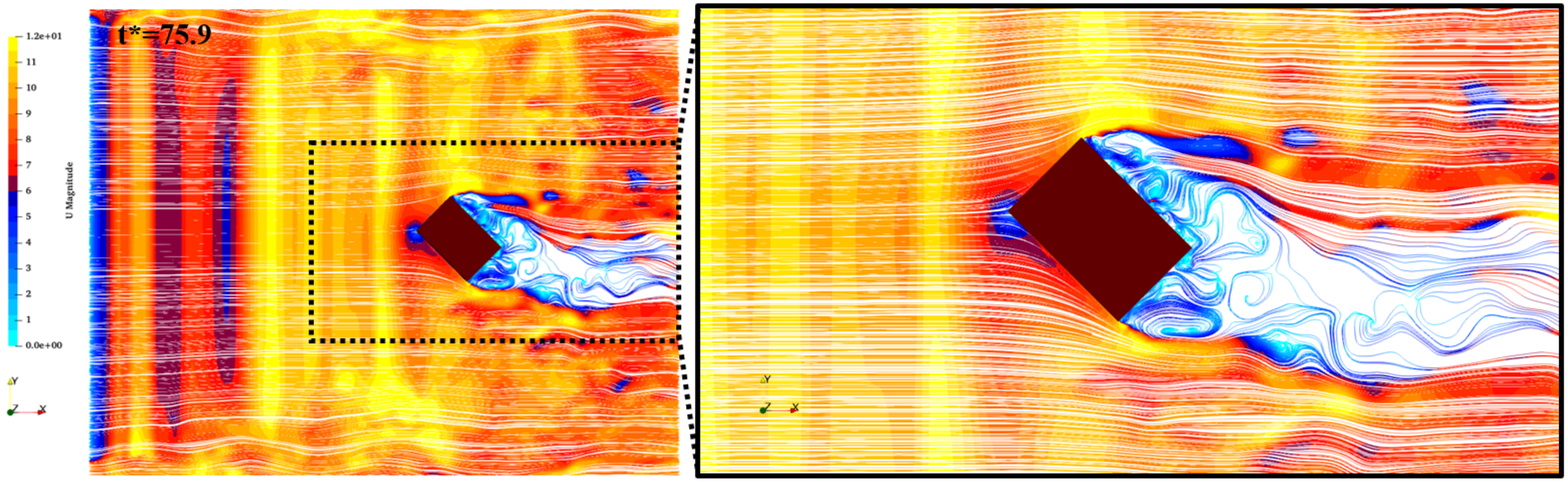

Figure 4.14: Velocity streamlines colored with the velocity magnitude in the XY plane for flow with oblique direction to the building

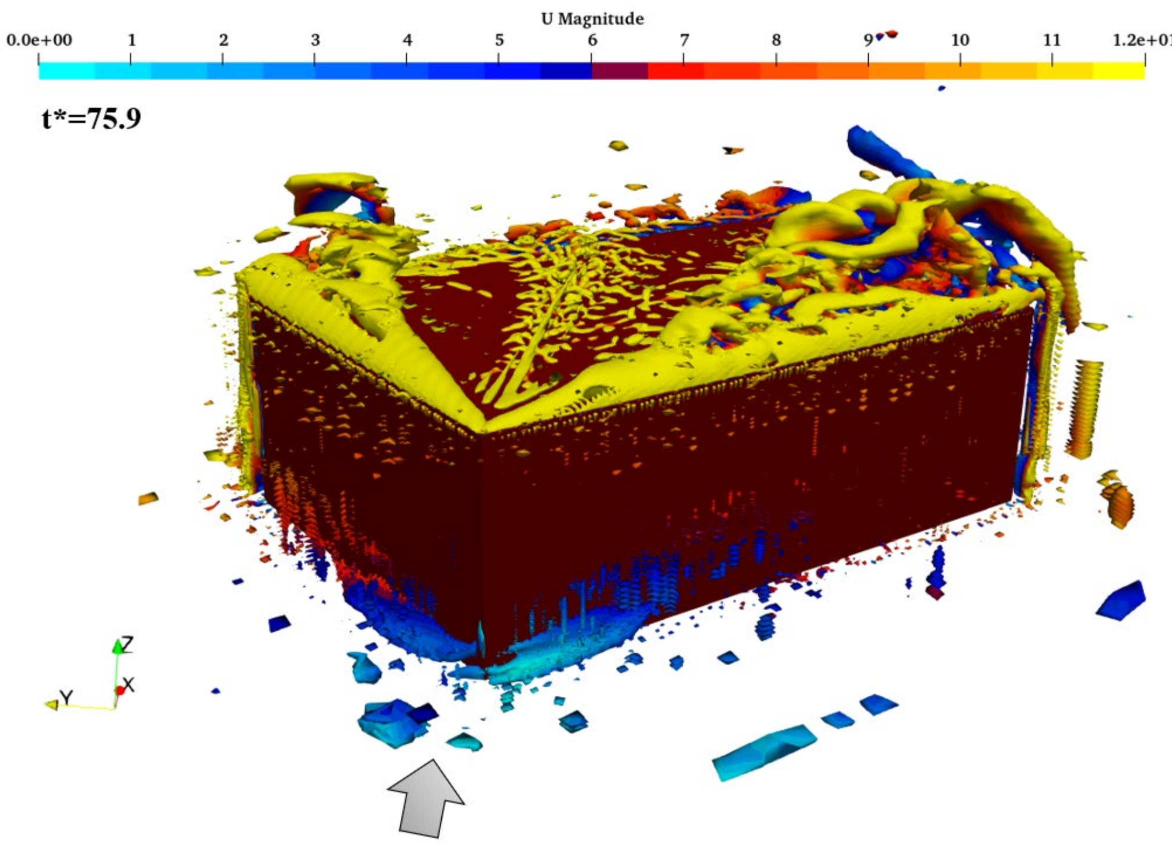

Figure 4.15: Q-criterion ~10^5 ($10*(U_h/H)^2$) contour of vorticial structures around the building envelope for the oblique wind direction.

4.3.4 Results

The validation metrics that were chosen for comparing experimental and numerical results are mean, std deviation and peak values on symmetric taps on the roof and correlation graphs of all pressure taps located on the roof. To further elaborate of this comparison two more metrics were used: the percentage of root mean square error (PRMSE) by fitting linearly the data and the percentage of accuracy (PoA) versus the tolerance of error (number of pressure taps with error less than the selected tolerance divided by the number of pressure taps included in the calculation). Both PoA and tolerance are defined in the range from 0 to 100% and are defined in Chapter 3.2.

- *Open exposure*

Starting with results of the open exposure, in Figure 4.16 the contours of the mean and peak pressure coefficients are presented for the roof. In the top row the mean values are displayed and, in the bottom, the peak values, that are colored based on the colormap below that. In the left and middle columns results from the database of NIST and from Concordia Wind Tunnel (CWT) are presented. In the right column the numerical results from the LES-DT methodology are displayed. Both for mean and peak values we see similar trends between the two experimental procedures, that vary more near the edges of the roof. The numerical results seem to agree more or less with the experimental findings, but visual comparisons are not enough to evaluate the level of agreement. Mean, std and peak values are presented on symmetric lines in Figure 4.17. Experimental results from NIST seem to be in good agreement for both wind directions examined, even for the pressure taps located near the corner, where the flow separates.

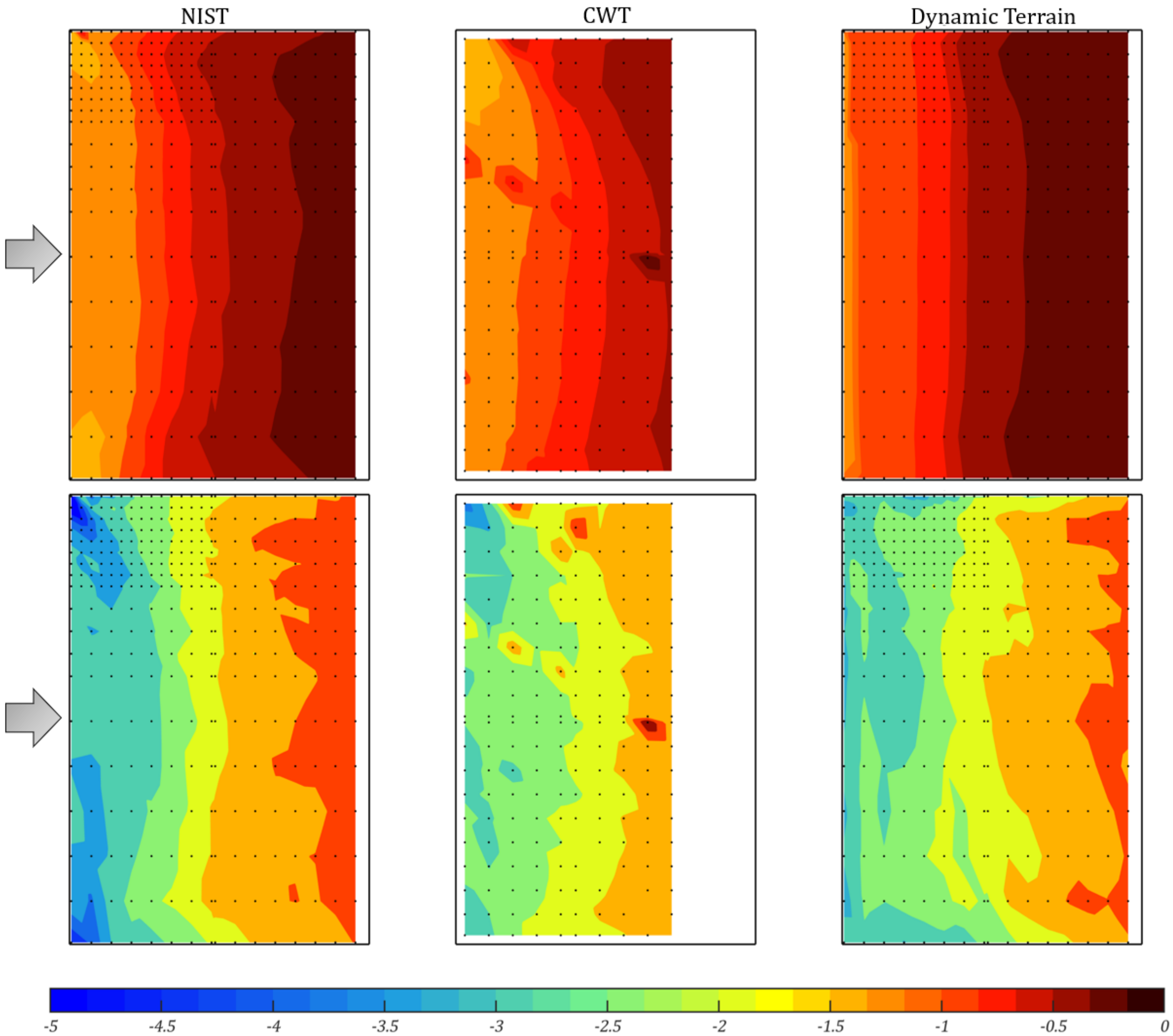

Figure 4.16: Mean (top) and peak (bottom) pressures on the roof of the experimental models from NIST (left), Concordia (middle) and the computational method of Dynamic Terrain (right) for perpendicular wind direction.

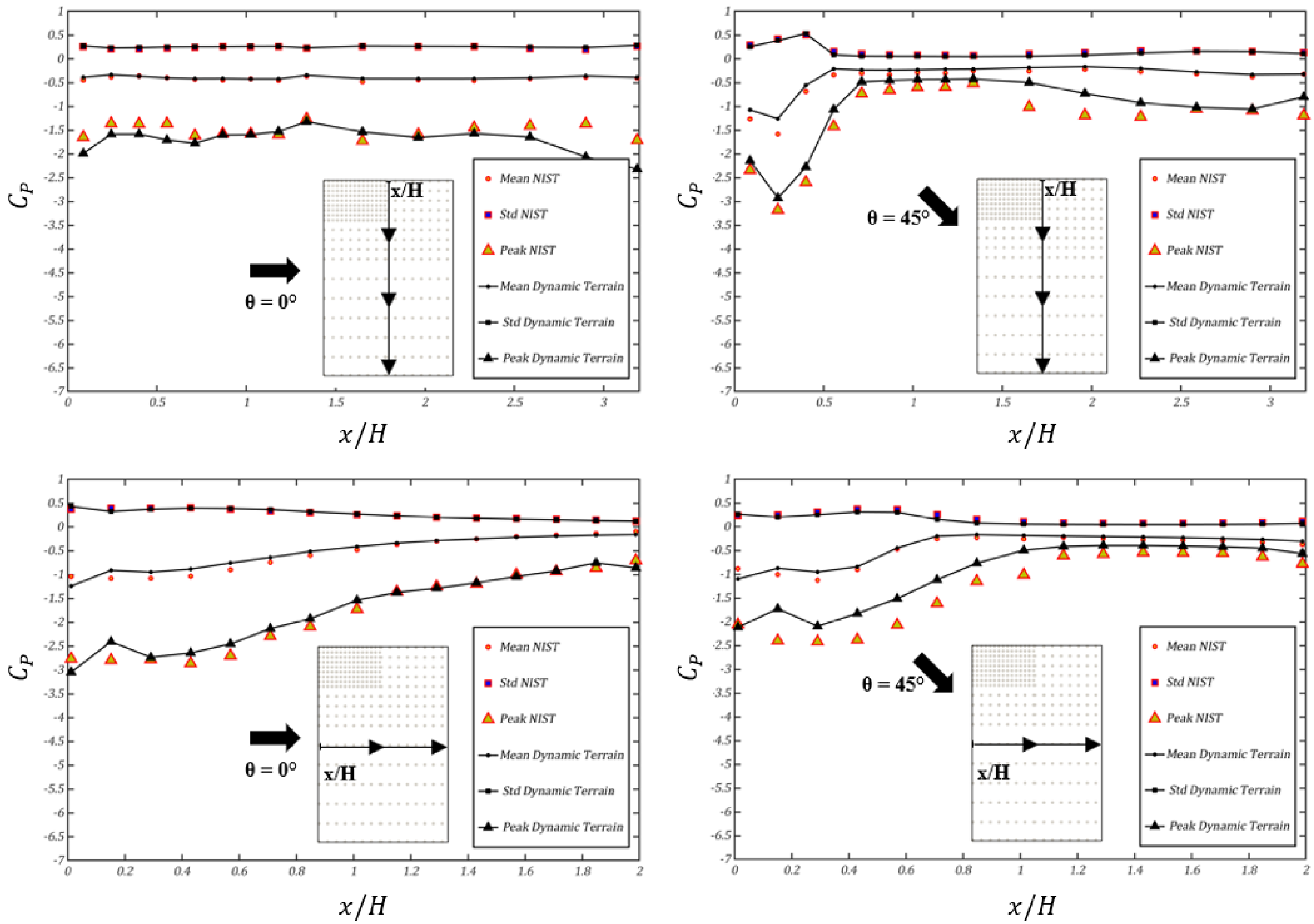

Figure 4.17: Mean, std and peak pressure coefficients on the two symmetric lines of pressure taps on the roof for perpendicular and oblique wind directions for open exposure.

These results were correlated with a paper that utilized the virtual wind tunnel method, to evaluate wind loads on the same building for an open exposure (Geleta and Girma, 2022). The exposure conditions were considered similar based on the mean speed and turbulence intensity profiles of the incident flow. In Figure 4.18, the PRMSE metric is presented for the mean, std and peak values of the symmetric taps presented in Figure 4.17, for perpendicular and oblique wind direction of 45°. As can be seen, PRMSE of the LES-DT method is slightly improved when compared with the virtual wind tunnel, but this is not the real advantage of the proposed method. In order to achieve these values with the virtual wind tunnel approach, the entire wind tunnel needs to be modeled as an initial step, that consists of a huge computational domain (168 million elements) – an unnecessary step with the LES-DT method. After this is done, the time series are extracted and introduced in the inlet plane of the secondary domain (with the building), which for the presented results have 9.6 million elements, more than two times bigger than the domain that was used for the present work, with bigger inflation of the mesh both locally near the building and at the inflow location. This leads to 45 days of analysis with 64 parallel processors (Geleta and Girma, 2022), in contrast to the 4 days of analysis with the same number of processors in order to extract similar results via the Dynamic Terrain. Thus, time efficiency is improved more than 11 times for this example.

Results for the pressures are extended to the entire roof of the building in terms of correlation graphs with experiments of Concordia Wind Tunnel (CWT) and NIST. In the first row of Figure 4.19 the correlation between the NIST and CWT experimental results are presented, regarding the mean, std and peak pressure coefficients. These results are presented as to define the threshold of accuracy that is to be expected from the computational results. The results from 192 similarly located pressure taps on the roof, are inserted into a linear model, and provide PRMSE of 6.2%, 8.69% and 7.03% for the mean, std and peak values accordingly. Similar studies that focus on comparing NIST and TPU databases results can be found, that present similar conclusions for the level of disagreement between the two experimental procedures for the peak values (Asmerom et al., 2014, Shelley et al., 2023). This is also discussed in Chapter 3.2 of this thesis. When selecting PRMSE as a validation metric, the accuracy of the peak values between experiments is related closer with the accuracy of the mean values in some cases and in other cases with the accuracy of the std (first row of Figure 4.19, Figure 4.21, Figure 4.25 and Figure 4.26). In Figure 4.18 both trends are noticed, either by using the virtual wind tunnel (Geleta and Bitsuamlak, 2022) or the LES-DT Method. Recently, a comparison between results from Concordia Wind Tunnel and University of Western, with full-scale measurements was conducted (Chavez et al., 2022). Results from this study for the peak values are in the same level of accuracy with those between CWT and NIST displayed in Figure 4.19.

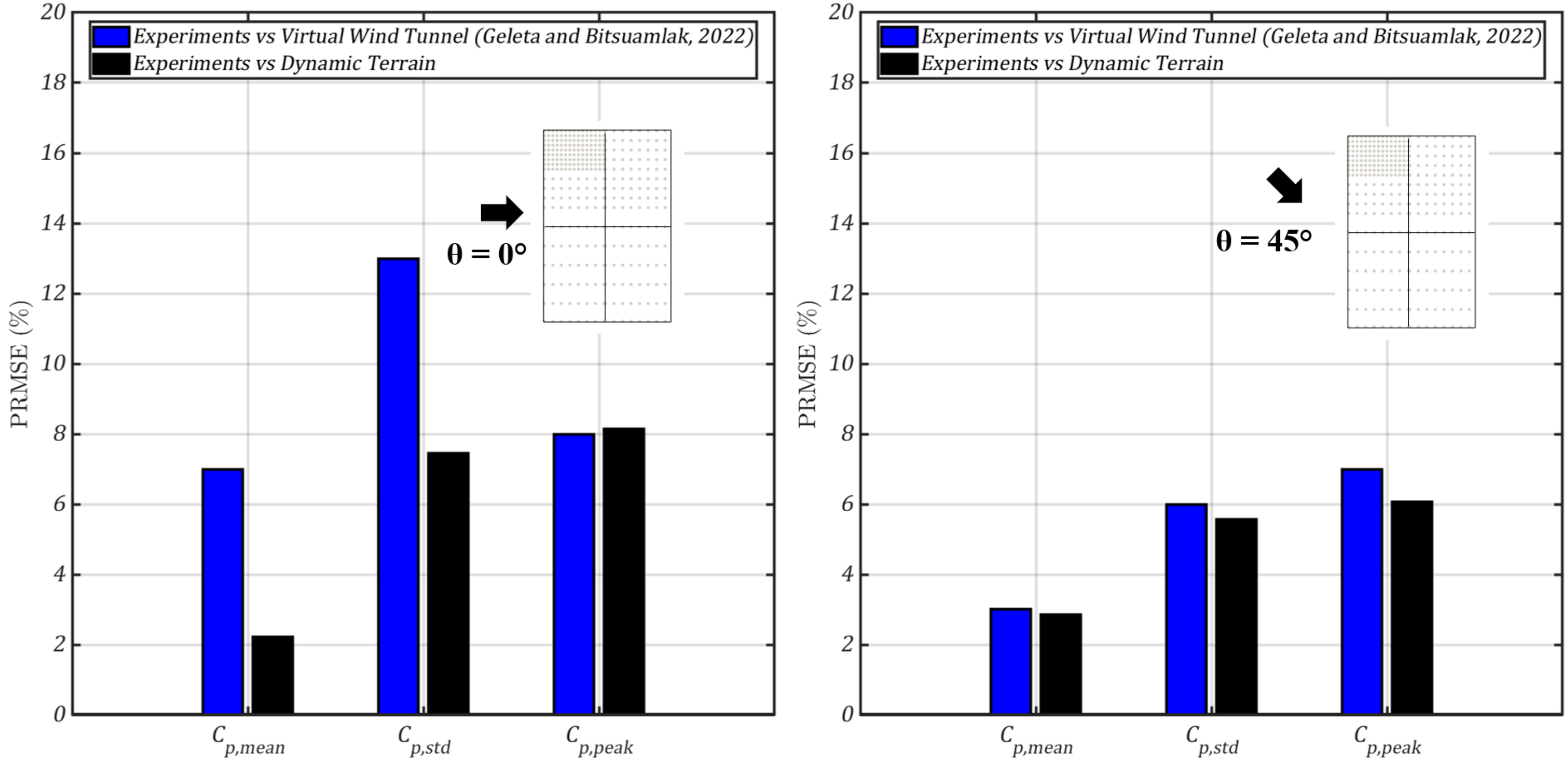

Figure 4.18: PRMSE of mean, std and peak pressure coefficients from Geleta and Bitsuamlak (2022) and the Dynamic Terrain for open exposure.

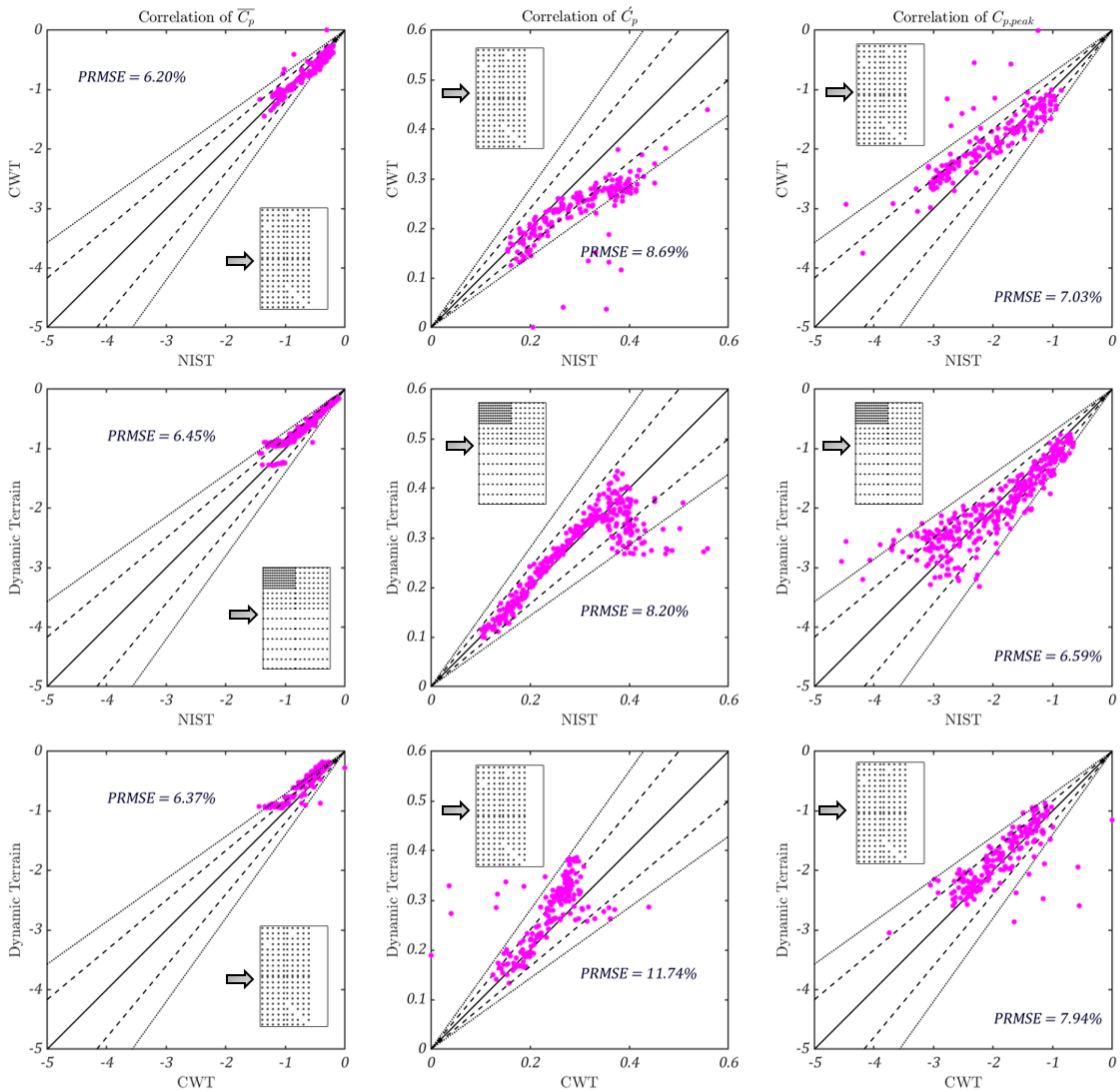

Figure 4.19: Correlation of mean, std and peak pressure coefficients of perpendicular wind direction for open exposure.

Keeping the experimental differences as a threshold, in the second and third row of Figure 4.19, similar comparisons are found between NIST and LES-DT for 336 pressure taps and CWT and LES-DT for 192 pressure taps, accordingly. In these cases, the pressure taps locations are exactly matched between the different procedures. For the mean values, LES-DT method has similar agreement as the one between the experimental procedures, while for the std values the comparison with NIST is slightly improved. Correlation of peak values provides PRMSE values of 6.59% with NIST and 7.94% with CWT.

The building was exposed to the same inlet conditions, with the same mesh, but being rotated for 45°. Contour of mean and peaks values are presented in Figure 4.20 from the experiments of NIST, CWT and the numerical data of the LES-DT method, similar to the perpendicular wind direction. In this case, from a visual point of view, it is obvious that the two experimental results differ more than the perpendicular wind direction presented in Figure 4.16. The numerical results seem to agree more with the experiments from NIST database.

Focusing now on the correlation graphs for all the pressure taps of the roof, results between the two experimental practices are found in the first row of Figure 4.21. Comparisons seem to disagree more for the oblique wind direction than for the perpendicular wind direction, as presented in Figure 4.19, which supports the visual observations. Results extracted from the numerical probes inside the computational domain with the LES-DT method are correlated in the second row with NIST and the third row with CWT in Figure 4.21. The agreement between the numerical results and NIST for the 336 pressure taps is improved when compared with the threshold between the two experimental results, for the mean from 12.02% to 4.04%, for the std from 17.07% to 5.62% and for the peak from 11.53% to 5.29%. The correlation of the results with CWT seems to be slightly above the threshold for the mean, std and peak values.

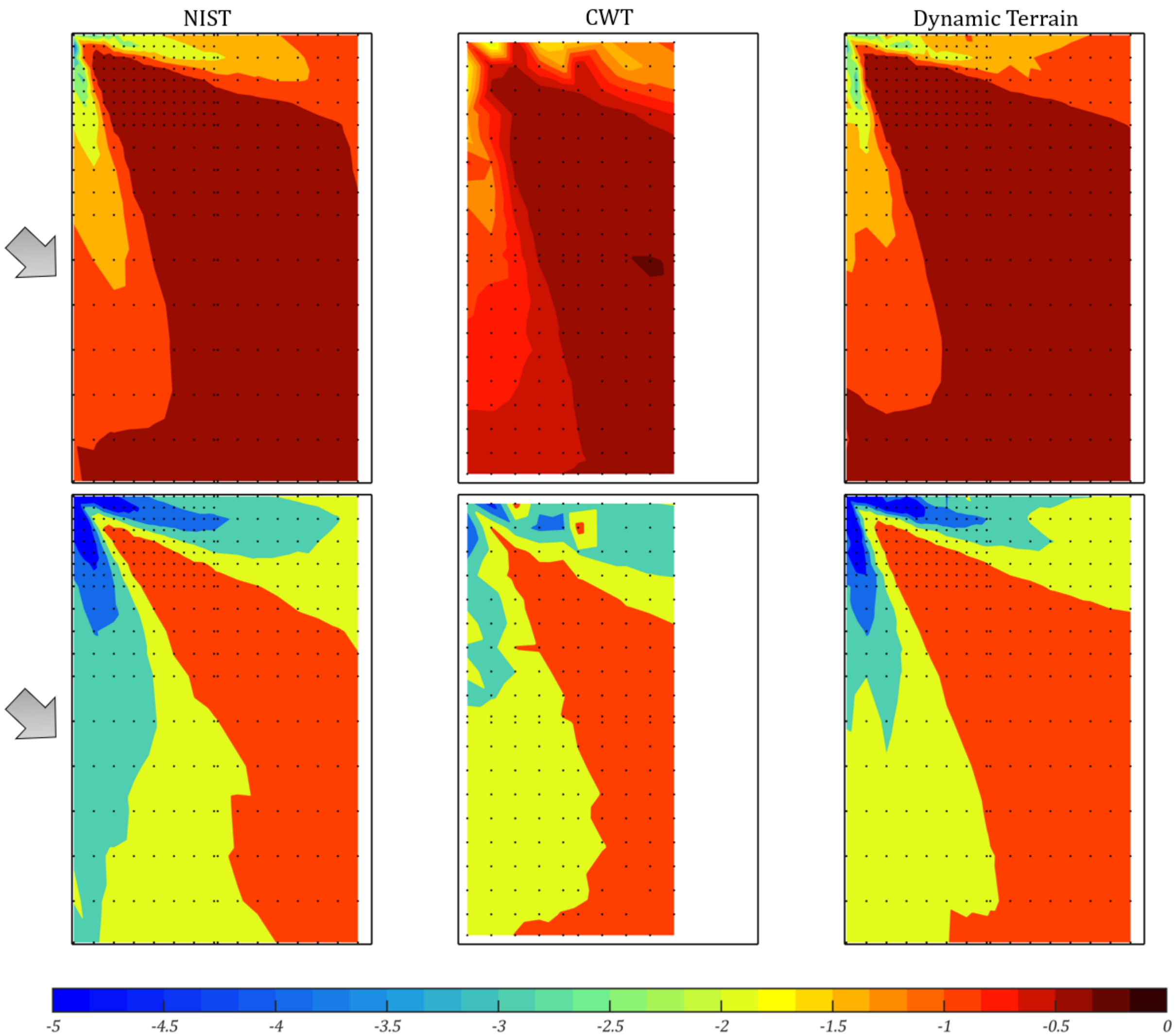

Figure 4.20: Mean (top) and peak (bottom) pressures on the roof of the experimental models from NIST (left), Concordia (middle) and the computational method of Dynamic Terrain (right) for oblique wind direction.

In Figure 4.22 the accuracy between the procedures is further elaborated in terms of tolerance versus the percentage of accuracy (PoA). For the mean and std values of the LES-DT results agree more with NIST than CWT. In general, the PoA between the two experimental procedures is lower for the entire range of the tolerance. For the peak values of the perpendicular wind, Dynamic

Terrain results are in great agreement with CWT where 80% of the pressure taps have less than 10% tolerance of error. The same level of accuracy is reached for a 20% tolerance between the Dynamic Terrain and NIST, and 25% between the two experimental procedures.

PoA for the oblique wind direction versus the tolerance is also presented in Figure 4.22. Although the PRMSE values seen in Figure 4.21 between the two experiments are above 10%, the PoA is similar to the perpendicular wind direction. As it seems, it's more difficult to fit the two experimental sets of pressure time series linearly for the oblique wind direction, but their actual values do not differ that much. In all cases, the PoA between the Dynamic Terrain method and NIST are similar with the PoA between the Dynamic Terrain method and CWT. Both are higher than the threshold of PoA, for most of the tolerance range.

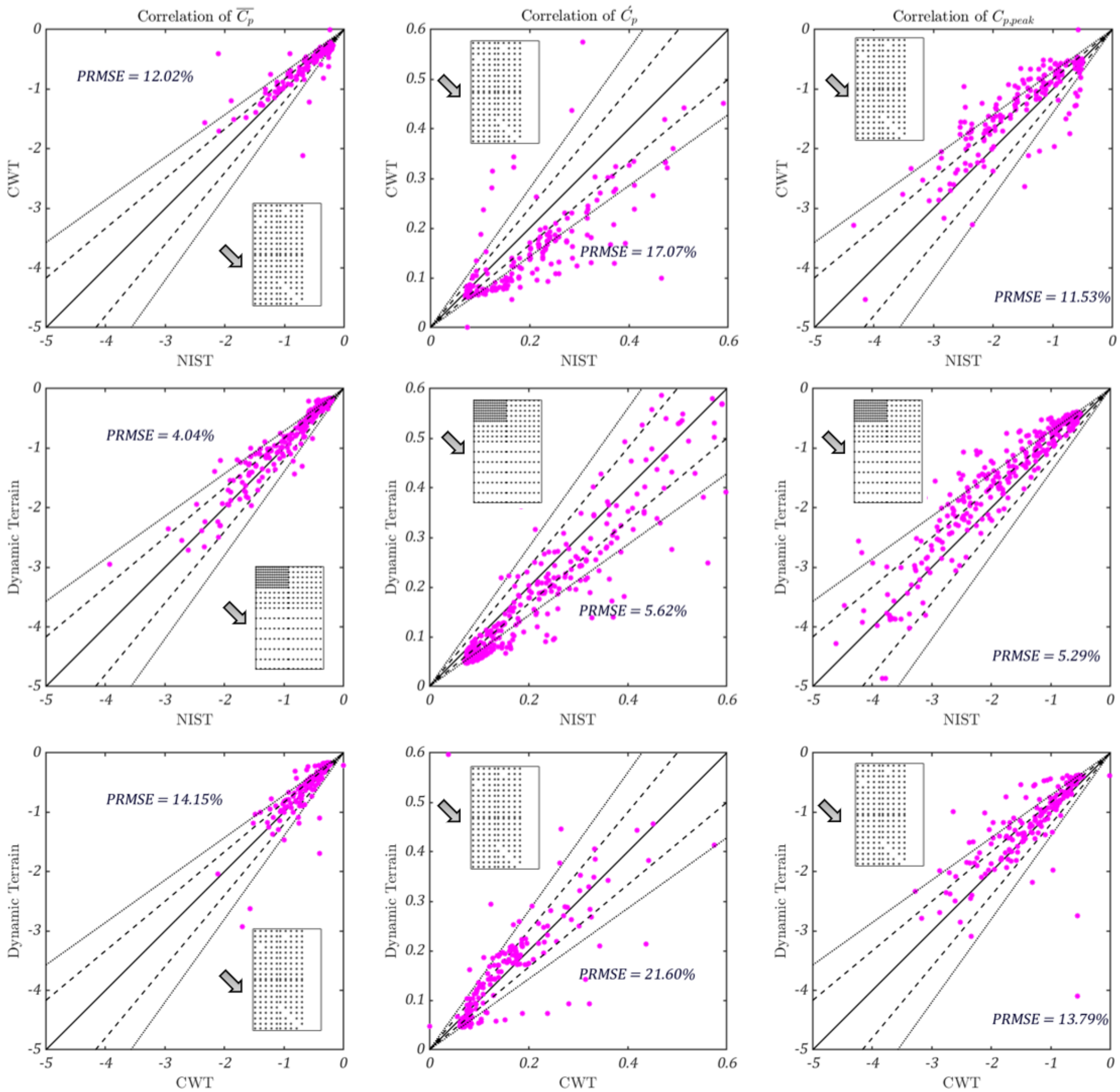

Figure 4.21: Correlation of mean, std and peak pressure coefficients of 45° wind direction for open exposure.

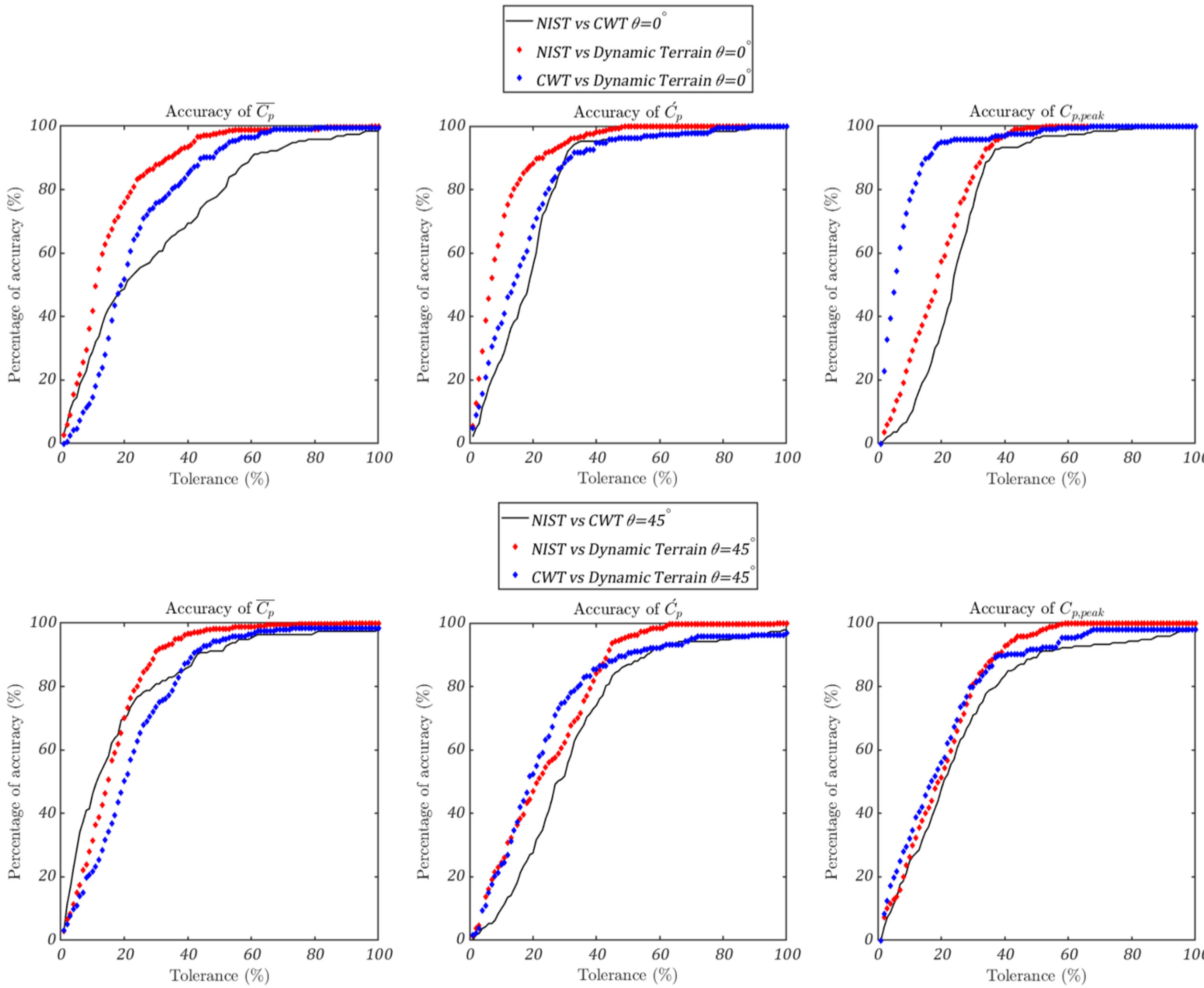

Figure 4.22: Percentage of accuracy versus tolerance between NIST, CWT and Dynamic Terrain method for perpendicular (top) and 45° (bottom) wind direction of open terrain.

- *Suburban exposure*

Exposing the same building into suburban conditions results in mean, std and peak pressure coefficients found in Figure 4.23, in symmetric taps of the roof. Similar to the open exposure, the computational results agree with the experiments found in the NIST database. To put the accuracy of these results into perspective, their validation metrics are compared with Ricci et al., (2017), that used the same building for the same exposure conditions – see Figure 4.24. In Ricci et al., (2017) the PoA is used as validation metric for the symmetric pressure taps for tolerance 10%, 20% and 30%, and not the PRMSE, which explains why this comparison is different than the corresponding open exposure results in Figure 4.18. To make this comparison fair with the results of the synthetic method of Ricci et al., (2017), fewer pressure taps were selected to be included in the calculation for PoA (Figure 4.24) and present their mean, std and peak values in Figure 4.23, in comparison with number of pressure taps used for Figure 4.17 and Figure 4.18. In this way the number of pressure taps for validation correspond to what was used in their study that utilized the synthetic inlet approach.

Dynamic terrain represents the PoA of std with a similar level of accuracy for the oblique wind direction and with an improvement for the perpendicular, as seen in Figure 4.24. Besides these improvements, the advantage of the Dynamic Terrain method in comparison with MDSRFG technique of Ricci et al., (2017) is threefold. First, the turbulence statistics are easier to be reproduced in the incident flow profile, and do not necessitate the modeling of the entire wind tunnel as to tune the synthetic inlet parameters. Another advantage is that with the Dynamic Terrain method there is no need to physically model roughness elements to mitigate the turbulence from inlet until the incident profile, that leads to increased computational cost in the main simulation (with the building). The scope of the inflow conditions of the Dynamic Terrain is to introduce small scale turbulence inside the computational domain, thus modeling of roughness elements or surroundings is not necessary. Finally, the domain that was used for the MDSRFG technique is huge compared with the mesh that was used in this study, thus time efficiency is greatly improved. Besides the above advantages, the complexity of the methodology of MDSRFG is higher, from a practical point of view, that necessitates more computational resources and parameterization of various parameters for the synthetic approach to be valid, while it still not proved that it can be used for different exposure conditions.

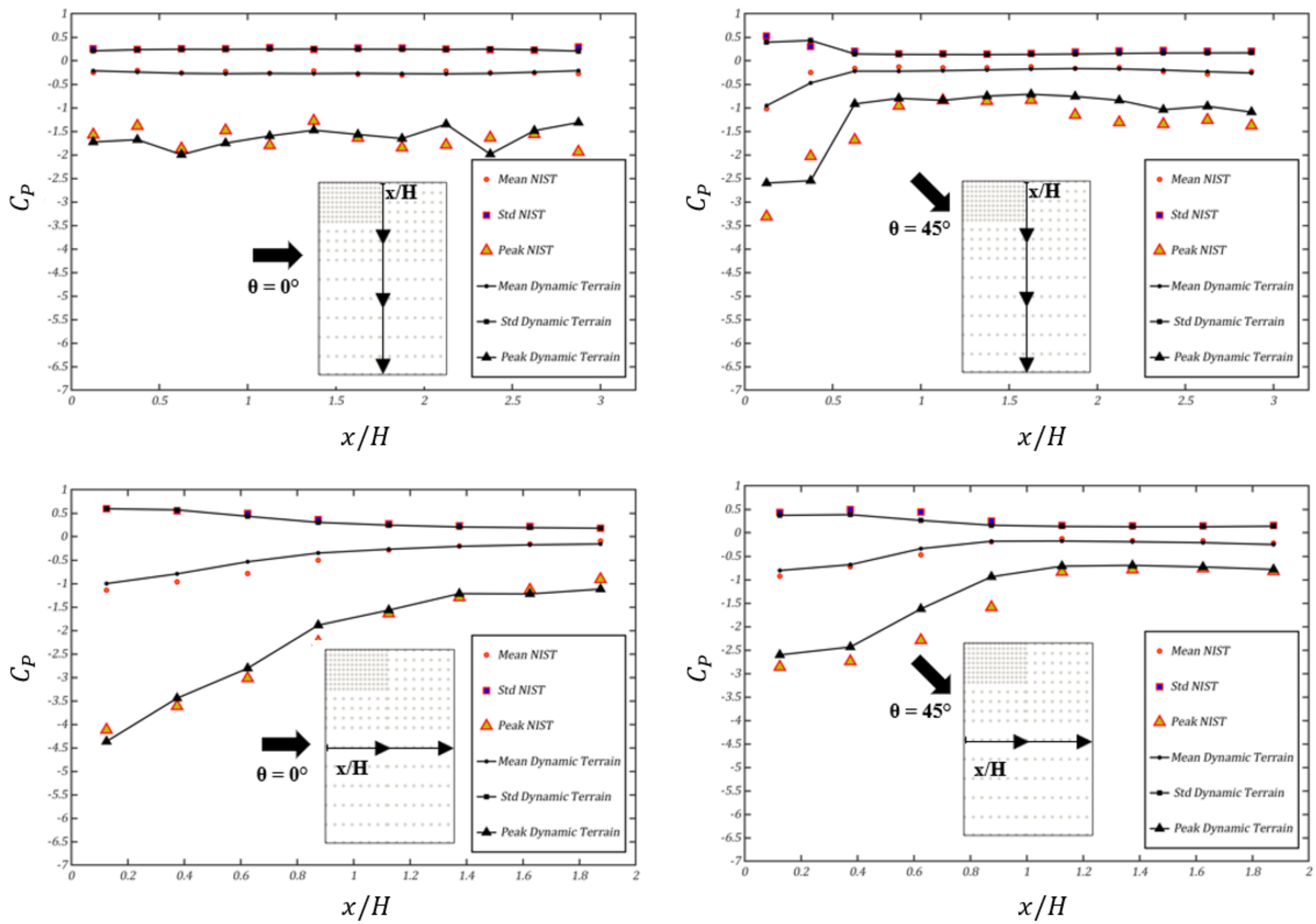

Figure 4.23: Mean, std and peak pressure coefficients on the two symmetric lines of pressure taps on the roof for perpendicular and oblique wind directions for suburban exposure.

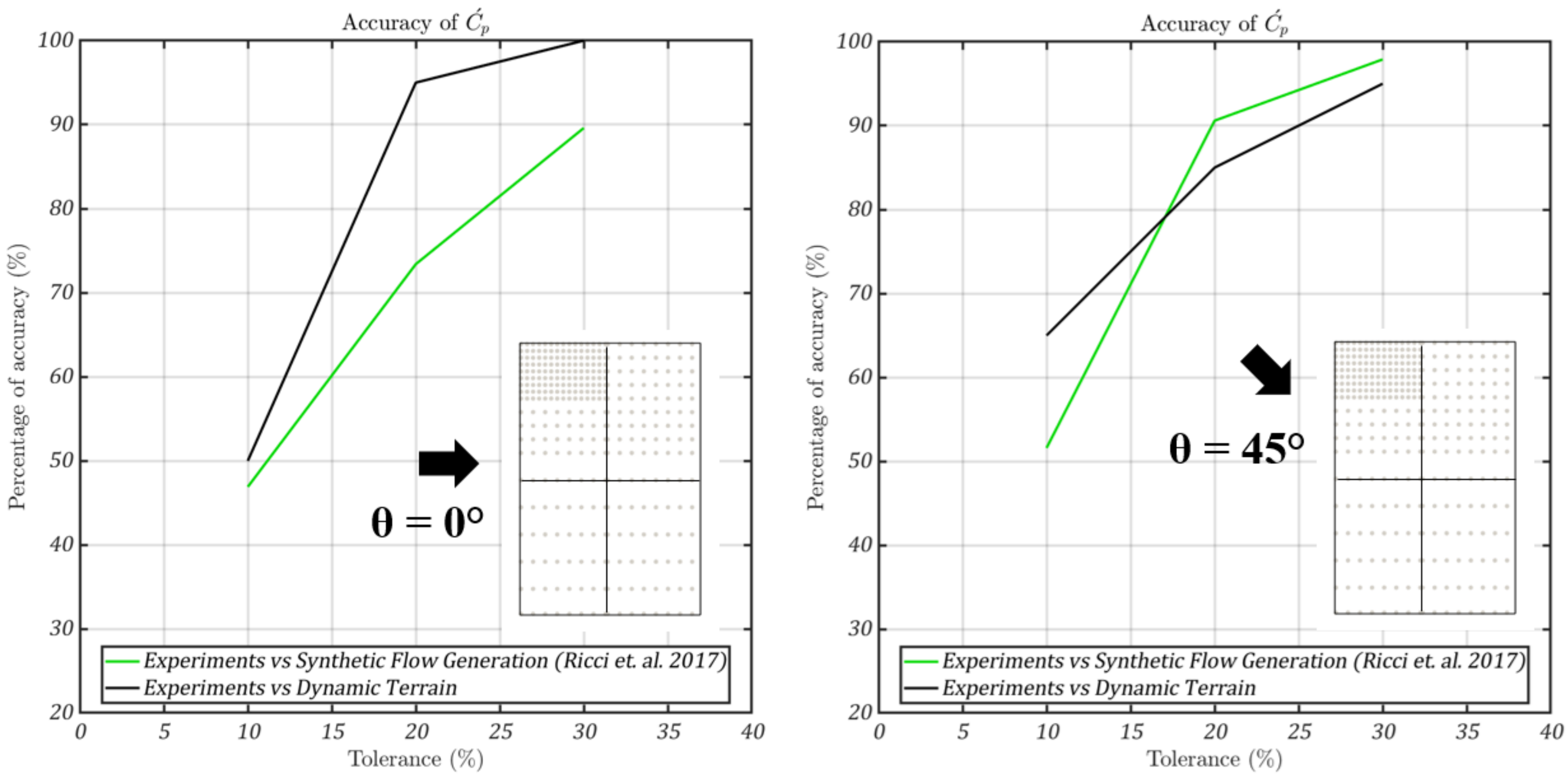

Figure 4.24: PoA of standard deviation of the pressure coefficient for the perpendicular and obliques wind direction for Ricci et al.., 2017 and the Dynamic Terrain for suburban exposure

The validity of the roof loads was also regarded for the entirety of the pressure taps of the model. Figure 4.25 presents the correlations of the mean, std and peak values for 92 pressure taps, whose location was based on the TPU model for perpendicular wind direction. Similar to the open exposure, the correlation of the two experimental procedures is considered a threshold for the validity of the method. For the mean values, experiments correlate with a PRSMSE of 7.38%, that is improved when comparing the Dynamic Terrain and NIST results. For the std values, Dynamic Terrain and TPU provide a PRMSE above 12%, but agree more with the NIST values. Finally, the peak values provide a slightly higher PRMSE for the computational comparisons, with values 9.03% and 9.94%, compared to the 8.43% between the experimental results.

Focusing of the oblique wind direction of 45° for the suburban exposure in Figure 4.26, it is evident that the correlation of mean, std and peak values among the two experiments deteriorates, compared to the perpendicular wind. In this case, the PRMSE are 10.96%, 9.6% and 9.87% respectively, while numerical results seem to be able to reduce the error for both experimental comparisons. Great interest is the peak values that PRMSE is 8.11% between the Dynamic Terrain and TPU. In Figure 4.27 the PoA versus the tolerance is plotted for the mean, std and peak values. The same issue reported for the perpendicular wind direction is again presented for the mean values, but the accuracy is increased for the std and peak pressure coefficients. Dynamic Terrain results agree more with TPU than NIST for the std, while the peak values are depicted slightly worse than the experimental error, in the tolerance range from 10% to 25%.

Although the mean values between the experimental results fit well in the linear model, the percentage of accuracy provides very low values for tolerance less than 40%, as seen in Figure

4.27. On the other side, the percentage of accuracy for the std and peak values are in very good agreement. Similar results for pressure taps located on the middle strip of the roof were presented on Shelley et al., (2023), with a thorough discussion as to which parameters play the most important role for this disagreement of the mean pressures. Dynamic Terrain results more accurately predict the NIST values for the mean and std, and the peak values are of the same order of agreement for among the three procedures.

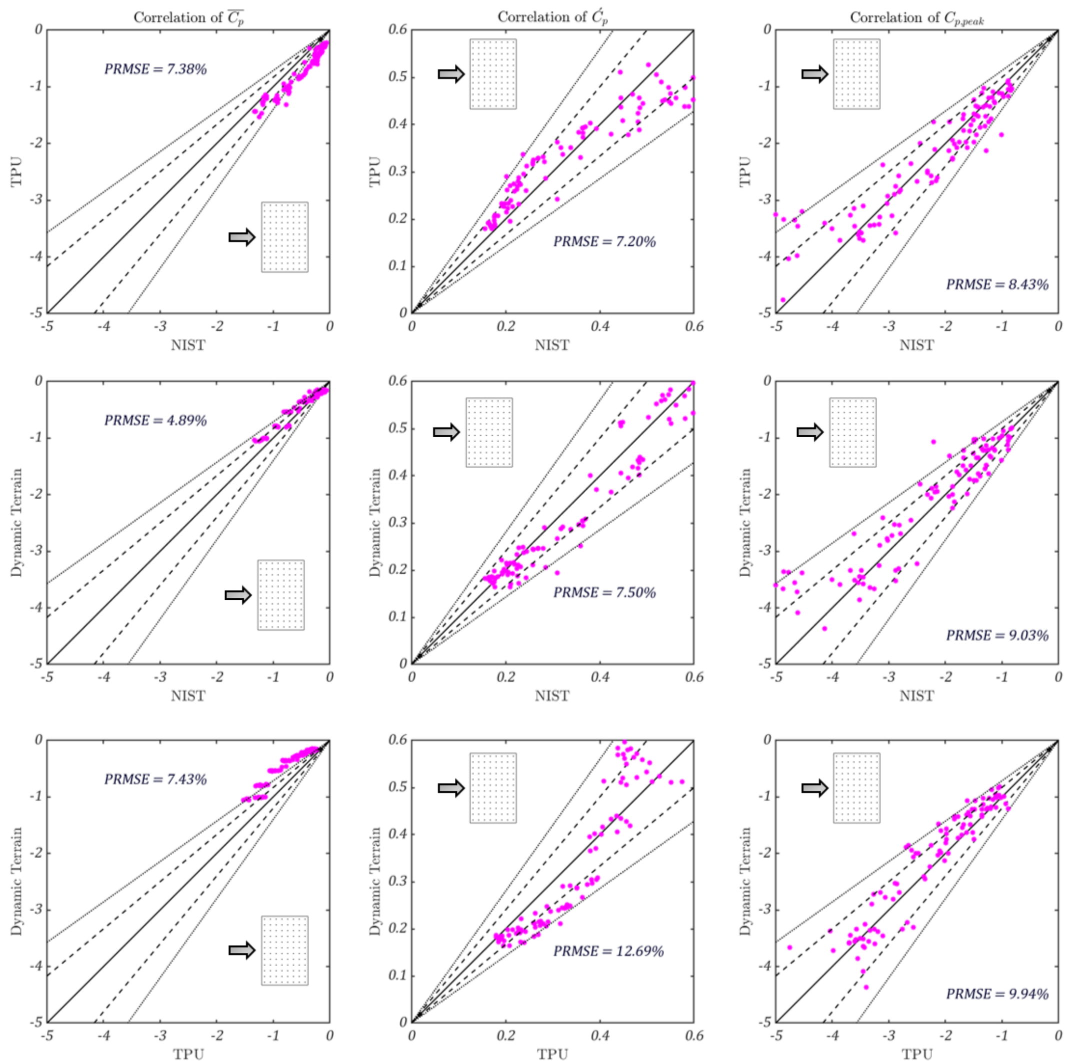

Figure 4.25: Correlation of mean, std and peak pressure coefficients of perpendicular wind direction for suburban exposure.

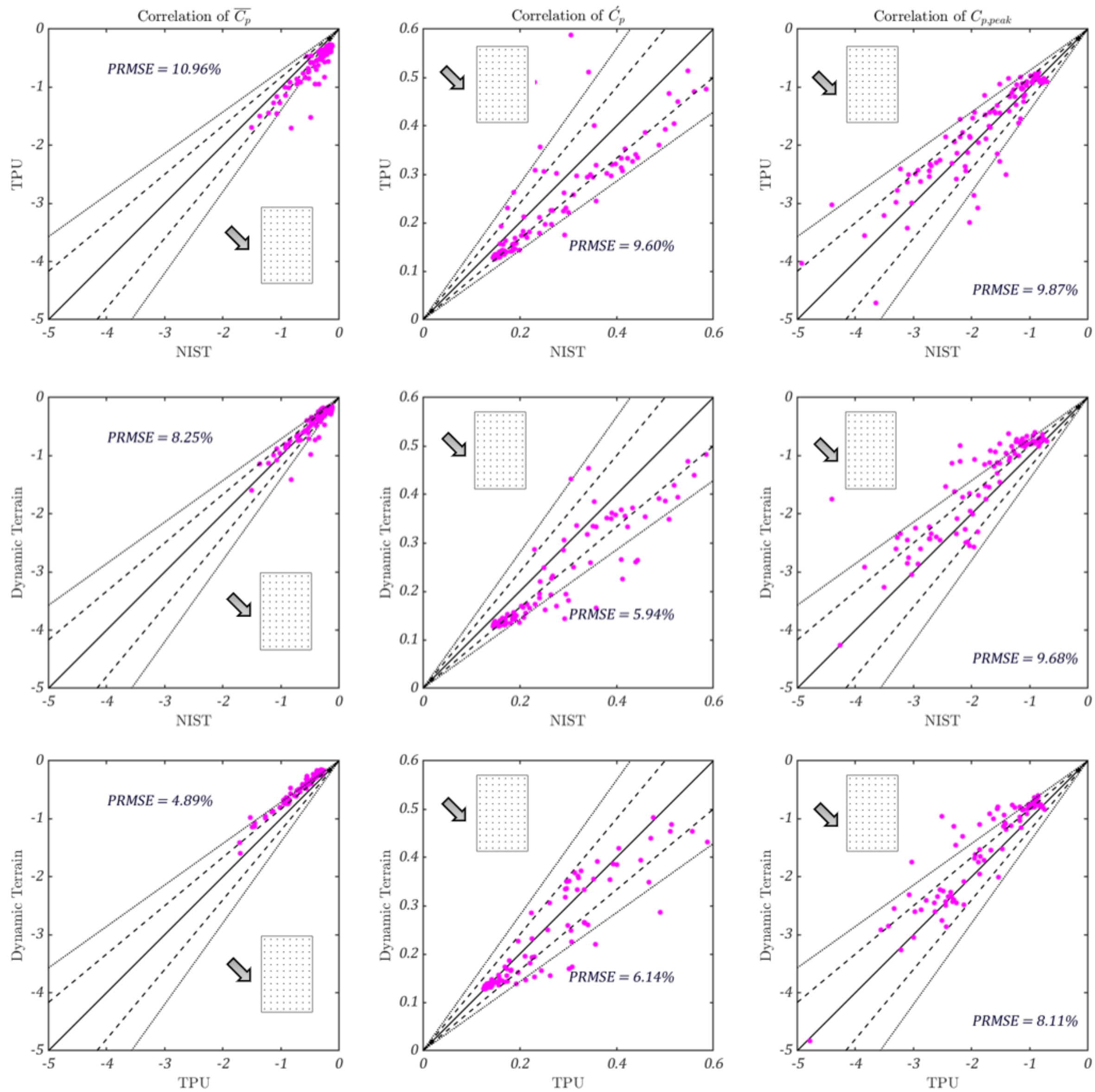

Figure 4.26: Correlation of mean, std and peak pressure coefficients of 45° wind direction for suburban exposure.

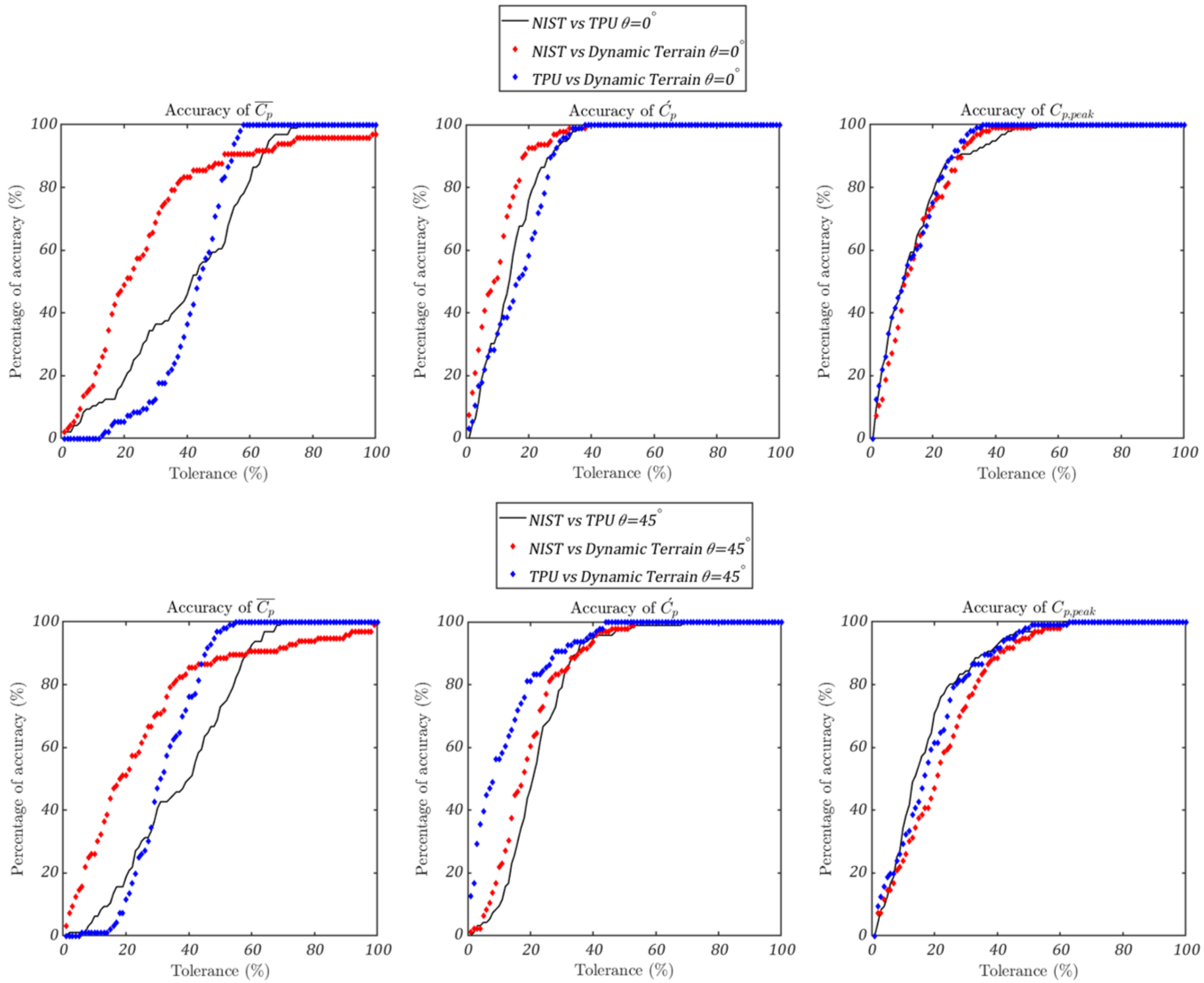

Figure 4.27: Percentage of accuracy versus tolerance between NIST, TPU and Dynamic Terrain method for perpendicular (top) and 45° (bottom) wind direction of suburban terrain.

4.4. Benefits of the methodology

The results of LES-DT presented in the previous sections, show its simplicity, accuracy, and ability to model wind induced loads on low-rise building roofs, with the current assumptions and techniques. By modeling the inlet conditions in this way, the method is successful regarding the following:

- Adopting coarse computational domains for practical applications of structural CWE.
- Accurately representing the high frequency fluctuations in the incident profile for higher frequencies than the cut-off limit of the sub-grid filter.
- Modelling mean and turbulence intensity profiles of the incident flow based on target experimental conditions.
- Avoiding the generation of non-physical pressures in the computational domain that need special treatment when using synthetic inlet techniques (e.g., divergent-free or mass flux corrections Patruno and de Miranda, 2020, Melaku and Bitsuamlak, 2021, Wang and Chen, 2022).
- Modelling accurately the mean, std and peak pressures on building envelopes, based on validation with experimental results.

Most of the limitations of LES-DT presented in Potsis and Stathopoulos, (2024) have been dealt with and presented in Chapter 5, where the documentation on how to use the LES-DT methodology is further discussed and some additional validation studies are presented.

4.5. Summary and Conclusions

Modeling the lower ABL for building design against wind induced loads has proven to be a challenging procedure for the wind engineering community in the last decades. In this Chapter some contributions and trends of the field were analyzed. In order to bridge the current gaps and shortcomings a novel modeling approach is proposed, based on coarse LES, the so-called Dynamic Terrain method (LES-DT).

Wind tunnel experimental results act as a database from which physical velocity time series are introduced in the computational domain. The process of the methodology to generate the appropriate inlet data was elaborated in the paper and the details of experimental and computational conditions were presented for a low-rise building, under open and suburban exposures. Visualization of the vorticial structures and their evolution in the empty computational domain are presented. High frequency energy content of turbulence spectrum in the longitudinal direction is represented accurately in the incident flow, that relates to the target of the method to model peak pressures on the building. Mean and turbulence intensity profiles of the incident flow are represented with good accuracy, based on the target experimental results. Streamlines of the flow field around the building and vortices from the q-criterion are displayed, that demonstrate the ability of the novel technique to model the interaction of low-rise buildings and the ABL. The pressures in symmetric taps of the roof of the low-rise building that was examined follow the experimental trends, and comparisons with state-of-the-art methods proved the ability of the proposed procedure and its advantages. Mean, std and peak local pressures situated in the entire roof for perpendicular and oblique wind direction, proved to be in good agreement with experimental results, for open and suburban exposures. The accuracy was estimated to be in the same order of magnitude as the accuracy achieved between experiments in different facilities. Coarse computational domain was used for all results, that is an encouraging outcome for the utilization of the method in practical applications.

CHAPTER 5: FURTHER DOCUMENTATION AND VALIDATION OF LES -DT

This chapter targets to expand on the practical usage, documentation and benefits of LES-DT that was presented in Chapter 4. An open database and source code are presented (https://github.com/tpotsis/DTv1.0) and applied to two case studies: one isolated low-rise building and a low-rise building inside a street canyon. Validation of numerical results is done based on experiments from the TPU database. Part of the material found in this Chapter was presented on BBAA IX of 2024 (Potsis and Stathopoulos, 2024b).

5.1 Introduction

Wind in the atmosphere can be considered a friend and an enemy. On the one side, wind energy and natural ventilation of cities can be impactful and beneficial to society. On the other side, wind can act as an extreme load on structures and influence their performance and their design process. Although wind engineering is a relatively young research field, it is widely accepted by the community that wind tunnel experiments are vital to estimate the aspects of wind as a friend and as an enemy. Since computers have developed so much during the last decades it is only reasonable to question: Can they aid in modeling the wind in the ABL as well?

The answer to the above question is yes, but there is one very important limitation. Wind turbulence in the lower Atmospheric Boundary Layer (ABL) interacts with human works and creates random and flow patterns. In order to have an accurate computational representation of this interaction Direct Numerical Simulations are necessary. Even with the most advanced High-Performance Computers (HPC), it is impossible to resolve this type of simulation within a reasonable time. Thus, the community of Computational Wind Engineering has turned its attention to Large Eddy Simulations (LES) and how the inlet conditions can be utilized in order to make the computational cost more practical.

In the state-of-the-art of CWE for structural applications there are three main categories of methods to model the inflow turbulence for efficient computational methods. Those are the recycling techniques, synthetic techniques and virtual wind tunnel. The last section is further decomposed to precursor method and entire wind tunnel modeling. In all methods available in the state-of-the-art, there are four aspects that need to be evaluated in order to have a representative wind flow according to the natural wind:

(a) *source of velocity time series*

(b) *temporal and spatial discretization of the inflow*

(c) *incident flow profiles*

(d) *pressure time series extraction* techniques from the computational domain

The above assumptions for each aspect, need to be combined with decisions of the computational set-up, such as subgrid model, mesh size, time step, solution and discretization schemes. All in all, there is high complexity in order to conduct numerical analyses that are able to replicate the natural wind in the same manner as wind tunnels do and have good validation and verification metrics.

This Chapter aims to further expand on details for the novel computational methodology of this thesis, that relies on simple steps in order to estimate wind loads on buildings via HPC. The Dynamic Terrain (LES-DT) inflow generation method is combined with widely adopted LES in order to numerically calculate the wind flow in lower ABL and its interaction with human works. In this Chapter, the assumption made via the LES-DT technique for each of the four aspects will be presented along with its differences with the state-of-the-art. Validation of LES -DT regarding wind loads on structures have been presented in Potsis and Stathopoulos, (2024) and regarding environmental application in Potsis et al.., (2024).

In Section 5.2, the procedure of the novel LES-DT method will be presented in contrast to other methods in the state-of-the-art regarding the four main aspects that were earlier discussed. In Appendix A the relevant data are presented, and some more specific guidelines are discussed for the LES-DT. In Section 5.3, the application of the LES -DT methodology will be displayed in order to model a suburban exposure for a low-rise building in isolated conditions and inside an urban canyon. Numerical results will be validated with experimental data from TPU. Finally, the Chapter concludes in Section 5.4 with the main findings.

5.2 Four aspects of inflow turbulence modeling for LES in the ABL

In this section, four main aspects of wind inflow for ABL modeling and wind-induced loads are discussed. The assumptions of the LES-DT are presented in contrast with similar assumptions in the state of the art, based on recycling, synthetic inlet and virtual wind tunnel techniques.

5.2.1 Source of velocity time series

Conducting LES for ABL flow to model peak and not only mean flow and load properties, changes the inlet conditions tremendously when compared with the stand ones for steady-RANS (Potsis et al.., 2023). Due to that, new inlet conditions have been researched since the milestone work by Kondo et al.., (1997). A first question that arises is what is the source of the velocity time series? Three answers can come into mind: numerical (from precursor analysis that use inlet similar to steady-RANS) or analytical. The first approach is used by any precursor domain method and the Virtual Wind Tunnel. These methods have proven to provide great results, although the very fine mesh, huge computational domains and inability to modify the incident flow efficiently make them inapplicable for practical applications as well (Potsis and Stathopoulos, 2022, 2024). Synthetic methods utilize the second approach by using various analytical expressions in order to create time series that represent the wind flow. Mainly due to the need for divergence-free inflow, synthetic inflow data have to undergo secondary complicated modification in order to have meaningful results. For this reason, and due to the need for very fine mesh, synthetic techniques are not yet adequate for practical use but have provided valuable insights in the CWE field (e.g. Melaku and Bitsuamlak, 2024).

In contrast to all the above techniques, the LES -DT method uses a third approach as a source of velocity time series for inflow: experimental data. Velocity time series from the Concordia Wind Tunnel are included in a public database, whose detailed information is presented in Appendix A and used to generate the inflow condition. In this way, they have a strong physical meaning since they come from experimental measurements that are validated in various studies (e.g., Stathopoulos, 1984, and more recently in Chavez et al.., 2022). Also, an important aspect of this method is that the inlet boundary condition is set as a quasi-steady, in the sense that the various velocity values are kept constant for a specific duration and then suddenly change. This means that by definition the inflow is divergent-free at the durations where the inflow data are constant. Each constant profile is convected downstream and interacts with the building of interest. In a fictitious way, each profile can be assumed as a mean profile of a different terrain, thus the name of the methodology was selected as Dynamic Terrain. More information regarding the experimental data can be found also in Potsis and Stathopoulos, (2022, 2024) and Chapter 4 of this thesis.

5.2.2 Temporal and spatial discretization of inflow

Temporal and spatial discretization of the inflow data is a vital step in order to express accurately the ABL via LES. It regards the choices of how fast the data will be introduced at the inlet (temporal aspects) and how they will be introduced in the lateral direction (spatial aspect). The assumptions used by various authors and methodologies differ, or in many cases, they are not even explicitly defined in their studies, which creates a problem in CWE.

The most usual practice in the precursor domain method is to map the velocity at the sampling plane for each time step of the precursor analysis. These data are saved and for each cell of the plane and fed to the main analysis. The mesh of the sampling and inlet planes need to be identical, which might create an extra computational restriction. Similar to the Virtual Wind Tunnel approach, it is impossible to modify the time or spatial discretization of the inflow data, thus these two methodologies lack the flexibility of introducing time series with different time steps or adjusting the lateral values according to the target.

On the other side, synthetic methods use various assumptions regarding temporal and spatial discretization of the inflow. Regarding the temporal discretization, it should be noted that most of the methodologies correlate the temporal discretization of the inflow with the computational time step, but do not have a clear proposal for these values, since they are dependent on the mesh size. For example, in the CDRFG (Aboshosha et al.., 2015) there is no restriction regarding the proper temporal discretization of the inlet data, thus they can be generated for any choice of the user. Besides that, the authors defined the f_{max} parameter as the maximum frequency that the inflow could resolve. Similar assumptions are used by various synthetic methods techniques such as (Kim et al.., 2013, Yu et al.., 2018, Lamberti et al.., 2018 and Bervida et al.., 2020). Melaku and Bitsuamlak, (2021), assumed an inlet frequency of 1250 Hz, that matched the computational time step size based on the frequency limit after which the spectrum of the longitudinal component can be assumed to be zero. More recently, in Al-Chalabi et al.., (2024), the CDRFG method was utilized for a parametric study of the f_{max} parameter that showed the sensitivity of the spectrum at the inlet and the pressures on building envelopes.

In contrast to that, the LES-DT method decouples the time step of the analysis and the time discretization of the inlet (hereafter inlet frequency) for two reasons. First, due to the fact that the data are introduced at the inlet in a quasi-steady manner, thus the analysis needs to conduct more time steps for each terrain at the inlet (usually more than 5) to extract appropriate the time series. Second, because by adjusting (tuning) properly the inlet frequency, an increased energy at the inflow can be achieved that when dissipated due to the filtering of LES results to a match at the high frequencies of the velocity spectrum inside the computational domain. To expand on that, starting on the theoretical aspect, high frequency velocity fluctuations are closely related to peak values on the building envelopes. This means that their representation is vital both in wind tunnel experiments and numerical simulations. More specifically, Morison and Kopp, (2018), concluded that the normalized frequency range of $0.1<n=f*H/U<2$ is very important in order to have proper development of peak wind induced pressures. This means that the cut-off frequency limit of LES should either be above this threshold, or different actions should be taken that utilize the inflow conditions to achieve that. If the cut-off filter of LES (indirectly the mesh size) is to be selected above this range, the mesh size will become so small that it will be impossible to apply for practical applications. This explains why in most of the studies found in the literature (that the authors actually present this data), the cut-off frequency of LES is less or close to 1 (Geleta and Bitsuamlak, 2022, Vranešević and Glumac, 2024).

Keeping the above in mind, in all of the studies found in the literature, either with synthetic inlet, precursor or virtual wind tunnel methods, a “dive-in” of the velocity spectrum is noticed at the incident flow, similar to what is presented in Figure 5.1a. What the LES-DT proposes is that the inlet frequency can be adjusted according to the mesh size and the numerical setup so that an augmented spectrum is assumed at the inlet. When these fluctuations dissipate due to the filtering process of LES, the spectrum inside the computational domain agrees very well with the target von Karman spectrum – see Figure 5.1b. Similar results have been presented in Potsis and Stathopoulos, 2022, 2024, Potsis et al.., (2024) and Chapter 4 of this thesis. This can be considered the main difference between the rest of the synthetic methods in the state-of-the-art and the LES-DT methodology. More information on how the tuning process should be conducted in practical application via the publicly available C++ code is presented in Appendix A.

Regarding the spatial discretization of the inflow, precursor domain methods use as control points all the mesh of the inlet plane, while for the Virtual Wind Tunnel method the inflow is uniform in the lateral direction. Similarly, synthetic methods calculate analytically the inlet time series in all mesh at the inlet and provide different instantaneous values. Still, these values should have the same statistical properties in the later direction as to generate a uniform flow with insignificant differences in the mean and turbulence intensity profiles in the lateral direction.

Via the LES-DT method the flow that is generated is uniform in the latter direction by assuming similar sets of control points located next to each other. The heights where the experimental velocity time series are extracted are considered as the z values of the control points, while the y values are equally spaced in the inlet plane. The control points feed the neighboring numerical cells of the inlet plane with the appropriate data for each time step. For example, in Figure 5.2 an instantaneous distribution of the velocity at the inlet plane is presented with three sets of control points (black dots). Various setups have been tested and the uniformity of the inlet in the y-direction can be achieved in various ways in OpenFOAM, with similar results. More details regarding these implementations can be found in Appendix A.

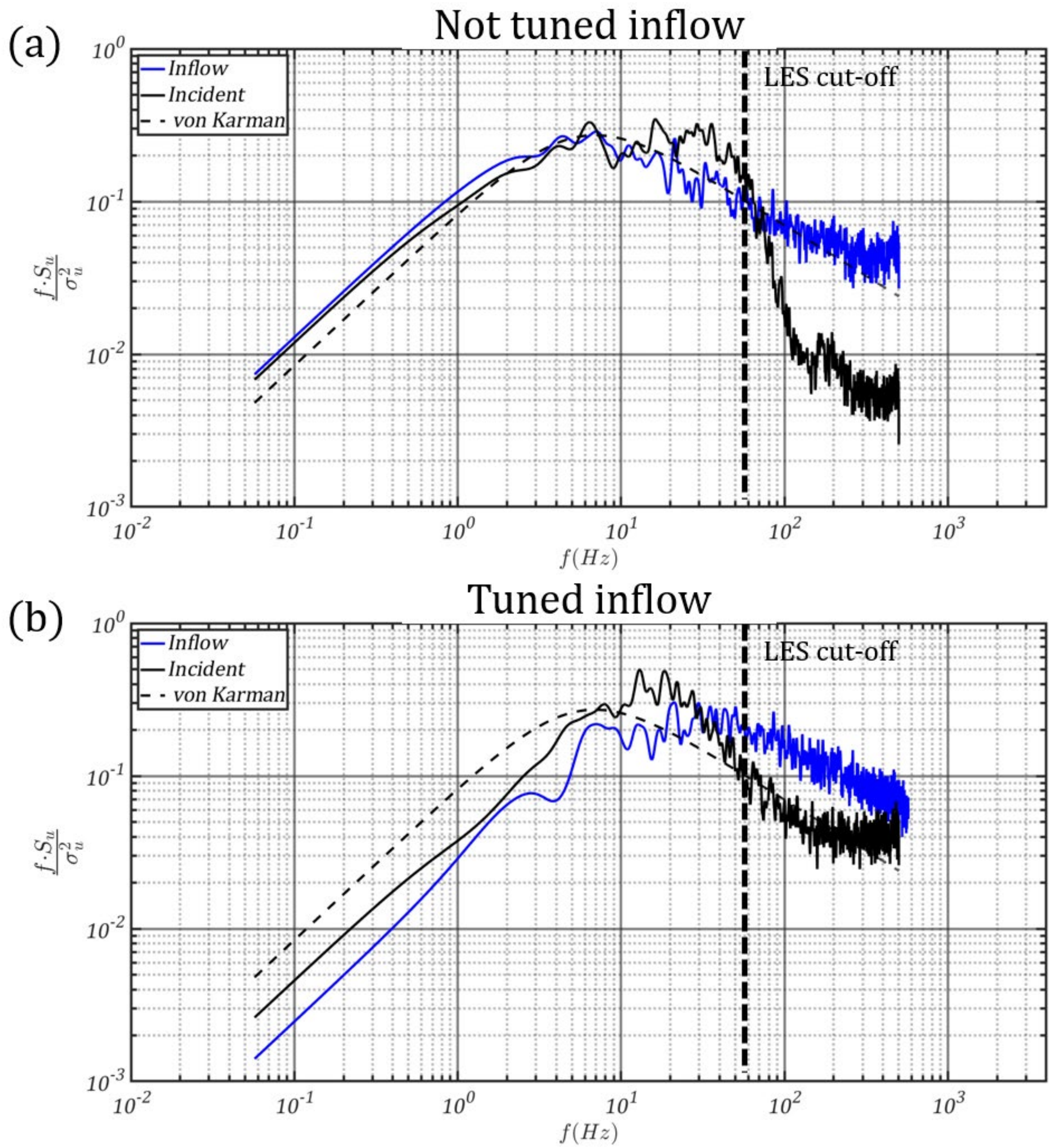

Figure 5.1: Spectrum of longitudinal velocity at inflow (blue) and incident flow (black) via (a) not tuned and (b) tuned process

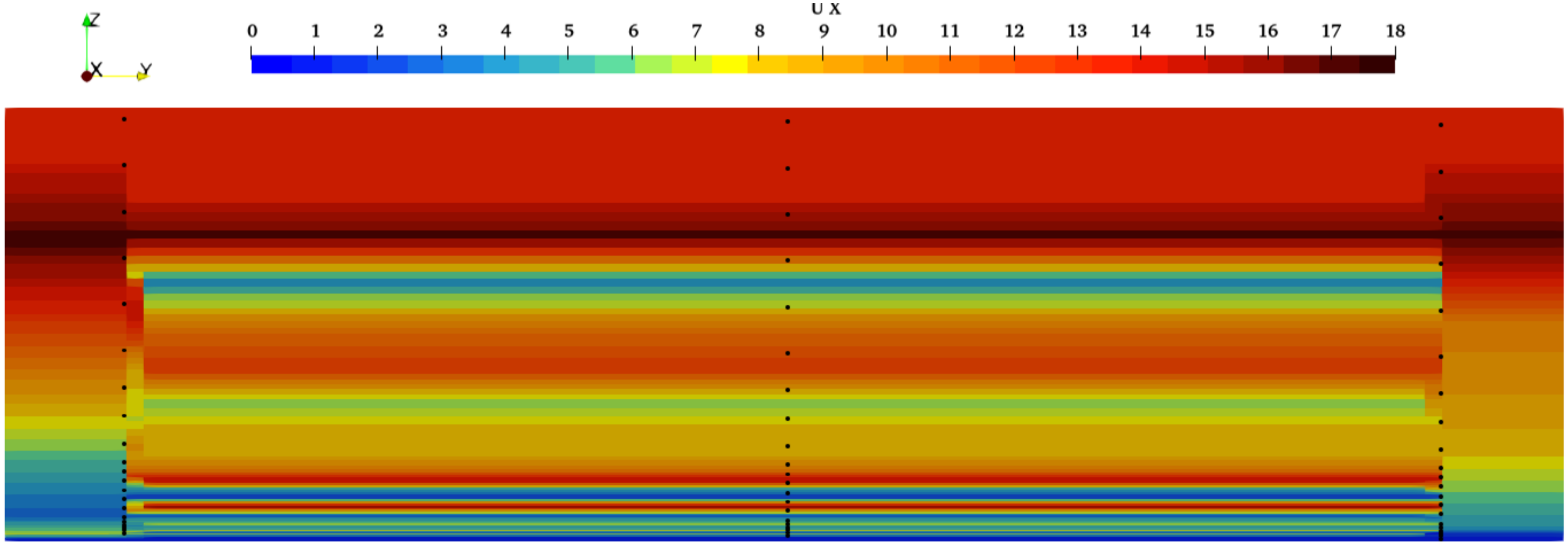

Figure 5.2: Spatial discretization of inflow at the inlet plane

5.2.3 Incident flow modification

Besides the spectral content, the pressures on building envelopes are closely related to the incident flow statistical profiles. Thus, it is also important to ensure that the incident profiles are as close as possible as the target exposure. The main problem with achieving easily the target incident profiles is the fact that turbulence tends to dissipate along the computational domain, that is from the inlet plane until the incident profile location.

Due to that, in various synthetic, precursor and virtual wind tunnel methods physical elements that resemble wind tunnel roughness blocks, are placed on the floor (Ricci et al.., 2017). Although this can help achieve the target statistics at the incident flow, it is not that efficient as to modify the exposure conditions and many iterations are needed to achieve the appropriate flow. Besides that, roughness elements necessitate more mesh at the final computational domain, thus making it less efficient. Other approaches used modification of the synthetic inlet parameters (e.g., mean values, shear stresses, length and time scales) to achieve various exposures to the incident flow. Most characteristic is the optimization process presented in Lamberti et al.., (2018) and the parametrization procedure of Al-Chalabi et al.., (2024), also discussed in 5.2.2. Melaku and Bitsuamlak, (2024) used a stress model as a ground boundary condition in order to sustain the turbulence characteristics from inlet until the incident flow, based on previous findings by Porte-Agel et al.., (2011). Wang and Chen, (2020) used a similar procedure to model the incident flow via a wall function. Forcing methods have also proven to be able to modify the incident flow characteristics by introducing a new forcing term in the NS at the fetch close to the inlet plane (e.g., Wang et al.., 2023). A more straightforward approach to modifying the inflow parameters to adjust the incident profiles was presented for the first time in Guichard (2019). In this case, a modification of the mean and std profiles at the inlet was enough to adjust the incident profile accordingly. Similar assumptions have been used by Melaku et al., (2022), Xing, (2023) and Sun et al.., (2024).

Given the fact that LES-DT is an engineering-based tool, the target is to provide a procedure able to be used by different computational setups, that at the same time can be efficient. For that reason, the flowchart of Figure 5.3 is used. The concept is to first modify the mean wind data at the inlet to match the target incident mean profile. After this is achieved, the altitude of the time series values is modified, which indirectly adjusts the std of the time series. A comparison of the turbulence intensity is needed to also make sure that the turbulence intensity profile is accurate. The above process is presented in Figure 5.4, by targeting a suburban exposure (A/B exposure based on ASCE 49-21). Similar results have been presented in Potsis and Stathopoulos, 2024 and in Chapter 4 of this thesis. The modification process is done by using the source code in C++ and more details are found in Appendix A.

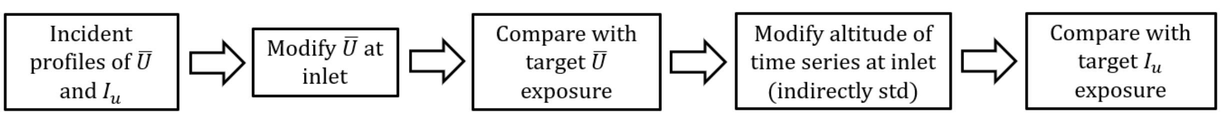

Figure 5.3: Flowchart of incident flow modification of LES-DT

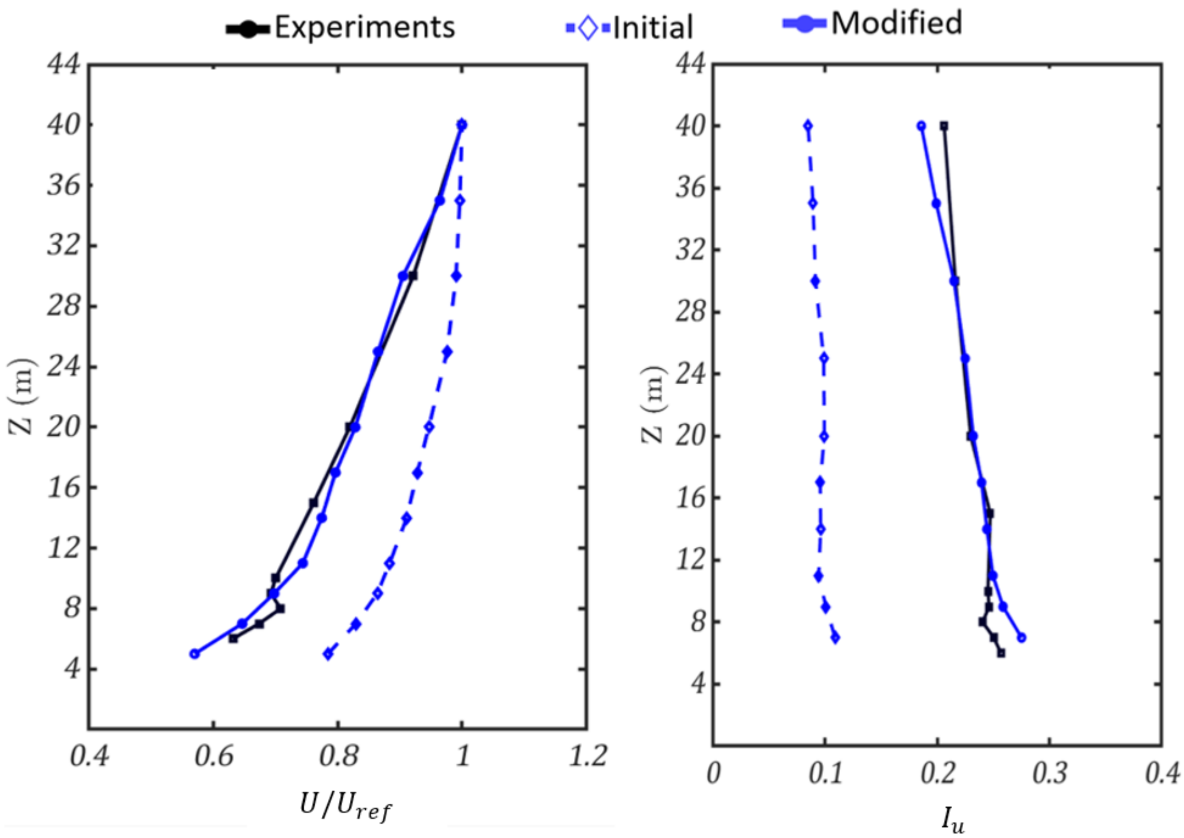

Figure 5.4: Example of initial and modified incident profiles for mean (left) and turbulence intensity (right)

5.2.4 Pressure time series extraction

From a structural engineering perspective, a CFD tool is helpful only if it can provide accurate and reliable results regarding the peak wind induced pressures. In this Subsection, the methodology of LES-DT in order to extract the pressure time series is presented. This step is vital for LES-DT, but it is not explicitly defined in other methods found in the state-of-the-art, which might lead to misunderstandings from a practical point of view.

As mentioned in 5.2.1, the inflow data of LES-DT have a quasi-steady character, thus there is an inherent discontinuity in the incoming wind. In order to compensate for the sudden change of the incoming flux in the NS, a large pressure gradient is created for the time steps close to the transition of the terrains. After various parametric studies of the behavior of the convergence of the pressure term in the NS, the LES-DT method proposes a flowchart presented in Figure 5.5, as to extract pressures that have valid physical meaning and can inform structural engineers regarding the peak pressure during a wind event. The scope is to first extract the time series for every time step from OpenFOAM, then discard the data that come from time steps close to the transition of terrain, thus keeping the data that correspond to a steady inlet. Finally, a new average is imposed on the time series to account for the target output frequency (e.g., in wind tunnels it ranges from 300 Hz – 1000Hz). Further explanation and documentation are presented in Appendix A.

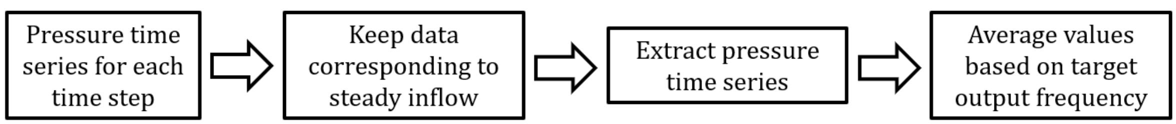

Figure 5.5: Flow chart of pressure time series extraction of LES-DT

Figure 5.6a presents the instantaneous flow field around a low rise structure and Figure 5.6b, is zoomed close to it. By utilizing the procedure presented in this subsection we can finally extract pressure time series like the one presented in Figure 5.6c. This one regards a pressure tap on the roof of the building. As seen, the time series has the characteristic skewness that is expected and measured in various experimental and numerical studies (e.g., Ciarlatani et al.., 2023). The pressure time series have to undergo a meticulous statistical procedure to extract mean, std and peak values. Validation of these values against experimental results are vital to estimate the accuracy of LES-DT. As discussed in Chapter 4, the procedure has been able to provide accurate results within the threshold of accuracy with good efficiency.

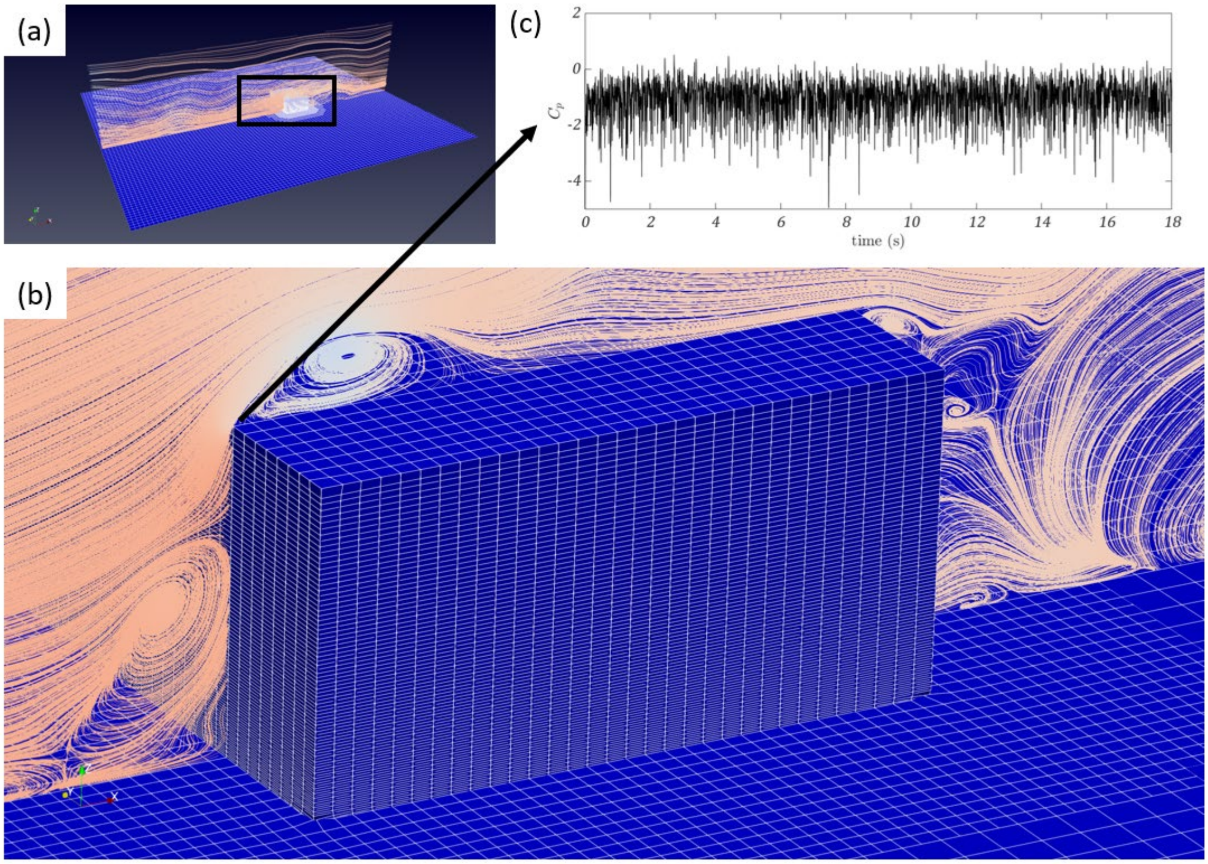

Figure 5.6: Instantaneous flow field around low building with instantaneous streamlines (a) entire computational domain (b) zoomed. (c) Pressure coefficient time series of LES-DT on building roof

5.3 Application of LES-DT for wind-induced loads on low-rise buildings

Low-rise buildings were selected as case studies due to the fact that the flow field has a strong three-dimensional character in contrast to high-rise buildings, where the flow field tends to be more two-dimensional. This gives an extra level of difficulty in this modelling approach. In addition, low-rise buildings are exposed to more turbulence due to the fact that they are closer to the ground, as discussed in Chapter 1. Combining both reasons, the accuracy of the LES-DT will be scrutinised under complex and realistic scenarios.

This Section is divided in three subsections. First the incident flow profiles are presented, that resemble a suburban exposure and are modelled based on the modifications of the inflow frequency and the mean and std profiles, as discussed in 5.2. The profiles are validated based on TPU results that correspond to a A/B exposure based on ASCE 49-21. Then, mean, std and peak pressures on 240 pressure taps are validated with TPU results for an isolated and a building in a street canyon for perpendicular wind direction.

5.3.1 Incident flow

Information on the incident flow profiles are vital in order to estimate the wind characteristics that interact with the building (or cluster of buildings) of interest. Due to that, the incident flow is measured inside the computational domain without any obstacles, before any building is placed. This approach is used in wind tunnel measurements as well.

For the purposes of this study a suburban exposure is modelled at the incident flow, after following the steps of the LES-DT that were presented in Sections 5.2 and Appendix A. Mean and turbulence intensity profiles of the incident flow are presented in Figure 5.7 and compared with the target experimental results from TPU public database. The accuracy of the numerical (LES-DT) and experimental results from TPU is within an acceptable margin of maximum error of 10%. This profile corresponds to exposure A/B in ASCE 49-21.

More importantly, according to what was stated in Section 5.2.2, at the incident flow the LES-DT results have the capacity to capture the proper energy content of the high-frequency fluctuations. This is done by the proper temporal discretization of the inflow. In Figure 5.8, the correlation of LES-DT results at the incident flow is shown with theoretical von Karman and experimental results from Concordia Wind Tunnel. This result regards the height of h = 12 m in full scale that corresponds to the building height analysed in Sections 5.3.2 and 5.3.3. The inflow frequency was selected as $50 \cdot f_c$ to achieve this outcome, as also discussed in Section 4.2, where f_c is the cut-off frequency of LES.

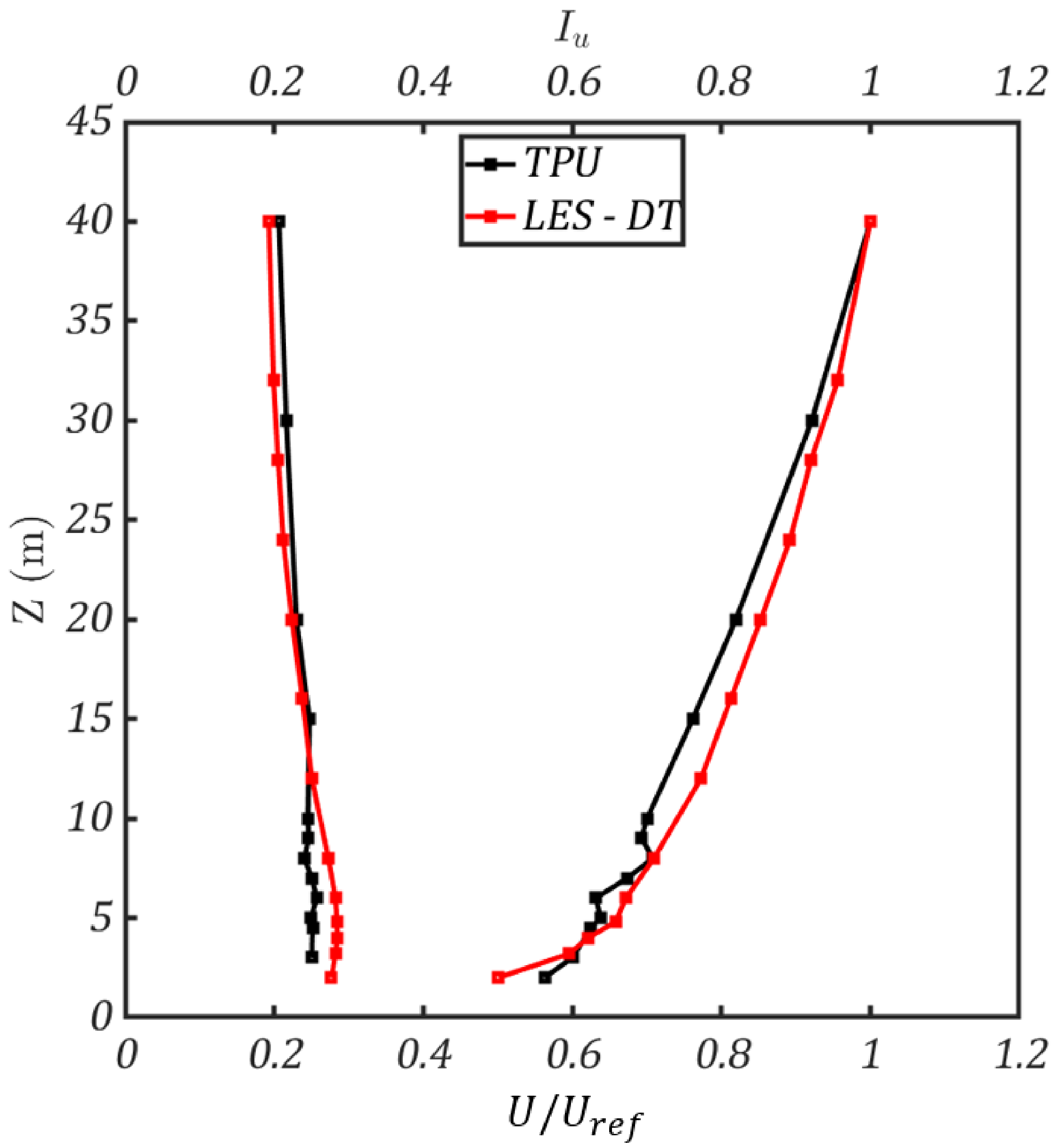

Figure 5.7: Mean and turbulence intensity profiles of LES-DT (red) compared with experimental results from TPU (black)

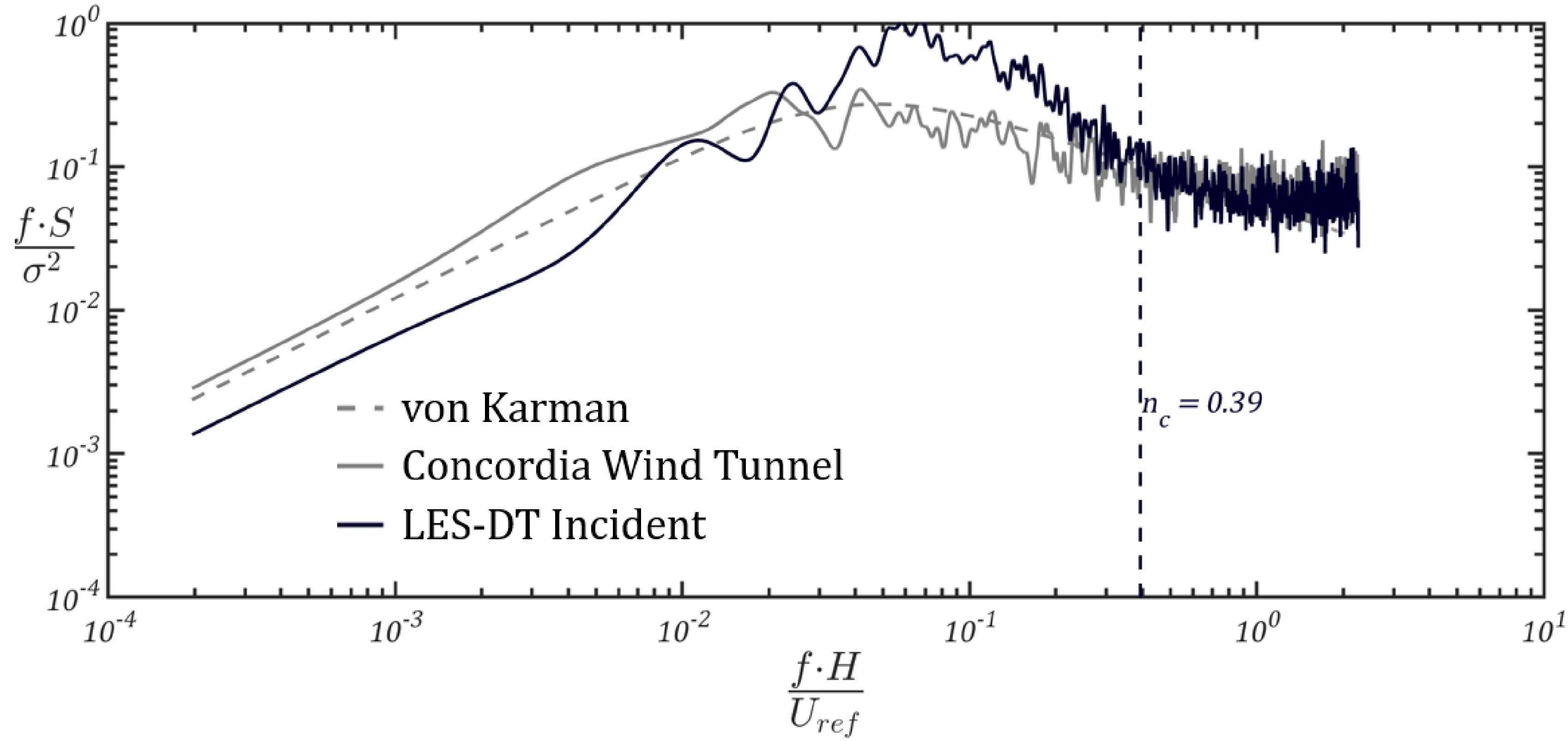

Figure 5.8: Spectrum of longitudinal velocity of von Karman (dotted grey line), Concordia Wind Tunnel (solid grey line) and LES- DT (solid black line) for h = 12 m in full scale

5.3.2 Wind loads on an isolated building

Firstly, an application of LES-DT was done for an isolated building with full-scale dimensions H x B x D = 12 m x 16 m x 24 m. The turbulence intensity at roof height is close to 22 % with a mean velocity of 8.4 m/s, in both experiments and numerical modeling. The mesh used is displayed in Figure 5.9, with inflation of three separate volumes around the building, similar to the mesh of Figure 4.8. The total number of mesh is around 1.8 million elements.

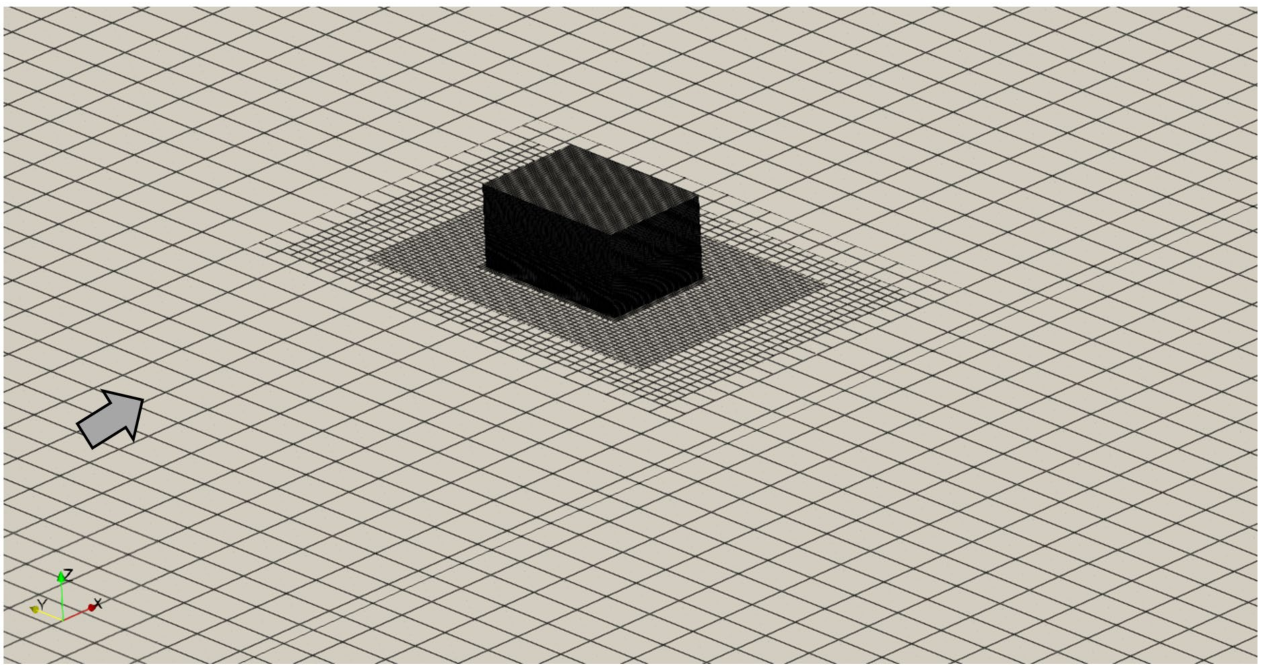

Figure 5.9: Mesh around the isolated building

In Figure 5.10, the mean flow around the building with the mean streamlines are presented in order to quantify the flow around the building subjected to the wind. As can be seen, there is a horseshoe standing vortex in front of the building, a detached vortex on the roof and a detached vortex on the lee ward. There are no experimental data available to validate the mean lengths of those vortices, but in theoretical terms, they seem to agree with bluff body aerodynamics theory. The main validation metric available is the pressure time series from 240 location on the entire building envelope. These results are compared between LES-DT and TPU in Figure 5.11and their accuracy is estimated based on the Percentage of Root Mean Square Error (PRMSE) from Equation 3.1.

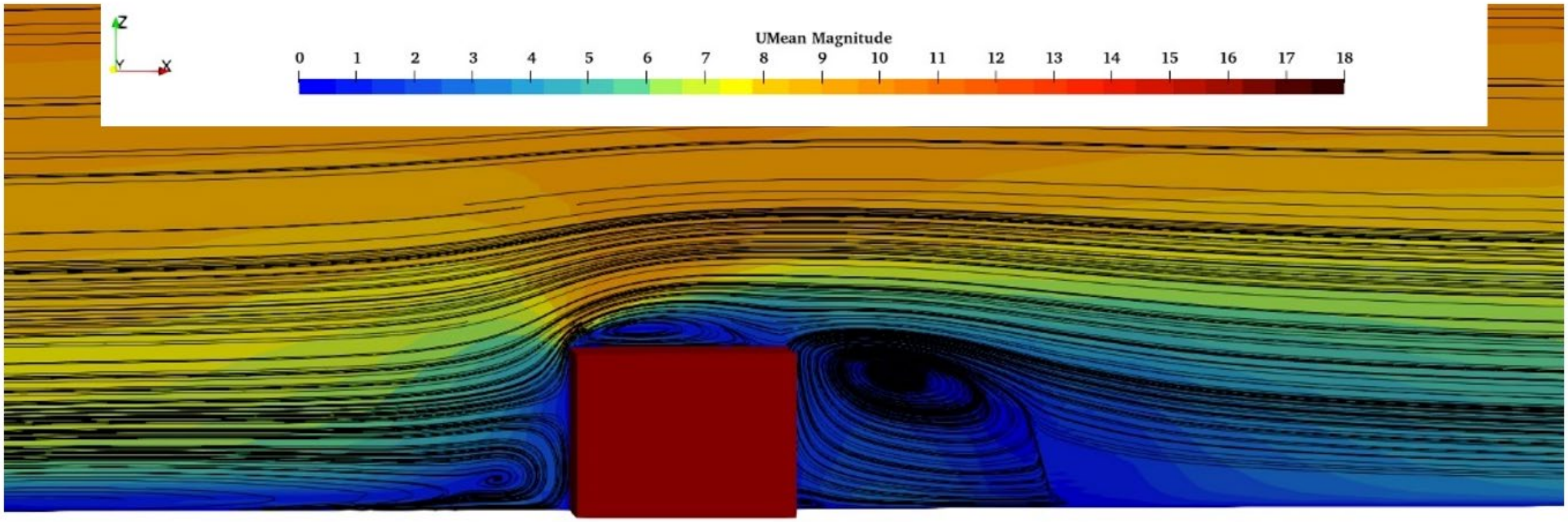

Figure 5.10: Contour of mean wind velocity magnitude and mean streamlines around isolated build

First in Figure 5.11a, the mean values are compared, and great accuracy is achieved, besides the lower energy of the low-frequency fluctuations seen in Figure 5.8 ($2 \cdot 10^{-4}<n<10^{-2}$). Similar findings for mean values on building roofs have been seen in Potsis and Stathopoulos, (2024). The std deviates more from the experimental results (Figure 5.11b), but still is well within the threshold of accuracy discussed in Chapter 3 and Chapter 4. Peak values also seem to have good accuracy in all 240 locations with a PRMSE of 6.10 % - see Figure 5.11c.

Another important metric of peak wind induced pressures is the Probability Density Function (PDF), which is shown in Figure 5.12, for four different locations: a) on the wind ward side, b) on the roof, c) on the side and d) on the leeward side. On the x-axis the pressure coefficients are normalized by subtracting the mean and dividing with the std, as to compare unbiased results. As seen in the aforementioned figure, LES-DT is able to reproduce the PDF distribution of pressures with excellent accuracy, even at the edges of the range, where the peak values are distributed. Regarding the windward side (Figure 5.12a), the PDF is skewed towards the positive values, since the flow is attached to the building surface, while for the rest of the sides the data are skewed towards the negative values. This is due to the fact that the flow is detached, thus higher negative peaks are measured at these locations. This is also seen at Figure 5.11c. Given the complex nature of the modeling due to high turbulence structures interacting with the building, the comparisons of PDFs can be considered good, also considering the efficiency of the computational setup. It is worth noting that the taps selected at Figure 5.12 are representative of all the taps found on the building envelope.

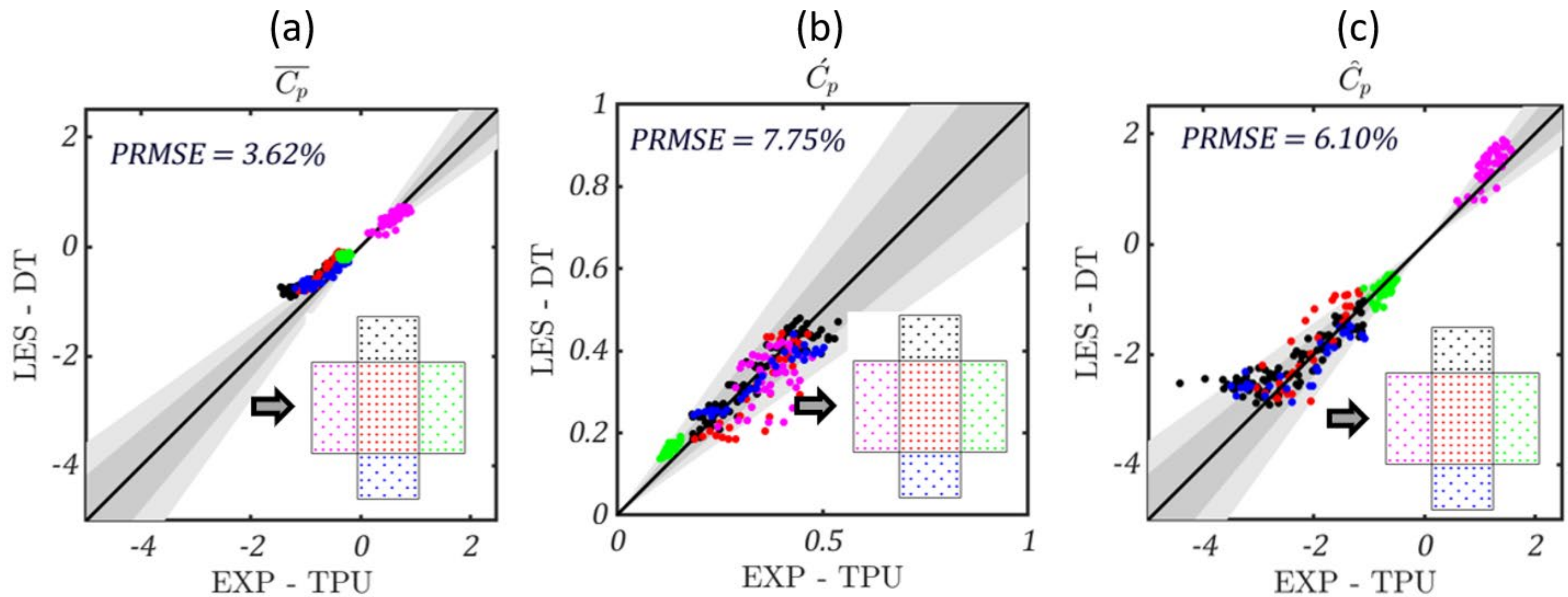

Figure 5.11: Comparison between LES-DT (y-axis) and TPU (x-axis) of (a) mean (b) std and (c) peak pressure coefficient on the isolated building envelope. Colors correspond to different sides of the building.

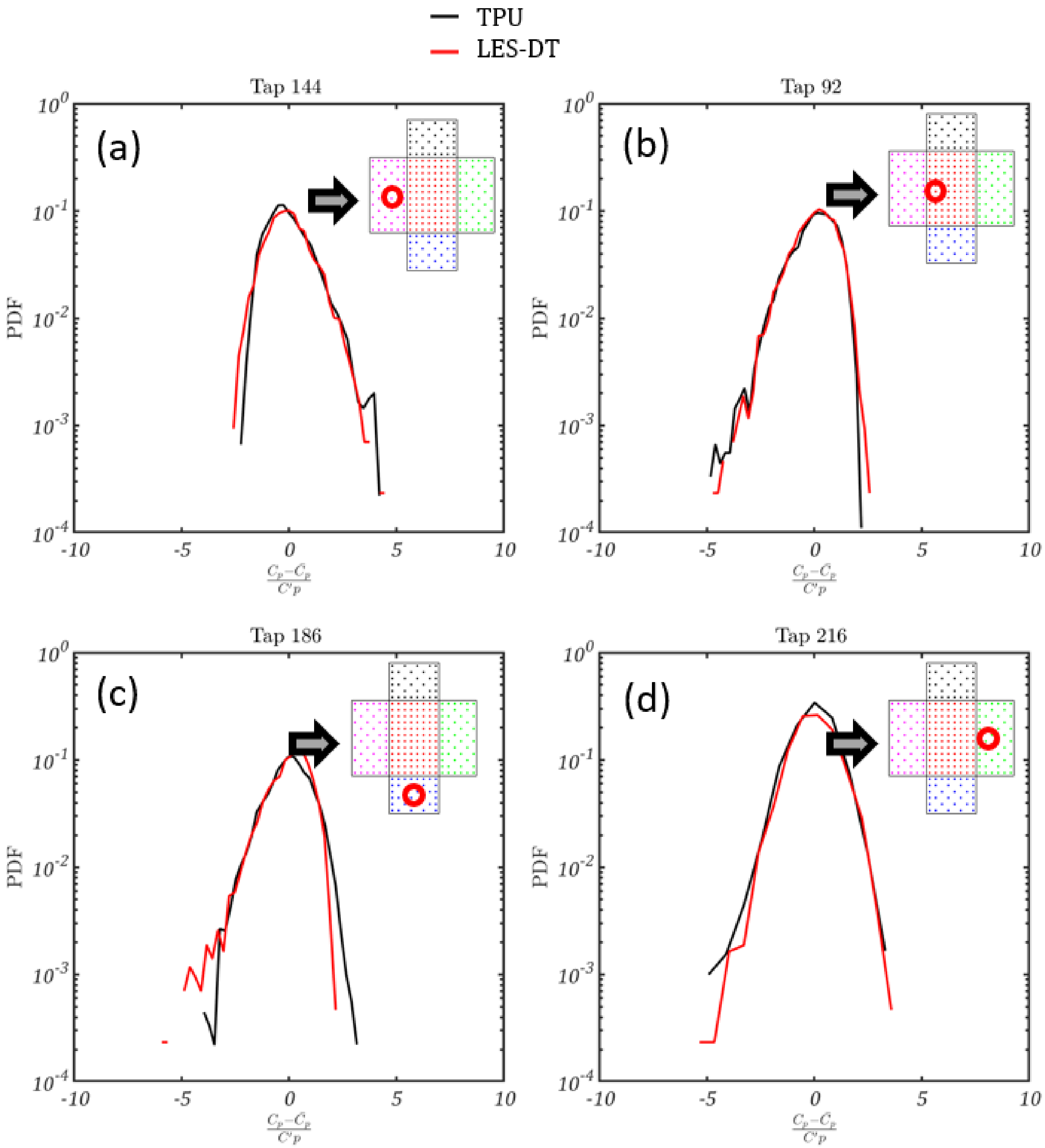

Figure 5.12: PDF of pressure coeffects on (a) wind ward side, (b) roof, (c) side wall and (d) leeward side of the isolated building

5.3.3 Wind loads on building inside an urban canyon

Similar to Section 5.3.2, here the results of a building inside a street canyon are validated against TPU experimental results. The mesh configuration can be seen in Figure 5.13. The building analyzed is the one in the middle and the mesh was kept exactly the same as the one in the isolated building case around it. The surrounding buildings have the same dimensions as the main building and correspond to a ratio of coverage of 0.1, according to the definition found in TPU, (2013). The computational domain, numerical setup, inflow and incident profiles are the same as the ones discussed previously, but due to the surrounding buildings, the mesh has a total number of 2.2 million elements.

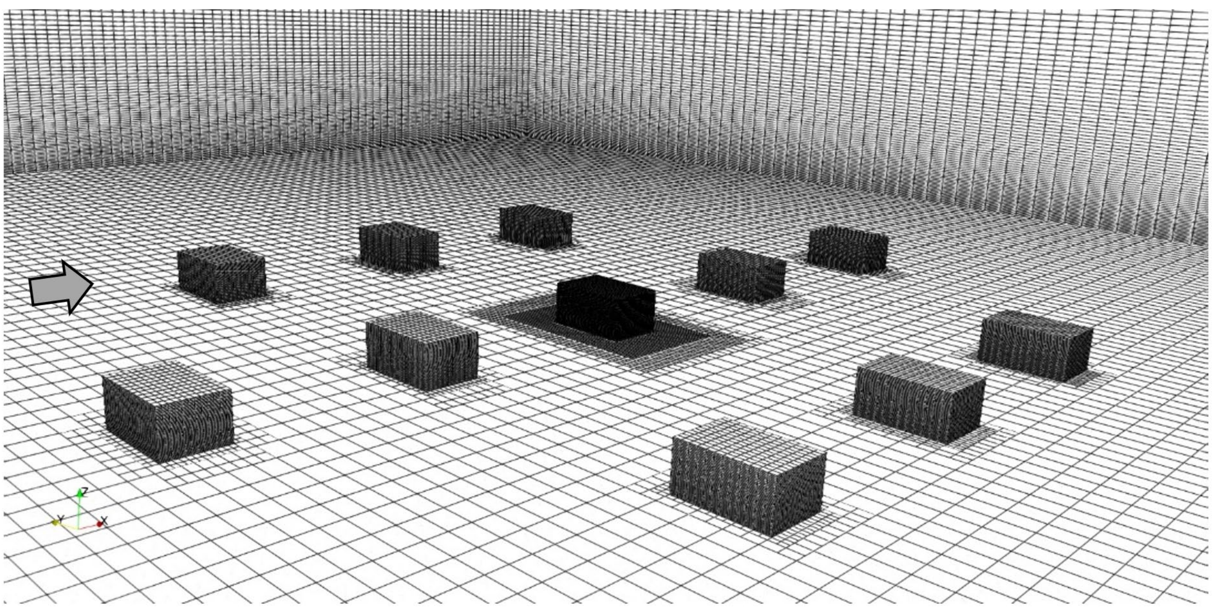

Figure 5.13: Mesh close to the urban canyon

As also seen in section 5.3.2, the mean velocity with the corresponding mean streamlines is presented in Figure 5.14 for the flow inside the street canyon. Recirculating vortices can be seen between the buildings with similar lengths between the canyons. As already mentioned, there are no experimental results to validate these numerical data, which consists of a big problem in the proper validation of CWE. Due to that, validation of numerical results is conducted with 256 pressure taps located on the building envelope of the target building that resides in the middle of the canyon.

Mean, std and peak local pressure coefficients are validated with TPU in Figure 5.15a, b, c accordingly. The PRMSE metric is shown in each subfigure. As seen, the accuracy is slightly decreased compared to the isolated building case at Section 5.3.2, but still within the threshold of accuracy discussed in this thesis. Once more, the effectiveness of the LES-DT is demonstrated for capturing peak pressures, while considering interference effects from surroundings.

PDF distributions for four locations of the building are presented in Figure 5.16. Despite the interference effects the accuracy of LES-DT is very good in the wind ward wall. On the roof, the accuracy is again in acceptable margins, but obviously less than the isolated case or the other sides of the building. This might be due to the fact that the mesh was kept the same, and more detail might be needed to capture more accurately the interference of the canyon to the roof load distribution. Regarding the side and leeward faces, the PDF agrees with the experimental results of TPU, similar to the isolated case. Since the local loads for peak pressure exhibit a very good correlation with the experimental results, the area-averaged loads are expected to behave in the same way, since their calculation comes from the local ones. Due to that, they were omitted from the thesis for clarity.

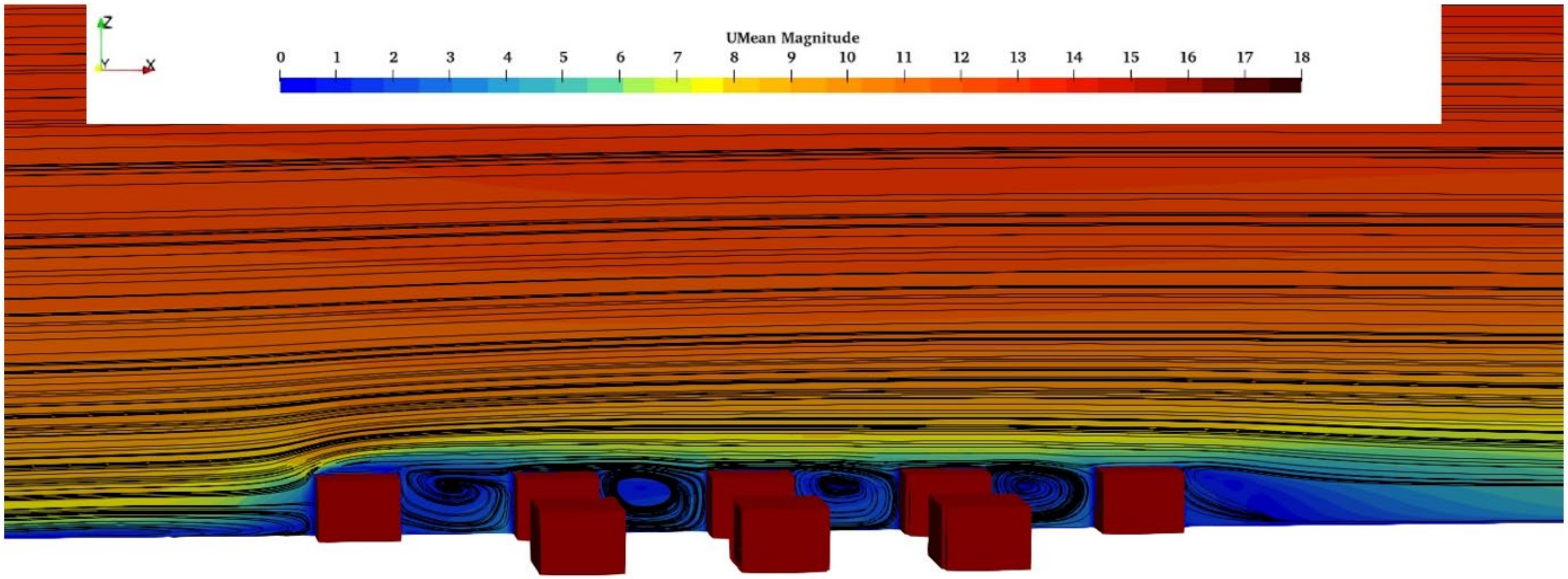

Figure 5.14: Contour of mean flow and mean streamlines inside the urban canyon

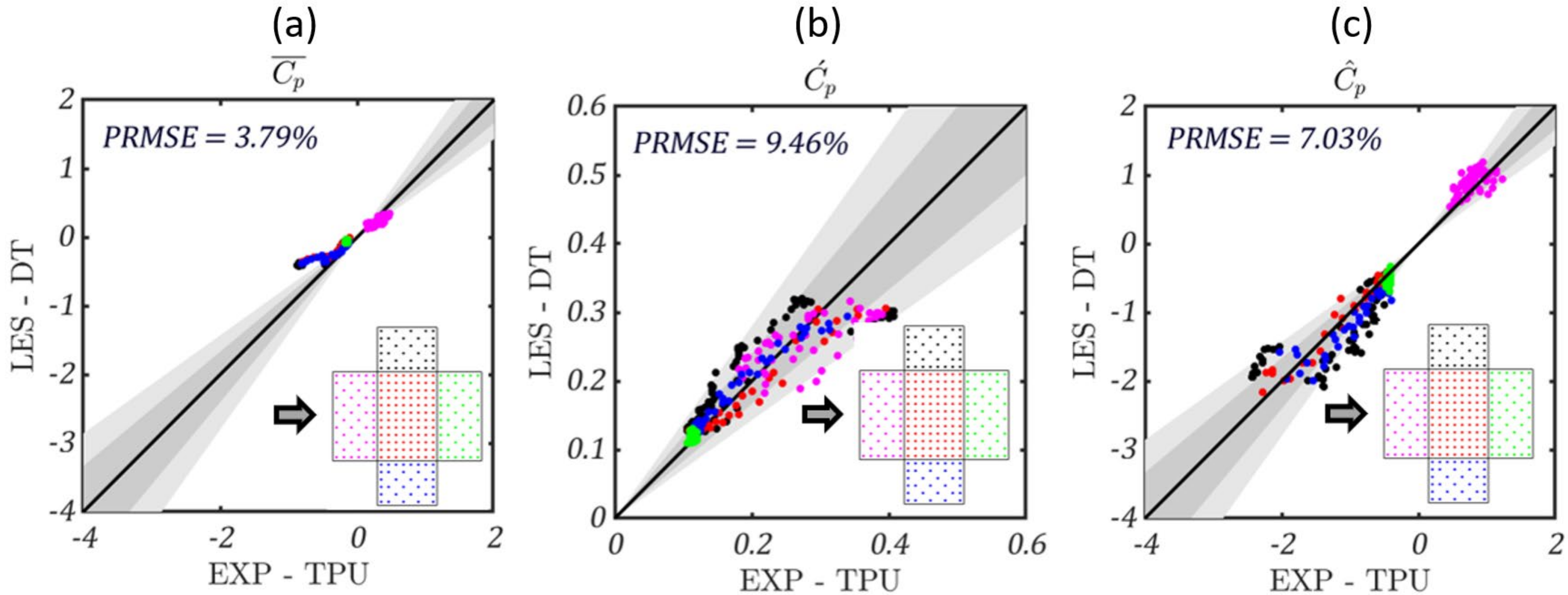

Figure 5.15 Comparison between LES-DT (y-axis) and TPU (x-axis) of (a) mean (b) std and (c) peak pressure coefficient on the building envelope inside the urban canyon. Colors correspond to different sides of the building.

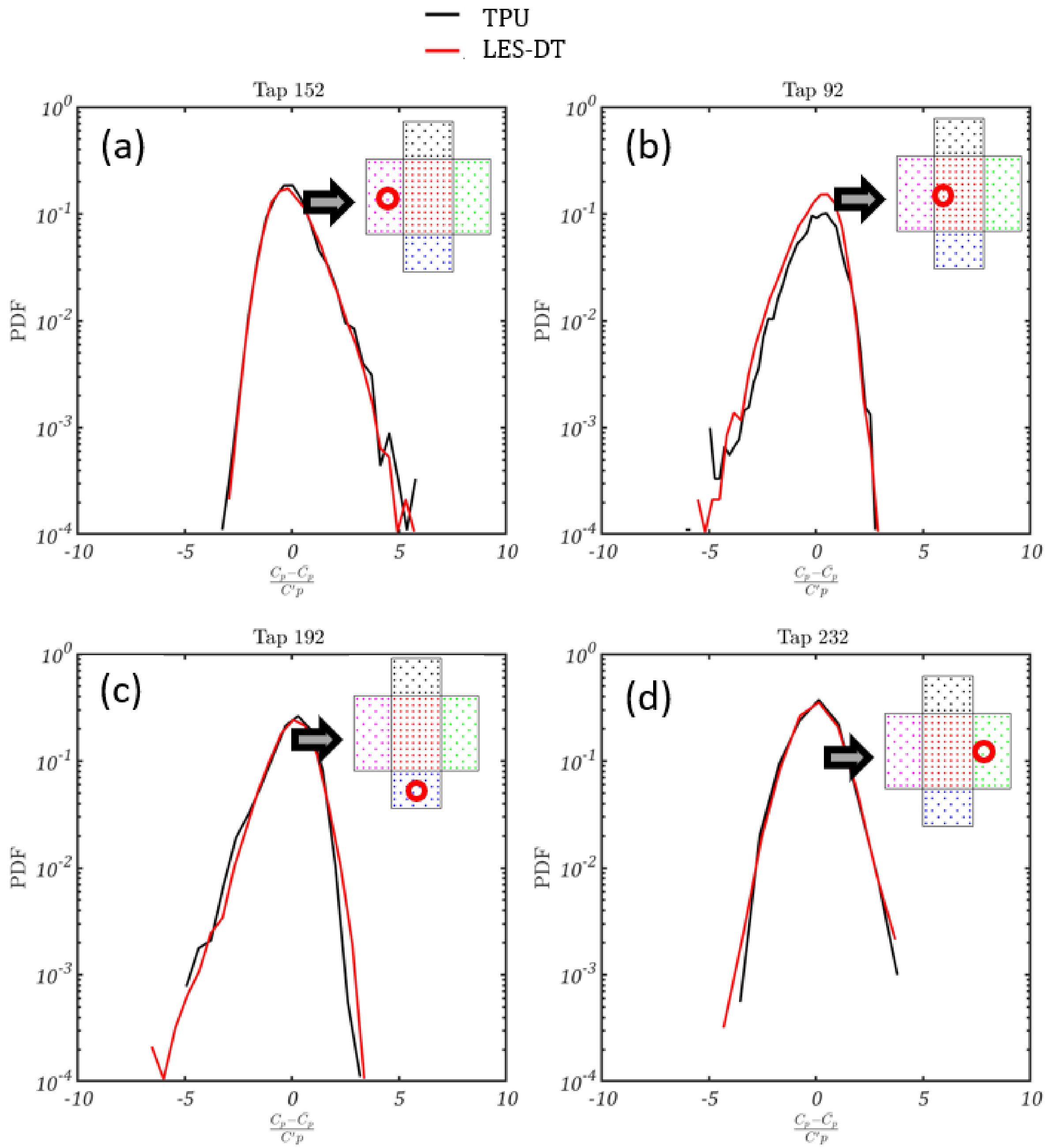

Figure 5.16: PDF of pressure coeffects on (a) wind ward side, (b) roof, (c) side wall and (d) leeward side of the building inside the urban canyon

5.4 Summary and conclusions

This Chapter targets to inform users regarding the Dynamic Terrain methodology via LES in order to model wind flow and wind-induced loads on buildings in the ABL. Four main aspects of turbulence modeling of wind in the ABL are thoroughly discussed, through the scope of benefits and guidelines via LES- DT. Two applications are presented for an isolated building and a building in a street canyon and the incident flow and local mean, std and peak pressures are validated from publicly available experiments. An open documentation and code of LES-DT can be found in https://github.com/tpotsis/DTv1.0. Some aspects of the practical importance of LES-DT are presented, that can be used with efficiency and accuracy for realistic structural wind engineering applications. Guidelines for efficient modeling of the interaction between ABL and structures should be expanded in the future in terms of mesh generation in realistic urban environments to account for various wind directions constructively and systematically.

CHAPTER 6: CONCLUDING REMARKS

In this thesis a novel technique to model numerically wind flow and wind-induced loads on the ABL was developed. The accuracy of this technique has been proven by Potsis and Stathopoulos, 2022, 2024. The technique is advantageous compared to similar methods found in the state-of-the-art in terms of simplicity and efficiency of computational cost. The main conclusions of the thesis can be summarised as follows:

1. The novelty of the computational procedure comes from its ability to introduce high-energy fluctuations to the high frequency vortices related to small turbulence lengths that are significantly smaller than the characteristic dimensions of the building. Also, these scales are mainly responsible for the peak wind-induced pressures on building envelopes. Due to the nature of LES modelling, the inability to correctly model the energy of these scales has been widely accepted by the scientific community. However, in this thesis this inability was considered as a research gap that was addressed with the Dynamic Terrain (LES-DT) technique.

2. The Dynamic Terrain methodology is an engineering tool that can be applied for practical applications that use straightforward procedures and coarser computational domains than similar techniques. The basic strategy of the methodology relates to scaling of the incoming turbulence in the frequency domain. In such a way, small scale turbulence is immediately introduced at the inlet plane by selecting the inlet frequency of the time series. This assumption has been able to consistently model accurately the energy level of the fluctuations in terms of spectral content when compared with experimental and theoretical results.

3. The spectral content was tested and verified at various heights of the ABL and produced similar results in the streamwise direction of the flow. Of great importance is this representation at the incident flow, where the building is introduced in the computational domain.

4. The inlet frequency in the range from $50 \cdot f_c$ to $100 \cdot f_c$ is proposed in order to model the energy of the frequency range of eddies smaller than the characteristic building dimension, where f_c is defined as the cut-off frequency of the filter of LES.

5. Open and suburban exposures were modeled properly by modifying the mean and std of the inlet time series to account for the turbulence losses in the computational domain. A linear scaling of mean values at the inlet proved adequate to model mean profiles for both exposures. The modification of std values at the inlet were tested with linear and non-linear expressions. Regarding the open exposure, a non-linear expression was used, while for the suburban the linear equation was adequate.

6. Quasi-steady conditions are assumed for the inlet time series in order to respect the divergence-free character of the wind flow. Consequently, a discontinuity of the numerical stability is introduced in the analyses, which is accounted by filtering the data appropriately. This can be interpreted as changing the terrain conditions during the analysis since the individual mean profiles are introduced at the inlet in a steady state for a prescribed period (inverse of inlet frequency). Each profile propagates in the computational domain and interacts with the building of interest, where a single value of the pressure time series is extracted for each interaction. This justifies the chosen name of the methodology as Dynamic Terrain.

7. The procedure can be utilized for various mesh sizes, numerical schemes and subgrid models. This makes it ideal for usage in various practical applications, where a variety of parameters is chosen by different practitioners.

8. The feasibility of the procedure has been demonstrated for structural wind engineering applications. This method can act as a tool to evaluate wind flow features and wind induced structural loads, within acceptable accuracy – as established by comparing experimental results from various wind tunnel facilities.

9. An open database has been formed from wind tunnel results from Concordia Aerodynamics Laboratory and libraries in OpenFOAM that makes the methodology accessible to practitioners and interested scientific groups.

CHAPTER 7: FUTURE PERSPECTIVES

Correct modeling of wind load goes hand by hand with correct modeling of the wind that interacts with the building of interest. In the future LES-DT method could be used for environmental studies to expand its realm of applicability. Its reliability has been expanded in the environmental applications in isolated and non-isolated buildings in Potsis et al.., (2024).

As presented in Chapter 5, LES-DT is a methodology that is based on previous assumptions and findings from research conducted by various authors during the last decades. Thus, the current assumptions of LES-DT could be expanded based on other inflow generation techniques in the future. Especially regarding the spectral tuning process, the findings of LES-DT could be beneficial to other methods in order to capture the proper energy content at the high-frequency fluctuations with coarser mesh. Some efforts toward this direction were already done by Al-Chalabi et al.., (2024), where the inflow frequency was parameterized based on the technique of Aboshosha et al.., 20215.

Another important aspect that should be investigated deeper in the future regards how code provisions will introduce guidelines for the use of CWE for structural applications. AIJ for example, is adopting a similar approach with the LES-DT in the sense that via a public database of inflow data, it allows users to model a pre-defined exposure, based on the precursor domain method. In Eurocode a similar direction has been published recently in Bruno et al., (2024). One of the most important aspects that need to be addressed so these endeavors are successful is the mesh that is needed to conduct accurate analysis for various wind directions. The applicability of the LES-DT could be beneficial in these codification efforts, due to the advantages and accuracy that have been displayed in this thesis and in the published papers.

Another interesting aspect is how to utilize the LES-DT by targeting realistic exposures (incident flow profiles) based on GIS data. For example, in Yu et al.., (2023), a method has been presented in order to estimate the z_0 based on Google Earth. This could improve the accuracy of LES-DT for realistic estimation of wind-induced pressures and expand its applicability in real-life applications more drastically, than the "usual" exposures presented in ASCE 49-21.

The public database available at https://github.com/tpotsis/DTv1.0 could be further expanded in the future in terms of code efficiency to generate inlet data that is embedded in OpenFOAM versions. This could facilitate the usage of the method by interested parties. The wind tunnel velocity database has proven adequate to model open and urban exposures at the incident flow, but more experimental data could be beneficial for validation purposes in future studies. This relates to the need to create more databases (or expand the existing ones) with wind profile measurements and velocity time series in urban environments and pressure time series in various building configurations. This will improve the impact of CFD results since their validation will be more properly documented.

For the purposes of this thesis, wind loads on low-rise buildings have been thoroughly investigated due to the three-dimensional character of the flow and the increased turbulence intensity that they interact due to the ground. LES-DT method could be expanded in high-rise buildings in the future and there is no reason to believe that its reliability will be less than low-rise buildings. Some initial results in high-rise buildings have proven to be accurate in the same manner as low-rise buildings but were omitted from the thesis for clarity. Applications of LES-DT in non-rectangular building shapes is also another target for future studies.

APPENDIX A: GUIDELINES FOR PUBLIC DATABASE OF LES-DT

For the purposes of LES-DT in practical application a public database and source code are available in https://github.com/tpotsis/DTv1.0. The core of the database is the DT.cpp C++ code, which reads all the information from the Data file and generates the corresponding directories in appropriate location of the numerical case. As an output is also prints the statistics of the wind tunnel data used to generate the turbulence inflow and the statistics of the data at the inlet plane. The modification of the inflow is done based on 22 vertical control points that start from 3 mm above the wind tunnel floor and reach 0.45 m. The location of these points on the inlet plane needs to be included in a file named points located at the inlet data directory. An example of this can be found in the case studies of the online database.

LES-DT database was deliberately selected as a non-embedded library in OpenFOAM, so it can be used with any version of OpenFOAM that includes the timeVarryingMappedFixedValue function. It reads the inlet data in space and time, thus introducing the necessary wind velocity in the computational domain from the inlet plane. Similar or identical functions have been utilized by various other synthetic methods (e.g., Bervida et al.., 2020, Aboshosha et al.., 2015, Melaku and Bitsuamlak, 2021). In Table A.1, there is a list of the keywords in the Data file and their corresponding options/explanations.

Table A.1: Keywords and options/explanation of Data file to generate inflow turbulence via DT.cpp

Keyword	**Options/Explanation**
inlet_frequency	- Options: positive integer - spectral tunning process in Chapter 4.2
time_start	- Options: positive real number - first time that creates data
time_end	- Options: positive real number -last time that creates data
write	- Options: yes/no - create directories of inlet data at /caseDirectoty/constant/boundaryData/inlet/
wind_tunnel	-Option: directory path (e.g., C:/user/Desktop/) -Directory path of wind tunnel data used to generate inflow turbulence
number_of_control_points	-Options: positive integer (default = 22) -number of points in the z-axis that are used to generate the inlet data on the plane
case	-Options: directory path -directory path of inlet of case study
include_v	-Options: yes/no -include data in the lateral direction or just put 0
include_w	-Options: yes/no -include data in the vertical direction or just put 0
inlet_nLines	-Options: positive integer -number of vertical lines at inlet plane that act as control points for the inflow -the algorithm rewrites the same data equal
modification_mean	-Options: none/linear/user_defined -based on the discussion at 5.2.3 -none: no modification -liner: linear modification based on mean data from previous step

	-user_defined: modification based on a user defined matrix that multiplies the mean data of previous step
targetProfileU_directory	-Options: directory path -directory path of mean target profile interpolated at the predefined 22 points
results_U0_directory	-Options: directory path -directory path of mean profile of previous step at the predefined 22 points
modification_rms	Options: none/linear/nonlinear/user_defined -based on the discussion at 5.2.3 -none: no modification -liner: linear modification based on rms data from previous step -nonliner: nonlinear modification (second order) based on rms data from previous step -user_defined: modification based on a user defined matrix that multiplies the mean data of previous step
targetProfileUrms_directory	-Options: directory path -directory path of rms target profile interpolated at the predefined 22 points
results_U0rms_directory	-Options: directory path -directory path of rms profile of previous step at the predefined 22 points
modification_rmsV	-Options: yes/no -modify lateral rms the same way as the longitudinal
modification_rmsW	-Options: yes/no -modify vertical rms the same way as the longitudinal

The timeVarryingMappedFixedValue function, besides the directories of the inflow data, reads a file named points located at /case/constant/boundaryData/inlet/. This file holds the coordinates of the control points, mentioned in Section 5.2.2. The choice of the distribution of the control points at the inlet plane gives insignificant differences at the generated flow as long as the flow is uniform in the lateral direction. For example, the same outcome can be achieved by using three sets of control points (see Figure 5.2) and only 2 (side ones) or just one in the middle. Minor differences can be spotted near the wall boundaries, that do not alter the flow field to significant values and have to do with the mapping method used. As a practice guideline for LES-DT the mapping method is set to the default (planarInterpolation).

Before the last analysis is run that consists of the computational domain with the building, it is vital to set up the pressure taps in the first cells on the building envelope. This is done by selecting their locations at the three dimensions and utilizing the probe function on OpenFOAM. Examples can be found in the case studies of the database. It is important to double check their location relative to the building to make sure that they are not placed slightly wrong, which might affect the results (e.g., slightly outside of the building footprint). Three-dimensional graphs are needed to ensure that, from the authors' opinion.

As discussed in Section 5.2.4, the utilization of LES-DT needs a code in order to extract the pressure time series, based on filtering the data to account for the inherent discontinuity of the inflow and average them based on the target output frequency. This is done by using the PTSE.cpp C++ code. There are two ways to filter the data in order to correspond to the steady inflow. The first way is to calculate the convergence residual Φ, where $\Phi = \frac{|p_i - p_{i+1}|}{|p_i|}$ and p_i is the value of the pressure at one pressure tap for time step i. Due to the inherent discontinuity of the data as they are imposed in a quasi-steady way, this value will be higher than 1 for time steps that the inflow data are transitioned from one terrain into another. By calculating this factor and removing the data where $\Phi>1$, the signal of the pressure has proven to consistently have a physical meaning and be in line with the modeling targets of LES-DT. The other way is simpler and regards removing all the data whose absolute value is larger than the static pressure at the top of the ABL. Both ways filter the data appropriately and provide similar statistical moments, but the second one is more advantageous in terms of simplicity and computational time, thus it is preferred.

Table A.2 presents the information that the PTSE.cpp code reads from the user, as direct inputs in the code. The final time series should be checked to make sure that the filtering was done properly. Then, it should be normalized with the reference velocity and the pressure coefficient time series should go under a statistical analysis to extract the mean, std and peak pressures (or any other value of interest).

Table A.2: Input and output of PTSE.cpp

Input	**Output**
Path directory of OpenFOAM results	Time series of pressures (first row is time and every row after that are each pressure tap)
Mean velocity at the top of the boundary layer	
Output frequency of pressure time series	
Path directory of the output file	

In the database, many case studies are found, as to facilitate its usage. It is proposed that, first these case studies are run, and then the methodology can be used for various numerical setups, target exposures and building characteristics. More specifically, in the directory Structural Applications the case studies of the results found in Section 5.3 are found, while the Environmental Studies directory includes the cases found in Potsis et al.., 2024.

REFERENCES

Aboshosha, H., Bitsuamlak, G., el Damatty, A., 2015a. Turbulence characterization of downbursts using LES. *Journal of Wind Engineering and Industrial Aerodynamics,* 136, 44–61. https://doi.org/10.1016/J.JWEIA.2014.10.020.

Aboshosha, H., Elshaer, A., Bitsuamlak, G.T., el Damatty, A., 2015b. Consistent inflow turbulence generator for LES evaluation of wind-induced responses for tall buildings. *Journal of Wind Engineering and Industrial Aerodynamics,* 142, 198–216. https://doi.org/10.1016/J.JWEIA.2015.04.004.

Abu-Zidan, Y., & Nguyen, K., 2023. A machine learning approach for calibrating ABL profiles in large-eddy simulations. *Journal of Wind Engineering and Industrial Aerodynamics*, *232*, 105277. https://doi.org/https://doi.org/10.1016/j.jweia.2022.105277

AIAA, 1998. Guide for the verification and validation of computational fluid dynamics simulations, American Institute of Aeronautics and Astronautics, AIAA, Reston, VA (AIAA-G-077-1998).

Al-Chalabi, R., Elshaer, A., & Aboshosha, H., 2024. Enhancing LES efficacy in wind load evaluation of low-rise buildings using synthesized inflow turbulence. *Journal of Building Engineering*, *95*, 110233. https://doi.org/10.1016/J.JOBE.2024.110233

Alminhana, G.W., Braun, A.L., Loredo-Souza, A.M., 2018. A numerical-experimental investigation on the aerodynamic performance of CAARC building models with geometric modifications. *Journal of Wind Engineering and Industrial Aerodynamics,* 180, 34–48. https://doi.org/10.1016/J.JWEIA.2018.07.001.

Architectural Institute of Japan, 2016. AIJ Benchmarks for Validation of CFD Simulations Applied to Pedestrian Wind Environment around Buildings, Architectural Institute of Japan. ISBN978-4-8189-5001-6. https://www.aij.or.jp/eng/publish/index_ddonly.htm.

Architectural Institute of Japan. https://www.aij.or.jp/jpn/publish/cfdguide/index.htm. (Retrieved 2023.07.07)

AIJ-2019. AIJ Recommendations for Loads on Buildings, 2015. Architectural Institute of Japan., March 25, 2019, ISBN978-4-8189-5003-0.

ASCE/SEI 49-21, 2022. Wind Tunnel Testing for Buildings and Other Structures, American Society of Civil Engineers. https://doi.org/10.1061/9780784415740.

Asmerom, H., Filmon, H., Gan, C. A., & DongHun, Y., 2014. Comparisons of Two Wind Tunnel Pressure Databases and Partial Validation against Full-Scale Measurements. *Journal of Structural Engineering*, *140*(10), 04014065. https://doi.org/10.1061/(ASCE)ST.1943-541X.0001001

Barlow, J.F., 2013. The wind that shakes the buildings: wind engineering from a boundary layer meteorology perspective, in: Fifty Years of Wind Engineering: Prestige Lectures from the Sixth European and African Conference on Wind Engineering, Owen J.S. et al. (Eds.), University of Birmingham, UK.

Barlow, J.F., 2014. Progress in observing and modelling the urban boundary layer. *Urban Climate*, 10, 216–240.

Bervida, M., Patruno, L., Stanič, S., de Miranda, S., 2020. Synthetic generation of the atmospheric boundary layer for wind loading assessment using spectral methods *Journal of Wind Engineering and Industrial Aerodynamics,* 196, 104040. https://doi.org/10.1016/J.JWEIA.2019.104040.

Blocken, B., 2014. 50 years of computational wind engineering: Past, present and future. *Journal of Wind Engineering and Industrial Aerodynamics,* 129, 69–102. https://doi.org/10.1016/j.jweia.2014.03.008.

Blocken, B., 2015. Computational Fluid Dynamics for urban physics: Importance, scales, possibilities, limitations and ten tips and tricks towards accurate and reliable simulations. *Building and Environment*, 91, 219–245.

Blocken, B., Stathopoulos, T., Carmeliet, J., 2007. CFD simulation of the atmospheric boundary layer: wall function problems. *Atmospheric Environment* 41(2), 238–252. https://doi.org/10.1016/J.ATMOSENV.2006.08.019.

Bruno, L., Coste, N., Mannini, C., Mariotti, A., Patruno, L., Schito, P., & Vairo, G., 2023. Codes and standards on computational wind engineering for structural design: State of art and recent trends. *Wind and Structures,* 37(2), 133-151. https://doi.org/10.12989/WAS.2023.37.2.133

Buffa, E., Jacob, J., Sagaut, P., 2021. Lattice-Boltzmann-based large-eddy simulation of high-rise building aerodynamics with inlet turbulence reconstruction *Journal of Wind Engineering and Industrial Aerodynamics,* 212, 104560. https://doi.org/10.1016/J.JWEIA.2021.104560.

Canadian Commission on Building and Fire Codes. 'National Building Code of Canada: 2020'. National Research Council of Canada, 28 March 2022. https://doi.org/10.4224/w324-hv93.

Cao, Y., Tamura, T., Kawai, H., 2019. Investigation of wall pressures and surface flow patterns on a wall-mounted square cylinder using very high-resolution Cartesian mesh. *Journal of Wind Engineering and Industrial Aerodynamics,* 188, 1–18. https://doi.org/10.1016/J.JWEIA.2019.02.013.

Castro, H.G., Paz, R.R., 2013. A time and space correlated turbulence synthesis method for Large Eddy Simulations. *Journal of Computational Physics*, 235, 742–763. https://doi.org/10.1016/J.JCP.2012.10.035.

CEDVAL, 2006. Compilation of Experimental Data for Validation of Microscale Dispersion Models. <https://mi-pub.cen.uni-hamburg.de/index.php?id=433> (retrieved 2022.12.13).

Celik, I. B., Cehreli, Z. N., & Yavuz, I., 2005. Index of Resolution Quality for Large Eddy Simulations. *Journal of Fluids Engineering*, *127*(5), 949–958. https://doi.org/10.1115/1.1990201

Cermak, J.E., 1975. Applications of fluid mechanics to wind engineering – A Freeman Scholar Lecture. *Journal of Fluids Engineering*, 97(1), 9–38.

Chavez, M., Baskaran, A., Aldoum, M., Stathopoulos, T., Geleta, T. N., & Bitsuamlak, G. T., 2022. Wind loading on a low-slope gabled roof: Comparison of field measurements, wind tunnel data, and code provisions. *Engineering Structures*, *267*, 114646. https://doi.org/https://doi.org/10.1016/j.engstruct.2022.114646

Cheng, Y., Lien, F.S., Yee, E., Sinclair, R., 2003. A comparison of large Eddy simulations with a standard k-ε Reynolds-averaged Navier-Stokes model for the prediction of a fully developed turbulent flow over a matrix of cubes. *Journal of Wind Engineering and Industrial Aerodynamics,* 91(11), 1301–1328. https://doi.org/10.1016/j.jweia.2003.08.001.

Ciarlatani, M. F., Huang, Z., Philips, D., & Gorlé, C., 2023. Investigation of peak wind loading on a high-rise building in the atmospheric boundary layer using large-eddy simulations. *Journal of Wind Engineering and Industrial Aerodynamics*, *236*, 105408. https://doi.org/10.1016/J.JWEIA.2023.105408

Daniels, S., Xie, Z.-T., 2022. Overview of large-eddy simulation for wind loading on slender structures. *Engineering and Computational Mechanics*, 175(2), 41–71. https://doi.org/10.1680/jencm.18.00028.

Daniels, S.J., Castro, I.P., Xie, Z.T., 2013. Peak loading and surface pressure fluctuations of a tall model building. *Journal of Wind Engineering and Industrial Aerodynamics,* 120, 19–28. https://doi.org/10.1016/J.JWEIA.2013.06.014.

Davenport, A., 1960. Rationale for determining design wind velocities. *ASCE Journal of the Structural Division*. 86, 39–68.

Davenport, A.G., 1961. The spectrum of horizontal gustiness near the ground in high winds. *Quarterly Journal of the Royal Meteorological Society*. 87(372), 194–211. https://doi.org/10.1002/qj.49708737208.

Delaunay, D., Lakehal, D., Pierrat, D., 1995. Numerical approach for wind loads prediction on buildings and structures *Journal of Wind Engineering and Industrial Aerodynamics*, 57(2–3), 307–321.

Dhamankar, N. S., & Blaisdell, G. A., 2018. Overview of Turbulent Inflow Boundary Conditions for Large-Eddy Simulations. *AIAA JOURNAL*, *56*(4). https://doi.org/10.2514/1.J055528

Di Sabatino, S., Buccolieri, R., Olesen, H.R., Ketzel, M., Berkowicz, R., Franke, J., Schatzmann, M.K., Schlunzen, H., Leitl, B., Britter, R., Borrego, C., Margari, A., 2011. COST 732 in practice: the MUST model evaluation exercise. *International Journal of Environment and Pollution*, 44, 403–418.

Elkhoury, M., 2016. Assessment of turbulence models for the simulation of turbulent flows past bluff bodies. *Journal of Wind Engineering and Industrial Aerodynamics* 154, 10–20. https://doi.org/10.1016/j.jweia.2016.03.011.

Elshaer, A., Aboshosha, H., Bitsuamlak, G., el Damatty, A., & Dagnew, A., 2016. LES evaluation of wind-induced responses for an isolated and a surrounded tall building. *Engineering Structures*, *115*, 179–195. https://doi.org/10.1016/J.ENGSTRUCT.2016.02.026

Emil Simiu, DongHun Yeo, Wind Effects on Structures, Fourth Edition, ©2019 John Wiley Sons Ltd

ESDU, 1993. Characteristics of atmospheric turbulence near the ground, Part II: single point data for strong winds (neutral atmosphere), Item No. 85020.

Feng, C., Gu, M., Zheng, D., 2019. Numerical simulation of wind effects on super high-rise buildings considering wind veering with height based on CFD. *Journal of Fluid and Structures*, 91, 102715. https://doi.org/10.1016/J.JFLUIDSTRUCTS.2019.102715.

Fernando, H.J.S., 2010. Fluid dynamics of urban atmospheres in complex terrain. *Annual Review of Fluid Mechanics*, 42, 365–389.

Fernando, H.J.S., Zajiic, D., Di Sabatino, S., Dimitrova, R., Hedquist, B., Dallman, A., 2010. Flow, turbulence and pollutant dispersion in urban atmospheres. *Physics of Fluids*, 22, 051301-1-20.

Ferziger, J.H., Peric M., 2002. Computational Methods for Fluid Dynamics, third ed. Springer-Verlag, ISBN 3-540-42074-6.

Gavanski, E., Gurley, K. R., & Kopp, G. A., 2016. Uncertainties in the Estimation of Local Peak Pressures on Low-Rise Buildings by Using the Gumbel Distribution Fitting Approach. *Journal of Structural Engineering*, *142*(11), 4016106. https://doi.org/10.1061/(ASCE)ST.1943-541X.0001556

Geleta, T. N., & Bitsuamlak, G., 2022. Validation metrics and turbulence frequency limits for LES-based wind load evaluation for low-rise buildings. *Journal of Wind Engineering and Industrial Aerodynamics*, *231*, 105210. https://doi.org/https://doi.org/10.1016/j.jweia.2022.105210

Germano M., Piomelli U., Moin P., et al., 1991. A dynamic subgrid-scale eddy viscosity model. *Physics of Fluids*, A 3 (3), 1760–1765.

Gimenez, J.M., Bre, F., 2019. Optimization of RANS turbulence models using genetic algorithms to improve the prediction of wind pressure coefficients on low-rise buildings. *Journal of Wind Engineering and Industrial Aerodynamics*, 193, 103978. https://doi.org/10.1016/j.jweia.2019.103978.

Gorlé, C., van Beeck, J., Rambaud, P., van Tendeloo, G., 2009. CFD modelling of small particle dispersion: the influence of the turbulent kinetic energy in the atmospheric boundary layer. *Atmospheric Environment*, 43, 673–681.

Gough, H., King, M.F., Nathan, P., Grimmond, C.S.B., Robins, A., Noakes, C.J., Luo, Z., Barlow, J.F., 2019. Influence of neighbouring structures on building façade pressures: Comparison between full-scale, wind-tunnel, CFD and practitioner guidelines *Journal of Wind Engineering and Industrial Aerodynamics,* 189, 22–33. https://doi.org/10.1016/J.JWEIA.2019.03.011.

Gousseau, P., Blocken, B., & van Heijst, G. J. F., 2013. Quality assessment of Large-Eddy Simulation of wind flow around a high-rise building: Validation and solution verification. *Computers & Fluids*, *79*, 120–133. https://doi.org/https://doi.org/10.1016/j.compfluid.2013.03.006

Guichard, R., 2019. Assessment of an improved Random Flow Generation method to predict unsteady wind pressures on an isolated building using Large-Eddy Simulation. *Journal of*

Wind Engineering and Industrial Aerodynamics, *189*, 304–313. https://doi.org/10.1016/J.JWEIA.2019.04.006

Guillas, S., Glover, N., Malki-Epshtein, L., 2014. Bayesian calibration of the constants of the k–ε turbulence model for a CFD model of street canyon flow. *Computer Methods in Applied Mechanics and Engineering*, 279, 536–553.

Harms, F., Leitl, B., Schatzmann, M., Patnaik, G., 2011. Validating LES-based flow and dispersion models. *Journal of Wind Engineering and Industrial Aerodynamics,* 99(4), 289–295.

Hertwig, D., Leitl, B., Schatzmann, M., 2011. Organized turbulent structures: Link between experimental data and LES. *Journal of Wind Engineering and Industrial Aerodynamics* 99(4), 296–307.

Hirsch, C., 2006. The development of a framework for CFD validation and best practice: The QNET-CFD knowledge base. *Chinese Journal of Aeronautics*, 19(2), 105–113. https://doi.org/10.1016/S1000-9361(11)60290-2.

Hu, J., Xuan, H.B., Kwok, K.C.S., Zhang, Y., Yu, Y., 2018. Study of wind flow over a 6 m cube using improved delayed detached Eddy simulation. *Journal of Wind Engineering and Industrial Aerodynamics* 179, 463–474. https://doi.org/10.1016/J.JWEIA.2018.07.003.

Huang, S.H., Li, Q.S., Wu, J.R., 2010. A general inflow turbulence generator for large eddy simulation. *Journal of Wind Engineering and Industrial Aerodynamics* 98(10–11), 600–617. https://doi.org/10.1016/J.JWEIA.2010.06.002.

Irtaza, H., Beale, R.G., Godley, M.H.R., Jameel, A., 2013. Comparison of wind pressure measurements on Silsoe experimental building from full-scale observation, wind-tunnel experiments and various CFD techniques. *International Journal of Engineering Science and Technology*, 5. 28–41. http://dx.doi.org/10.4314/ijest.v5i1.3.

Jarrin, N., Benhamadouche, S., Laurence, D., & Prosser, R., 2006. A synthetic-eddy-method for generating inflow conditions for large-eddy simulations. *International Journal of Heat and Fluid Flow*, 27(4), 585–593. https://doi.org/10.1016/J.IJHEATFLUIDFLOW.2006.02.006

Jayakumari, A. K. R., Gillmeier, S., Ricci, A., Guichard, R., & Blocken, B., 2023. Scaling effects on experimentally obtained pressures on an idealized building: Possible implications towards asbestos containment. *Journal of Wind Engineering and Industrial Aerodynamics*, *239*, 105442. https://doi.org/10.1016/J.JWEIA.2023.105442

Jeong, J., & Hussain, F., 1995. On the identification of a vortex. *Journal of Fluid Mechanics*, *285*, 69–94. https://doi.org/10.1017/S0022112095000462

Khaled, M. F., & Aly, A. M., 2022. Assessing aerodynamic loads on low-rise buildings considering Reynolds number and turbulence effects: a review. *Advances in Aerodynamics*, *4*(1), 24. https://doi.org/10.1186/s42774-022-00114-0

Kim, J., Hangan, H., 2007. Numerical simulations of impinging jets with application to downbursts. *Journal of Wind Engineering and Industrial Aerodynamics* 95(4), 279–298. https://doi.org/10.1016/J.JWEIA.2006.07.002.

Kim, Y., Castro, I. P., & Xie, Z. T., 2013. Divergence-free turbulence inflow conditions for large-eddy simulations with incompressible flow solvers. *Computers and Fluids*, *84*, 56–68. https://doi.org/10.1016/J.COMPFLUID.2013.06.001

Klein, M., Sadiki, A., & Janicka, J., 2003. A digital filter based generation of inflow data for spatially developing direct numerical or large eddy simulations. *Journal of Computational Physics*, 186(2), 652–665. https://doi.org/10.1016/S0021-9991(03)00090-1

Kondo, K., Murakami, S., & Mochida, A., 1997. Generation of velocity fluctuations for inflow boundary condition of LES. *Journal of Wind Engineering and Industrial Aerodynamics*, *67–68*, 51–64. https://doi.org/10.1016/S0167-6105(97)00062-7

Lamberti, G., García-Sánchez, C., Sousa, J., Gorlé, C., 2018. Optimizing turbulent inflow conditions for large-eddy simulations of the atmospheric boundary layer. *Journal of Wind Engineering and Industrial Aerodynamics* 177, 32–44. https://doi.org/10.1016/J.JWEIA.2018.04.004.

Lamberti, G., Gorlé, C., 2020. Sensitivity of LES predictions of wind loading on a high-rise building to the inflow boundary condition. *Journal of Wind Engineering and Industrial Aerodynamics* 206, 104370. https://doi.org/10.1016/J.JWEIA.2020.104370.

Lamberti, G., Gorlé, C., 2021. A multi-fidelity machine learning framework to predict wind loads on buildings. *Journal of Wind Engineering and Industrial Aerodynamics* 214, 104647. https://doi.org/10.1016/J.JWEIA.2021.104647.

Lettau, H., 1969. Note on Aerodynamic Roughness-Parameter Estimation on the Basis of Roughness-Element Description. *Journal of Applied Meteorology (1962-1982)*, *8*(5), 828–832. http://www.jstor.org/stable/26174682

Lim, H.C., Thomas, T.G., Castro, I.P., 2009. Flow around a cube in a turbulent boundary layer: LES and experiment. *Journal of Wind Engineering and Industrial Aerodynamics* 97(2), 96–109. https://doi.org/10.1016/J.JWEIA.2009.01.001.

Lund, T. S., Wu, X., & Squires, K. D., 1998. Generation of Turbulent Inflow Data for Spatially-Developing Boundary Layer Simulations. *Journal of Computational Physics*, 140(2), 233–258. https://doi.org/10.1006/JCPH.1998.5882

Luo, Y., Liu, H., Huang, Q., Xue, H., Lin, K., 2017. A multi-scale synthetic eddy method for generating inflow data for LES. *Computers and Fluids*, 156, 103–112. https://doi.org/10.1016/J.COMPFLUID.2017.06.017.

Melaku, A. F., & Bitsuamlak, G. T., 2024. Prospect of LES for predicting wind loads and responses of tall buildings: A validation study. *Journal of Wind Engineering and Industrial Aerodynamics*, *244*, 105613. https://doi.org/10.1016/J.JWEIA.2023.105613

Melaku, A. F., Doddipatla, L. S., Bitsuamlak, G. T., 2022. Large-eddy simulation of wind loads on a roof-mounted cube: application for interpolation of experimental aerodynamic data. *Journal of Wind Engineering and Industrial Aerodynamics* 231, 105230. https://doi.org/https://doi.org/10.1016/j.jweia.2022.105230

Melaku, A.F., Bitsuamlak, G.T., 2021. A divergence-free inflow turbulence generator using spectral representation method for large-eddy simulation of ABL flows. *Journal of Wind Engineering and Industrial Aerodynamics* 212, 104580. https://doi.org/10.1016/J.JWEIA.2021.104580.

Mochida, A., Iizuka, S., Tominaga, Y., Lun, I.Y.-F., 2011. Up-scaling CWE models to include mesoscale meteorological influences. *Journal of Wind Engineering and Industrial Aerodynamics* 99, 187–198.

Mochida, A., Murakami, S., Shoji, M., Ishida, Y., 1993. Numerical Simulation of flow field around Texas Tech Building by Large Eddy Simulation. *Journal of Wind Engineering and Industrial Aerodynamics* 46–47, 455–460. https://doi.org/10.1016/0167-6105(93)90312-C.

Mochida, A., Tabata, Y., Iwata, T., Yoshino, H., 2008. Examining tree canopy models for CFD prediction of wind environment at pedestrian level. *Journal of Wind Engineering and Industrial Aerodynamics* 96, 1667–1677.

Mochida, A., Tominaga, Y., Murakami, S., Yoshie, R., Ishihara, T., Ooka, R., 2002. Comparison of various k-ε models and DSM applied to flow around a high-rise building. *Wind and Structures*, 5, 227–244.

Moen, A., Mauri, L., Narasimhamurthy, V.D., 2019. Comparison of k-ε models in gaseous release and dispersion simulations using the CFD code FLACS. *Process Safety and Environmental Protection*, 130, 306–316. https://doi.org/10.1016/j.psep.2019.08.016.

Morrison, M. J., & Kopp, G. A., 2018. Effects of turbulence intensity and scale on surface pressure fluctuations on the roof of a low-rise building in the atmospheric boundary layer. *Journal of Wind Engineering and Industrial Aerodynamics*, *183*, 140–151. https://doi.org/10.1016/J.JWEIA.2018.10.017

Murakami, S., 1990. Computational wind engineering. *Journal of Wind Engineering and Industrial Aerodynamics* 36, 517–538.

Murakami, S., 1993. Comparison of various turbulence models applied to a bluff body. *Journal of Wind Engineering and Industrial Aerodynamics*, 46-47, 21–36.

Murakami, S., 1997. Current status and future trends in computational wind engineering. *Journal of Wind Engineering and Industrial Aerodynamics,* 67 & 68, 3–34.

Murakami, S., Mochida, A., Hayashi, Y., 1990. Examining the k-ε model by means of a wind tunnel test and large-eddy simulation of the turbulence structure around a cube. *Journal of Wind Engineering and Industrial Aerodynamics* 35, 87–100.

Murakami, S., Mochida, A., Hayashi, Y., Sakamoto, S., 1992. Numerical study on velocity-pressure field and wind forces for bluff bodies by k-e, ASM and LES. *Journal of Wind Engineering and Industrial Aerodynamics* 41–44, 2841–2852.

Murakami. S., Mochida, A., Ooka, R., Kato, Iizuka, S., 1996. Numerical prediction of flow around a building with various turbulence models - Comparison of k-ε EVM, ASM, DSM, and LES with wind tunnel tests. *ASHRAE Transactions*, 102 (Part1), 741–753.

Nicoud, F., & Ducros, F., 1999. Subgrid-Scale Stress Modelling Based on the Square of the Velocity Gradient Tensor. *Flow, Turbulence and Combustion* (Vol. 62).

Nicoud, F., Ducros, F., 1999. Subgrid-scale stress modelling based on the square of the velocity gradient tensor. *Flow, Turbulence and Combustion,* 62, 183–200.

NIST, 2003. <https://www.nist.gov/el/materials-and-structural-systems-division-73100/nist-aerodynamic-database> (retrieved 2022.12.13)

Nozawa, K., & Tamura, T., 2002. Large eddy simulation of the flow around a low-rise building immersed in a rough-wall turbulent boundary layer. *Journal of Wind Engineering and Industrial Aerodynamics*, *90*(10), 1151–1162. https://doi.org/10.1016/S0167-6105(02)00228-3

Nozawa, K., 2003. Numerical prediction of pressure on a high-rise building immersed in a turbulent boundary layer using LES. Proc. Annual Meeting of JACWE 95. https://cir.nii.ac.jp/crid/1572824500080232448.

Nozu, T., Tamura, T., Takeshi, K., Akira, K., 2015. Mesh-adaptive LES for wind load estimation of a high-rise building in a city. *Journal of Wind Engineering and Industrial Aerodynamics* 144, 62–69. https://doi.org/10.1016/J.JWEIA.2015.05.007.

Oberkampf, W.L., Trucano, T.G., 2002. Verification and validation in computational fluid dynamics. *Progress in Aerospace Sciences*, 38(3), 209–272. https://doi.org/10.1016/S0376-0421(02)00005-2.

Oberkampf, W.L., Trucano, T.G., Hirsch, C., 2004. Verification, validation, and predictive capability in computational engineering and physics. *Applied Mechanics Reviews*, 57(5), 345–384.

Oke, T.R., 1987. Boundary layer climates, 2nd ed. Routledge, London, 435 pp.

Ong, R.H., Patruno, L., Yeo, D., He, Y., Kwok, K.C.S., 2020. Numerical simulation of wind-induced mean and peak pressures around a low-rise structure. *Engineering Structures*, 214, 110583. https://doi.org/10.1016/J.ENGSTRUCT.2020.110583.

Ono, Y., Tamura, T., Kataoka, H., 2008. LES analysis of unsteady characteristics of conical vortex on a flat roof. *Journal of Wind Engineering and Industrial Aerodynamics* 96(10–11), 2007–2018. https://doi.org/10.1016/J.JWEIA.2008.02.021.

Papp, B., Kristóf, G., Gromke, C., 2021. Application and assessment of a GPU-based LES method for predicting dynamic wind loads on buildings. *Journal of Wind Engineering and Industrial Aerodynamics* 217, 104739. https://doi.org/10.1016/J.JWEIA.2021.104739.

Parente, A., Gorlé, C., van Beeck, J., Benocci, C., 2011. Improved k-ε model and wall function formulation for the RANS simulation of ABL flows. *Journal of Wind Engineering and Industrial Aerodynamics* 99(4), 267–278. https://doi.org/10.1016/j.jweia.2010.12.017.

Paterson, D.A., 1993. Predicting r.m.s. pressures from computed velocities and mean pressures. *Journal of Wind Engineering and Industrial Aerodynamics* 46–47, 431–437. https://doi.org/10.1016/0167-6105(93)90309-C.

Patruno, L., & de Miranda, S., 2020. Unsteady inflow conditions: A variationally based solution to the insurgence of pressure fluctuations. *Computer Methods in Applied Mechanics and Engineering*, *363*, 112894. https://doi.org/10.1016/J.CMA.2020.112894

Patruno, L., & Ricci, M., 2018. A systematic approach to the generation of synthetic turbulence using spectral methods. *Computer Methods in Applied Mechanics and Engineering*, 340, 881–904. https://doi.org/10.1016/J.CMA.2018.06.028

Peng, X., Yang, L., Gavanski, E., Gurley, K., & Prevatt, D., 2014. A comparison of methods to estimate peak wind loads on buildings. *Journal of Wind Engineering and Industrial Aerodynamics*, *126*, 11–23. https://doi.org/10.1016/J.JWEIA.2013.12.013

Piringer, M., Joffre, S., Baklanov, A., 2007. The surface energy balance and the mixing height in urban areas—activities and recommendations of COST-Action 715. *Boundary Layer Meteorology*, 124, 3–24. https://doi.org/10.1007/s10546-007-9170-0.

Poletto, R., Craft, T., & Revell, A., 2013. A new divergence free synthetic eddy method for the reproduction of inlet flow conditions for les. *Flow, Turbulence and Combustion*, 91(3), 519–539. https://doi.org/10.1007/S10494-013-9488-2

Pope, S. B., 2000. *Turbulent Flows*. Cambridge University Press. https://doi.org/DOI: 10.1017/CBO9780511840531

Porté-Agel, F., Wu, Y. T., Lu, H., & Conzemius, R. J., 2011. Large-eddy simulation of atmospheric boundary layer flow through wind turbines and wind farms. *Journal of Wind Engineering* *and Industrial Aerodynamics*, *99*(4), 154–168. https://doi.org/10.1016/J.JWEIA.2011.01.011

Potsis, T., Stathopoulos, T., 2022. A Novel Computational Approach for an Improved Expression of the Spectral Content in the Lower Atmospheric Boundary Layer. *Buildings* 12(6). https://doi.org/10.3390/buildings12060788.

Potsis, T., Tominaga, Y., & Stathopoulos, T., 2023. Computational wind engineering: 30 years of research progress in building structures and environment. *Journal of Wind Engineering and Industrial Aerodynamics*, *234*, 105346. https://doi.org/https://doi.org/10.1016/j.jweia.2023.105346

Potsis, T., & Stathopoulos, T., 2024. Wind induced peak pressures on low-rise building roofs via dynamic terrain computational methodology. *Journal of Wind Engineering and Industrial Aerodynamics*, *245*, 105630. https://doi.org/10.1016/J.JWEIA.2023.105630

Potsis, T., Ricci, A., & Stathopoulos, T., 2024. On the reliability of the dynamic terrain method to generate ABL winds for environmental applications. *Meccanica*. https://doi.org/10.1007/s11012-024-01810-5

Potsis, Theodore and Stathopoulos, Ted, Evaluation of Wind Flow and Structural Loads by the Dynamic Terrain Approach (June 2, 2024b). Available at SSRN: https://ssrn.com/abstract=4944018 or http://dx.doi.org/10.2139/ssrn.4944018

Potsis, T. and Stathopoulos, T. 2024c, Design criteria for wind loads on buildings in Canada: Review of current Code provisions, wind tunnel data and CFD results, *CSCE 2024*, Conference Proceedings

Potsis. T., 2024. "DTv1.0" Github. https://github.com/tpotsis/DTv1.0 (accessed Oct. 14, 2024)

Ricci, M., Patruno, L., de Miranda, S., 2017. Wind loads and structural response: Benchmarking LES on a low-rise building. *Engineering Structures*,144, 26–42. https://doi.org/10.1016/J.ENGSTRUCT.2017.04.027.

Ricci, M., Patruno, L., Kalkman, I., de Miranda, S., Blocken, B., 2018. Towards LES as a design tool: Wind loads assessment on a high-rise building. *Journal of Wind Engineering and Industrial Aerodynamics* 180, 1–18. https://doi.org/10.1016/J.JWEIA.2018.07.009.

Richards, P. J., & Hoxey, R. P., 1992. Computational and wind tunnel modelling of mean wind loads on the Silsoe structures building. *Journal of Wind Engineering and Industrial Aerodynamics*, *43*(1–3), 1641–1652. https://doi.org/10.1016/0167-6105(92)90574-T

Richards, P. J., & Hoxey, R. P., 2012. Pressures on a cubic building—Part 1: Full-scale results. *Journal of Wind Engineering and Industrial Aerodynamics*, *102*, 72–86. https://doi.org/10.1016/J.JWEIA.2011.11.004

Richards, P., Norris, S., 2015. LES modelling of unsteady flow around the Silsoe cube. *Journal of Wind Engineering and Industrial Aerodynamics* 144, 70–78. https://doi.org/10.1016/J.JWEIA.2015.03.018.

Richards, P.J., Hoxey, R.P., 1993. Appropriate boundary conditions for computational wind engineering models using the k-ϵ turbulence model. *Journal of Wind Engineering and Industrial Aerodynamics* 46–47, 145–153. https://doi.org/http://dx.doi.org/10.1016/0167-6105(93)90124-7.

Richards, P.J., Norris, S.E., 2011. Appropriate boundary conditions for computational wind engineering models revisited. *Journal of Wind Engineering and Industrial Aerodynamics* 99(4), 257–266. https://doi.org/10.1016/j.jweia.2010.12.008.

Robins, A.G., Hall, R., Cowan, I.R., Bartzis, J.G., Albergel, A., 2000. Evaluating modelling uncertainty in CFD predictions of building affected dispersion. *International Journal of Environment and Pollution,* 14, 52–64.

Rodi, W., 1997. Comparison of LES and RANS calculations of the flow around bluff bodies. *Journal of Wind Engineering and Industrial Aerodynamics* 69–71, 55–75.

Rotach, M.W., Vogt, R., Bernhofer, C., Batchvarova, E., Christen, A., Clappier, A., Feddersen, B., Gryning, S.-E., Martucci, G., Mayer. H., Mitev. V., Oke. T.R., Parlow. E., Richner. H., Roth. M., Roulet, Y.A., Ruffieux, D., Salmond, J., Schatzmann, M., Voogt, J.A., 2005. BUBBLE – an Urban Boundary Layer Meteorology Project. *Theoretical and Applied Climatology*. 81, 231–261.

Sagaut, P., 2006. *Large Eddy Simulation for Incompressible Flows*. https://doi.org/10.1007/b137536

Schatzmann, M., Olesen, H., Franke, J., 2010. Cost 732 Model Evaluation Case Studies: Approach and Results, COST Action 732, *COST Office*.

Scott, D., Goupil, J., Burton, M., Gorle, C., Kareem, A., Stathopoulos, T., and Young, B., 2023. Advancements in Computational Wind Engineering: Workshop Report. (National Institute of Standards and Technology, Gaithersburg, MD), NIST Grant Contractor Report (GCR) NIST GCR 23-047. https://doi.org/10.6028/NIST.GCR.23-047

Selvam, R.P., 1992. Computation of pressures on Texas Tech Building. *Journal of Wind Engineering and Industrial Aerodynamics* 43(1–3), 1619–1627. https://doi.org/10.1016/0167-6105(92)90572-R.

Selvam, R.P., 1997. Computation of pressures on Texas Tech University building using large eddy simulation. *Journal of Wind Engineering and Industrial Aerodynamics* 67–68, 647–657. https://doi.org/10.1016/S0167-6105(97)00107-4.

Shelley, E., Hubbard, E., & Zhang, W., 2023. Comparison and uncertainty quantification of roof pressure measurements using the NIST and TPU aerodynamic databases. *Journal of Wind Engineering and Industrial Aerodynamics*, *232*, 105246. https://doi.org/https://doi.org/10.1016/j.jweia.2022.105246

Shirzadi, M., Mirzaei, P.A., Tominaga, Y., 2020c. RANS model calibration using stochastic optimization for accuracy improvement of urban airflow CFD modeling. *Journal of Building Engineering*. 32, 101756. https://doi.org/10.1016/j.jobe.2020.101756.

Smagorinsky J., 1963. General Circulation Experiments with the Primitive Equations: I. the Basic Experiment. *Monthly Weather Review,* 91(3), 99–164.

Smirnov, A., Shi, S., & Celik, I., 2001. Random Flow Generation Technique for Large Eddy Simulations and Particle-Dynamics Modeling. *Journal of Fluids Engineering*, *123*(2), 359–371. https://doi.org/10.1115/1.1369598

Solari, G., Burlando, M., Repetto, M.P., 2020. Detection, simulation, modelling and loading of thunderstorm outflows to design wind-safer and cost-efficient structures. *Journal of Wind Engineering and Industrial Aerodynamics* 200, 104142. https://doi.org/10.1016/J.JWEIA.2020.104142.

Stathopoulos, T. (1984). Design and fabrication of a wind tunnel for building aerodynamics. *Journal of Wind Engineering and Industrial Aerodynamics*, *16*(2–3), 361–376. https://doi.org/10.1016/0167-6105(84)90018-7

Stathopoulos, T., & Surry, D., 1983. Scale effects in wind tunnel testing of low buildings. *Journal of Wind Engineering and Industrial Aerodynamics*, *13*(1–3), 313–326. https://doi.org/10.1016/0167-6105(83)90152-6

Stathopoulos, T., & Zhou, Y. S., 1993. Numerical simulation of wind-induced pressures on buildings of various geometries. *Journal of Wind Engineering and Industrial Aerodynamics*, *46–47*(C), 419–430. https://doi.org/10.1016/0167-6105(93)90308-B

Stathopoulos, T., 1997. Computational wind engineering: Past achievements and future challenges. *Journal of Wind Engineering and Industrial Aerodynamics* 67–68, 509–532. https://doi.org/10.1016/S0167-6105(97)00097-4.

Stathopoulos, T., 2002. The numerical wind tunnel for industrial aerodynamics-Real or virtual in the new millennium? *Wind and Structures*, 5(2–4), 193–208.

Stathopoulos, T., Zhou, Y.S., 1993. Numerical simulation of wind-induced pressures on buildings of various geometries. *Journal of Wind Engineering and Industrial Aerodynamics* 46–47, 419–430. https://doi.org/10.1016/0167-6105(93)90308-B.

Stathopoulos, T., Zhou, Y.S., 1995. Numerical evaluation of wind pressures on flat roofs with the k-ε model. *Building and Environment*, 30(2), 267–276. https://doi.org/10.1016/0360-1323(94)00038-T.

Stathopoulos, T., 2020, "Wind on the globe", Lecture, BLDG 6071 Wind Engineering and Building Aerodynamics, Concordia University, Montreal, Canada.

Sun, L., Wu, J., & Tamura, Y., 2024. Large eddy simulation of aerodynamic wind pressure on a tall rectangular building by modified synthetic volume forcing method. *Journal of Wind Engineering and Industrial Aerodynamics*, *247*, 105697. https://doi.org/10.1016/J.JWEIA.2024.105697

Tamura, T., 1999. Reliability on CFD estimation for wind-structure interaction problems. *Journal of Wind Engineering and Industrial Aerodynamics* 81(1–3), 117–143. https://doi.org/10.1016/S0167-6105(99)00012-4.

Tamura, T., 2008. Towards practical use of LES in wind engineering. *Journal of Wind Engineering and Industrial Aerodynamics* 96(10–11), 1451–1471. https://doi.org/10.1016/j.jweia.2008.02.034.

Tamura, T., Kawai, H., Kawamoto, S., Nozawa, K., Sakamoto, S., Ohkuma, T., 1997. Numerical prediction of wind loading on buildings and structures — Activities of AIJ cooperative project on CFD. *Journal of Wind Engineering and Industrial Aerodynamics* 67–68, 671–685. https://doi.org/10.1016/S0167-6105(97)00109-8.

Tamura, T., Nozawa, K., Kondo, K., 2008. AIJ guide for numerical prediction of wind loads on buildings. *Journal of Wind Engineering and Industrial Aerodynamics* 96(10–11), 1974–1984. https://doi.org/10.1016/J.JWEIA.2008.02.020.

Thordal, M.S., Bennetsen, J.C., Capra, S., Koss, H.H.H., 2020a. Towards a standard CFD setup for wind load assessment of high-rise buildings: Part 1 – Benchmark of the CAARC building. *Journal of Wind Engineering and Industrial Aerodynamics* 205, 104283. https://doi.org/10.1016/J.JWEIA.2020.104283.

Thordal, M.S., Bennetsen, J.C., Capra, S., Koss, H.H.H., 2020b. Engineering approach for a CFD inflow condition using the precursor database method. J. W. Ind. Aerod. 203, 104210. https://doi.org/10.1016/j.jweia.2020.104210.

Thordal, M.S., Bennetsen, J.C., Capra, S., Kragh, A.K., Koss, H.H.H., 2020c. Towards a standard CFD setup for wind load assessment of high-rise buildings: Part 2 – Blind test of chamfered and rounded corner high-rise buildings. *Journal of Wind Engineering and Industrial Aerodynamics* 205, 104282. https://doi.org/10.1016/j.jweia.2020.104282.

Tieleman, H. W., Reinhold, T. A., & Hajj, M. R., 1997. Importance of turbulence for the prediction of surface pressures on low-rise structures. *Journal of Wind Engineering and Industrial Aerodynamics*, *69–71*, 519–528. https://doi.org/10.1016/S0167-6105(97)00182-7

Tokyo Polytechnic University, TPU Aerodynamic Database, 2013. <http://wind.arch.t-kougei.ac.jp/system/eng/contents/code/tpu> (retrieved 2022.12.13)

Tominaga, Y., Mochida, A., Murakami, S., &Sawaki, S., 2008a. Comparison of various revised k–ε models and LES applied to flow around a high-rise building model with 1:1:2 shape placed within the surface boundary layer. *Journal of Wind Engineering and Industrial Aerodynamics*, *96*(4), 389–411. https://doi.org/10.1016/J.JWEIA.2008.01.004

Tominaga, Y., Mochida, A., Yoshie, R., Kataoka, H., Nozu, T., Yoshikawa, M., & Shirasawa, T., 2008b. AIJ guidelines for practical applications of CFD to pedestrian wind environment around buildings. *Journal of Wind Engineering and Industrial Aerodynamics*, *96*(10–11), 1749–1761. https://doi.org/10.1016/J.JWEIA.2008.02.058

Tominaga, Y., Stathopoulos, T., 2009. Numerical simulation of dispersion around an isolated cubic building: Comparison of various types of k-ε models. *Atmospheric Environment*, 43, 3200–3210.

Tsuchiya, M., Murakami, S., Mochida, A., Kondo, K., Ishida, Y., 1997. Development of a new k-ε, model for flow and pressure fields around bluff body. *Journal of Wind Engineering and*

Industrial Aerodynamics 67 & 68, 169–182. https://doi.org/10.1016/S0167-6105(97)00071-8.

Vatistas G.., 2020, "Control volume of a fluid in incompressible flow conditions", Lecture, ENGR 6201 Fluid Mechanics, Concordia University, Montreal, Canada,

Vasaturo, R., Kalkman, I., Blocken, B., & van Wesemael, P. J. V. 2018. Large eddy simulation of the neutral atmospheric boundary layer: performance evaluation of three inflow methods for terrains with different roughness. *Journal of Wind Engineering and Industrial Aerodynamics*, *173*, 241–261. https://doi.org/10.1016/J.JWEIA.2017.11.025

Versteeg, H.K., Malalasekera, W., 2007. An introduction to computational fluid dynamics, Second ed. Pearson Education, ISBN: 978-0-13-127498-3.

von Kármán, T. (1948). Progress in the Statistical Theory of Turbulence*. *Proceedings of the National Academy of Sciences*, *34*(11), 530–539. https://doi.org/10.1073/pnas.34.11.530

Vranešević, K.K., Vita, G., Bordas, S.P.A., Glumac, A.Š., 2022. Furthering knowledge on the flow pattern around high-rise buildings: LES investigation of the wind energy potential. *Journal of Wind Engineering and Industrial Aerodynamics* 226, 105029. https://doi.org/10.1016/J.JWEIA.2022.105029.

Vranešević, K. K., & Glumac, A. Š., 2024. Peak pressures on high-rise buildings roof: A dual approach through validated LES and wind tunnel experiments with uncertainty quantification. *Journal of Wind Engineering and Industrial Aerodynamics*, *250*, 105784. https://doi.org/10.1016/J.JWEIA.2024.105784

Wang, J., Li, C., Huang, S., Zheng, Q., Xiao, Y., & Ou, J., 2023. Large eddy simulation of turbulent atmospheric boundary layer flow based on a synthetic volume forcing method. *Journal of Wind Engineering and Industrial Aerodynamics*, *233*, 105326. https://doi.org/https://doi.org/10.1016/j.jweia.2023.105326

Wang, Y., & Chen, X., 2022. Evaluation of wind loads on high-rise buildings at various angles of attack by wall-modeled large-eddy simulation. *Journal of Wind Engineering and Industrial Aerodynamics*, *229*, 105160. https://doi.org/10.1016/J.JWEIA.2022.105160

Wang, Y., Chen, X., 2020. Simulation of approaching boundary layer flow and wind loads on high-rise buildings by wall-modeled LES. *Journal of Wind Engineering and Industrial Aerodynamics* 207, 104410. https://doi.org/10.1016/J.JWEIA.2020.104410.

Wang, Y., Vita, G., Fraga, B., Lyu, C., Wang, J., & Hemida, H., 2022. Influence of Turbulent Inlet Boundary Condition on Large Eddy Simulation Over a Flat Plate Boundary Layer. *International Journal of Computational Fluid Dynamics*, *36*(3), 232–259. https://doi.org/10.1080/10618562.2022.2085255

Xing, J., 2023. Simulation of a ground-mounted prism in ABL flow using LES: on overview of error metrics and distribution. *Advances in Aerodynamics*, *5*(1), 9. https://doi.org/10.1186/s42774-023-00139-z

Xing, J., Patruno, L., Pozzuoli, C., Pedro, G., de Miranda, S., & Ubertini, F., 2022. Wind loads prediction using LES: Inflow generation, accuracy and cost assessment for the case of Torre

Gioia 22. *Engineering Structures*, *262*, 114292. https://doi.org/https://doi.org/10.1016/j.engstruct.2022.114292

Yan, B. W., & Li, Q. S. 2015. Inflow turbulence generation methods with large eddy simulation for wind effects on tall buildings. *Computers & Fluids*, *116*, 158–175. https://doi.org/10.1016/J.COMPFLUID.2015.04.020

Yan, B., Yuan, Y., Ma, C., Dong, Z., Huang, H., Wang, Z., 2022. Modeling of downburst outflows and wind pressures on a high-rise building under different terrain conditions. J. Build. Eng. 48, 103738. https://doi.org/10.1016/J.JOBE.2021.103738.

Yang, Y., Gu, M., Chen, S., Jin, X., 2009. New inflow boundary conditions for modelling the neutral equilibrium atmospheric boundary layer in computational wind engineering. *Journal of Wind Engineering and Industrial Aerodynamics* 97, 88–95.

Yoshie, R., Mochida, A., Tominaga, Y., Kataoka, H., Harimoto, K., Nozu, T., Shirasawa, T., 2007. Cooperative project for CFD prediction of pedestrian wind environment in the Architectural Institute of Japan. *Journal of Wind Engineering and Industrial Aerodynamics* 95(9-11), 1551–1578. http://dx.doi.org/10.1016/j.jweia.2007.02.023.

Yu, Y., Yang, Y., Xie, Z., 2018. A new inflow turbulence generator for large eddy simulation evaluation of wind effects on a standard high-rise building. Build. Environ. 138, 300–313. https://doi.org/10.1016/J.BUILDENV.2018.03.059.

Yu, J., Stathopoulos, T., & Li, M., 2023. Exposure factors and their specifications in current wind codes and standards. *Journal of Building Engineering*, *76*, 107207. https://doi.org/10.1016/J.JOBE.2023.107207